



UvA-DARE (Digital Academic Repository)

Search for Higgs boson decays into two new low-mass spin-0 particles in the $4b$ channel with the ATLAS detector using pp collisions at $\sqrt{s} = 13$ TeV

Aad, G.; ATLAS Collaboration

DOI

[10.1103/PhysRevD.102.112006](https://doi.org/10.1103/PhysRevD.102.112006)

Publication date

2020

Document Version

Final published version

Published in

Physical Review D. Particles, Fields, Gravitation, and Cosmology

License

CC BY

[Link to publication](#)

Citation for published version (APA):

Aad, G., & ATLAS Collaboration (2020). Search for Higgs boson decays into two new low-mass spin-0 particles in the $4b$ channel with the ATLAS detector using pp collisions at $\sqrt{s} = 13$ TeV. *Physical Review D. Particles, Fields, Gravitation, and Cosmology*, 102(11), [112006]. <https://doi.org/10.1103/PhysRevD.102.112006>

General rights

It is not permitted to download or to forward/distribute the text or part of it without the consent of the author(s) and/or copyright holder(s), other than for strictly personal, individual use, unless the work is under an open content license (like Creative Commons).

Disclaimer/Complaints regulations

If you believe that digital publication of certain material infringes any of your rights or (privacy) interests, please let the Library know, stating your reasons. In case of a legitimate complaint, the Library will make the material inaccessible and/or remove it from the website. Please Ask the Library: <https://uba.uva.nl/en/contact>, or a letter to: Library of the University of Amsterdam, Secretariat, Singel 425, 1012 WP Amsterdam, The Netherlands. You will be contacted as soon as possible.

UvA-DARE is a service provided by the library of the University of Amsterdam (<https://dare.uva.nl>)

Search for Higgs boson decays into two new low-mass spin-0 particles in the $4b$ channel with the ATLAS detector using pp collisions at $\sqrt{s} = 13$ TeV

G. Aad *et al.**
(ATLAS Collaboration)

 (Received 26 May 2020; accepted 30 September 2020; published 7 December 2020)

This paper describes a search for beyond the Standard Model decays of the Higgs boson into a pair of new spin-0 particles subsequently decaying into b -quark pairs, $H \rightarrow aa \rightarrow (b\bar{b})(b\bar{b})$, using proton-proton collision data collected by the ATLAS detector at the Large Hadron Collider at center-of-mass energy $\sqrt{s} = 13$ TeV. This search focuses on the range $15 \text{ GeV} \leq m_a \leq 30 \text{ GeV}$, where the decay products are collimated; it is complementary to a previous search in the same final state targeting the range $20 \text{ GeV} \leq m_a \leq 60 \text{ GeV}$, where the decay products are well separated. A novel strategy for the identification of the $a \rightarrow b\bar{b}$ decays is deployed to enhance the efficiency for topologies with small separation angles. The search is performed with 36 fb^{-1} of integrated luminosity collected in 2015 and 2016 and sets upper limits on the production cross section of $H \rightarrow aa \rightarrow (b\bar{b})(b\bar{b})$, where the Higgs boson is produced in association with a Z boson.

DOI: [10.1103/PhysRevD.102.112006](https://doi.org/10.1103/PhysRevD.102.112006)

I. INTRODUCTION

The Higgs boson is a particle with a particularly narrow natural width, and its branching fractions to new light particles can be sizable even if they interact weakly with it. Because of this, several new weakly interacting light particles that would not be visible in inclusive searches can be probed by searching for “beyond the Standard Model” (BSM) Higgs boson decays at the LHC [1]. These new light particles are predicted in several BSM theories with extended Higgs sectors [2–6] that address open questions in high-energy physics. Theories with new light particles weakly coupled to the Higgs boson provide an explanation for electroweak baryogenesis [7,8] and contain fields that mediate interactions between Standard Model (SM) particles and dark matter [9–13]. This paper presents a search for a new spin-0 singlet a that couples to the SM Higgs boson.

When the mass of the spin-0, m_a , is less than half of the mass of the Higgs boson, m_H , i.e., $2m_a < m_H$, the decay $H \rightarrow aa$ is kinematically allowed. The search in this paper is performed with events in which each a boson decays into a pair of b quarks, and the Higgs boson is produced in association with a Z boson which decays into electrons or

muons. The final state with multiple b quarks has the highest branching ratio in several BSM theories when it is kinematically accessible. The Z boson with leptonic decay provides a simple strategy for triggering and selecting events, as well as powerful background rejection. Figure 1 depicts the main production mechanism of the events sought in this paper.

The Higgs boson has been observed by the ATLAS and CMS collaborations [14,15]. A comprehensive program is being pursued to measure its branching ratios to SM particles and to search for decays into exotic or non-SM particles. Current measurements constrain the non-SM branching ratio of the Higgs boson to be less than approximately 21% at 95% confidence level (C.L.) with several assumptions [16], leaving enough room for exotic Higgs boson decays.

ATLAS has previously performed a search where each of the four b quarks was experimentally identified as an individual jet in the detector [17]. The search set upper limits on the production cross section of ZH , followed by $H \rightarrow aa \rightarrow (b\bar{b})(b\bar{b})$, of approximately 0.5 pb at 95% C.L. for $m_a \gtrsim 30$ GeV. However, when the mass of the a boson is small, it is produced with large momentum and the jets created in the hadronization of the two b quarks from a single $a \rightarrow b\bar{b}$ decay are reconstructed as a single jet in the calorimeter using the standard ATLAS reconstruction algorithms. Because of this, the previous search that covered the range $20 \text{ GeV} \leq m_a \leq 60 \text{ GeV}$ rapidly loses efficiency for masses $m_a \lesssim 30$ GeV.

This article extends the previous analysis in the mass regime $15 \text{ GeV} \leq m_a \leq 30 \text{ GeV}$ by relying on a novel

*Full author list given at the end of the article.

Published by the American Physical Society under the terms of the [Creative Commons Attribution 4.0 International license](https://creativecommons.org/licenses/by/4.0/). Further distribution of this work must maintain attribution to the author(s) and the published article's title, journal citation, and DOI. Funded by SCOAP³.

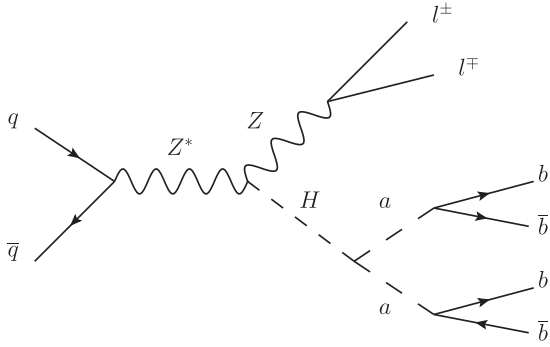


FIG. 1. Representative tree-level Feynman diagram for the ZH production processes with the subsequent decays $Z \rightarrow \ell\ell$ ($\ell = e, \mu$) and $H \rightarrow aa \rightarrow (b\bar{b})(b\bar{b})$.

strategy for the reconstruction and identification of $a \rightarrow b\bar{b}$ decays. The article is structured as follows. Section II describes the relevant features of the ATLAS detector. Section III lists the data collected for this search and details the simulated signal and background event samples that were used to describe the composition of the selected events. Section IV describes the basic reconstruction and identification of leptons and jets using the ATLAS detector. Section V presents the dedicated method for the reconstruction and identification of low-mass $a \rightarrow b\bar{b}$ decays. Section VI explains the strategy for event selection and categorization. Section VII discusses the systematic uncertainties considered in this search, and Sec. VIII presents the results. Finally, Sec. IX presents the conclusion.

II. ATLAS DETECTOR

The ATLAS experiment [18–20] at the LHC is a multipurpose particle detector with a forward-backward symmetric cylindrical geometry and a near 4π coverage in solid angle.¹ It consists of an inner tracking detector surrounded by a thin superconducting solenoid providing a 2 T axial magnetic field, electromagnetic and hadron calorimeters, and a muon spectrometer. The inner tracking detector covers the pseudorapidity range $|\eta| < 2.5$. It consists of silicon pixel, silicon microstrip, and transition radiation tracking detectors. Lead/liquid-argon (LAr) sampling calorimeters provide electromagnetic (EM) energy measurements with high granularity. A steel/scintillator-tile sampling calorimeter provides hadronic energy measurements in the central pseudorapidity range ($|\eta| < 1.7$).

¹ATLAS uses a right-handed coordinate system with its origin at the nominal interaction point (IP) in the center of the detector and the z axis along the beam pipe. The x axis points from the IP to the center of the LHC ring, and the y axis points upwards. Cylindrical coordinates (r, ϕ) are used in the transverse plane, with ϕ being the azimuthal angle around the z axis. The pseudorapidity is defined in terms of the polar angle θ as $\eta = -\ln \tan(\theta/2)$. Angular distance is measured in units of $\Delta R \equiv \sqrt{(\Delta\eta)^2 + (\Delta\phi)^2}$.

The end cap and forward regions are instrumented with LAr calorimeters for EM and hadronic energy measurements up to $|\eta| = 4.9$. The muon spectrometer surrounds the calorimeters and is based on three large air-core toroidal superconducting magnets with eight coils each. The field integral of the toroids ranges between 2.0 and 6.0 T m across most of the detector. The muon spectrometer includes a system of precision tracking chambers and fast detectors for triggering. A two-level trigger system is used to select events. The first-level trigger is implemented in custom hardware and uses a subset of the detector information to keep the accepted rate below 100 kHz. This is followed by a software-based trigger that reduces the accepted event rate to 1 kHz on average depending on the data-taking conditions.

III. DATA SET AND SIMULATED EVENT SAMPLES

Events are selected from proton-proton (pp) collisions collected by the ATLAS detector at the LHC at $\sqrt{s} = 13$ TeV in 2015 and 2016. Only collisions recorded when all relevant subsystems were operational are considered in the analysis. The data set corresponds to an integrated luminosity of $3.2 \pm 0.1 \text{ fb}^{-1}$ recorded in 2015 and $32.9 \pm 0.7 \text{ fb}^{-1}$ recorded in 2016, for a total of $36.1 \pm 0.8 \text{ fb}^{-1}$ [21]. The uncertainty is obtained from the primary luminosity measurements using the LUCID-2 detector [22]. The data used for this search were collected using the single-electron or single-muon triggers with transverse momentum (p_T) thresholds of 20 (26) GeV for muons and 24 (26) GeV for electrons in 2015 (2016) [23].

Simulated event samples are used to study the characteristics of signal events and to calculate the signal efficiency and acceptance, as well as for most aspects of the background estimation. Monte Carlo (MC) samples were produced using the full ATLAS detector simulation [24] based on GEANT4 [25]. To simulate the effects of simultaneous inelastic collisions (pileup), additional interactions were generated using PYTHIA 8.186 [26] with the A2 set of tuned parameters [27] and the MSTW2008LO [28] parton distribution function (PDF) set, and overlaid on the simulated hard-scatter event. Simulated events were reweighted to match the pileup conditions observed in the data. All simulated events are processed through the same reconstruction algorithms and analysis chain as the data. Decays of b and c hadrons were performed by EvtGen v1.2.0 [29], except in events simulated with the SHERPA event generator [30].

Signal samples of associated Higgs boson production with a Z boson, $pp \rightarrow ZH$, were generated with POWHEG-BOX v2 [31–34] using the CT10 PDF set [35] at next-to-leading order (NLO). The sample include gluon-initiated processes at LO. The Higgs boson decay into two spin-0 a bosons and the subsequent decay of each a boson into a pair of b quarks were simulated with PYTHIA 8.186. The a -boson decay was performed in the narrow-width approximation and the

coupling to the b quarks is assumed to be that of a pseudoscalar. The information about the parity of the a boson assumed in the simulation is lost in the hadronization of the b quarks and, therefore, the results of this search apply equally to scalars and pseudoscalars. PYTHIA 8.186 was also used for the parton showering, hadronization, and underlying-event simulation with the A14 tune [36]. Signal events were generated for several a -boson mass hypotheses: 15, 17.5, 20, 22.5, 25, 27.5, and 30 GeV.

The background samples were generated following exactly the same procedure as described in Ref. [17] and only a summarized description is given here. A sample of top-quark pair events was generated using POWHEG-BOX v2 [37] with the NNPDF3.0NLO PDF set. The parton showers and hadronization were modeled by PYTHIA 8.210 [38] with the A14 tune. To model the $t\bar{t} + b\bar{b}$ background with better precision, the relative contributions of the different heavy-flavor categories in the $t\bar{t}$ sample are scaled to match the predictions of an NLO $t\bar{t} + b\bar{b}$ sample including parton showering and hadronization [39], generated with SHERPA+OPENLOOPS [30,40], using the procedure described in Ref. [41].

The production of Z bosons in association with jets was simulated with SHERPA 2.2.1 [30,42] using the NNPDF3.0NNLO PDF set [43]. The matrix element calculation was performed with COMIX [44] and OPENLOOPS [40] and was matched using the MEPS@NLO prescription [45].

Several subleading backgrounds were also simulated. The diboson + jets samples were generated using SHERPA 2.1.1 [46] and the CT10 PDF set. Associated production of $t\bar{t}W$ and $t\bar{t}Z$ ($t\bar{t}V$) were generated with an NLO matrix element using MadGraph5_aMC@NLO interfaced to PYTHIA 8.210 and the NNPDF3.0NNLO PDF set. Samples of Wt single-top-quark backgrounds were generated with POWHEG-BOX v1 at NLO accuracy using the CT10 PDF set. The production of four top quarks ($t\bar{t}t\bar{t}$) and $t\bar{t}WW$ was simulated with MadGraph5_aMC@NLO at LO accuracy and interfaced to PYTHIA 8.186. Background sources with non-prompt leptons contribute negligibly to this search.

Multijet samples are used to compare the data identification efficiency of the $a \rightarrow b\bar{b}$ decays with simulation. These samples were generated using PYTHIA 8.186, with the LO NNPDF2.3 PDF set and the A14 tune. To increase the number of simulated events with semileptonically decaying hadrons used in this analysis, samples of multijet events filtered to have at least one muon with p_T above 3 GeV and $|\eta| < 2.8$ were produced with PYTHIA using the same version, PDF set, and underlying-event tunes as the unfiltered multijet samples. Both the filtered and unfiltered multijet samples produced with PYTHIA were processed through the same ATLAS detector simulation.

IV. OBJECT RECONSTRUCTION AND SELECTION

This search relies on the efficient reconstruction of electrons and muons in order to identify leptonically

decaying Z bosons and the reconstruction of jets to identify $a \rightarrow b\bar{b}$ decays.

Electrons are reconstructed from energy deposited in clusters of cells in the electromagnetic calorimeter matched to tracks in the inner detector [47] and are required to have $p_T > 15$ GeV and $|\eta| < 2.47$. Candidates in the transition region between the barrel and end-cap calorimeters, $1.37 < |\eta| < 1.52$, are excluded. Electrons are identified using the ‘‘Tight’’ criterion based on a likelihood discriminant [48]. Muons are reconstructed by combining matching tracks in the inner detector and the muon spectrometer, and are required to have $p_T > 10$ GeV and $|\eta| < 2.4$. Muon candidates must satisfy the ‘‘Medium’’ identification criterion [49]. An isolation requirement based on the momentum of the tracks and the calorimeter energy around each lepton candidate is imposed to distinguish between leptons coming from the decay of a Z boson and those from nonprompt sources [48,49]. Additionally, all lepton candidates are required to be consistent with the primary vertex, chosen as the reconstructed vertex with the highest sum of the p_T^2 of its associated tracks.

Jets are reconstructed from three-dimensional topological energy clusters [50] in the calorimeter using the anti- k_t jet algorithm [51] implemented in the FastJet package [52] with a radius parameter of 0.4. Jets are calibrated using energy- and η -dependent corrections [53] and are required to have $p_T > 20$ GeV and $|\eta| < 2.5$. Events containing jets arising from noncollision sources or detector noise are removed [54]. Finally, a track-based criterion, the jet vertex tagger (JVT), is used to reduce contributions from jets arising from pileup [55]. In the region $|\eta| < 2.5$, jets are tagged as containing b -hadrons using a multivariate discriminant (MV2) score [56]. The MV2 score is obtained from a boosted decision tree (BDT) that combines several algorithms that identify tracks with large impact parameters, secondary vertices, and the topological structure of weak b - and c -hadron decays inside jets. The BDT was trained using jets reconstructed with the anti- k_t algorithm with a radius parameter $R = 0.4$ from $t\bar{t}$ simulated events to discriminate b jets from c jets and light-flavor jets [57]. In this search, the same BDT is used with a novel strategy described in Sec. VA.

V. IDENTIFICATION OF LOW-MASS RESONANCES DECAYING INTO b -QUARK PAIRS

A. Reconstruction and identification of $a \rightarrow b\bar{b}$ decays

For low-mass a bosons, the b quarks from a -boson decay tend to have small angular separation ΔR and can be reconstructed either as a single jet or as multiple jets in the calorimeter depending on their angular separation and the clustering algorithm used. In order to include both cases, all calibrated jets reconstructed using the anti- k_t jet algorithm with radius parameter $R = 0.4$ and $p_T > 20$ GeV are clustered again, using an anti- k_t algorithm with radius parameter $R = 0.8$ [58]. The radius parameter was chosen

to optimize the signal acceptance in the mass range considered. Each $R = 0.8$ jet is considered as a reconstructed $a \rightarrow b\bar{b}$ candidate. The $R = 0.8$ jet will often contain a single anti- k_t constituent jet with radius parameter $R = 0.4$ when the angular separation ΔR between the b quarks from the $a \rightarrow b\bar{b}$ decay is less than 0.4. The four-momentum of an $a \rightarrow b\bar{b}$ candidate is the sum of all four-momenta of the set of constituent $R = 0.4$ jets. Since the $R = 0.4$ constituent jets are calibrated, no additional momentum calibration is necessary.

The hadronization of the two b quarks which come from an a -boson decay is identified using variables sensitive to the number of b hadrons and the mass of the a boson. The values of these variables are calculated using tracks with $p_T > 0.4$ GeV matched to the reconstructed $a \rightarrow b\bar{b}$ candidate. The matching is performed using the ghost-association method [59], which treats the tracks as four-vectors of infinitesimal magnitude during the jet reconstruction and assigns them to the $a \rightarrow b\bar{b}$ candidate with which they are clustered. Tracks from the hadronization of different b quarks are separated by splitting the set of tracks matched to an $a \rightarrow b\bar{b}$ candidate into multiple track jets. Ideally, the decay of each b quark should be associated with a different track jet. In this search, the track jets are reconstructed by clustering all matched tracks using an exclusive- k_t algorithm that produces either two ($\text{Ex}k_t^{(2)}$) or three ($\text{Ex}k_t^{(3)}$) final jets [60]. The exclusive- k_t algorithm implements a sequential clustering in which the two tracks with the smallest k_t distance, defined as the product of the minimum p_T of the two tracks and their distance ΔR , are clustered together if this distance is smaller than the transverse momentum of all tracks. If two tracks are clustered together, their momenta are summed and the two are considered as a single object in the next iteration of the sequential clustering. If the transverse momentum of a track is smaller than all k_t distances, the track is discarded. Tracks clustered together are considered a final-state track jet. The sequential clustering is interrupted after the step in which all the tracks have been clustered in the desired number of final-state track jets [61]. The splitting into three final jets attempts to capture cases where significant additional radiation is present. The strategy presented here to identify the two b -quark flight directions as different track jets differs from the method documented in Ref. [62], where the inclusive version of the anti- k_t algorithm is used. At low a -boson momenta, the exclusive- k_t algorithm is able to identify the two b -quark flight directions in separate track jets more often than the inclusive anti- k_t algorithm. For a simulated signal event sample with $m_a = 20$ GeV, the inclusive anti- k_t algorithm associates the b -quark flight directions with different track jets in 46% of cases. In contrast, the flight directions are associated with different exclusive- k_t track jets in nearly 100% of cases.

The variables used for the $a \rightarrow b\bar{b}$ identification are calculated using the exclusive- k_t track jets. For the track jets

calculated with the $\text{Ex}k_t^{(2)}$ algorithm, the variables used are the MV2 scores of the two track jets, as well as their angular separation ΔR and their p_T asymmetry, defined as $(p_{T1} - p_{T2}) / (p_{T1} + p_{T2})$. For $\text{Ex}k_t^{(3)}$ track jets, the same variables are used, but they are calculated with the two track jets with highest and lowest MV2 scores among the three track jets. The eight variables are used simultaneously. The MV2 scores identify the presence of a b hadron in the track jets. Track jets with large ΔR separation occur in the decay of a massive state. Track jets with very large p_T asymmetry can arise from final-state radiation. The variables calculated with $\text{Ex}k_t^{(2)}$ track jets provide most of the discriminating power between signal and background, while the variables calculated in $\text{Ex}k_t^{(3)}$ help disentangle cases where $\text{Ex}k_t^{(2)}$ would fail to identify the flight direction of the $a \rightarrow b\bar{b}$ decay products.

A BDT is trained with these variables to obtain an efficient identification criterion that distinguishes $a \rightarrow b\bar{b}$ candidates in signal events that have two b quarks produced in the decay of a low-mass resonance, from those in top-quark pair events that contain a single b -quark decay. A sample of simulated SM $t\bar{t}$ events is used as a source of $a \rightarrow b\bar{b}$ candidates with a single b -quark decay, while a simulated signal event sample with $m_a = 20$ GeV is used as a source of $a \rightarrow b\bar{b}$ candidates with two b -quark decays. The transverse momentum and angular distributions are not included as inputs for the BDT training, but the differences in these distributions among signal and background are partially taken into account since they are correlated with other variables. In order to classify the b -quark multiplicity of an $a \rightarrow b\bar{b}$ candidate, b hadrons in the simulation of the b -quark hadronization with $p_T > 5$ GeV are matched to the candidates using the same ghost-association method as described above. Figure 2 shows the predicted score and efficiency for signal and background events using the trained BDT. The BDT discriminator is also efficient in rejecting events without b quarks, even if such a sample was not explicitly included in the BDT training. Two event categories based on the BDT score are defined for the analysis using a tight and a loose working point (WP). A high-purity category (HPC) for $a \rightarrow b\bar{b}$ candidates is selected by requiring a BDT score larger than the tight WP, while a low-purity category (LPC) is selected from candidates with a BDT score between the loose and the tight WPs. The tight WP is defined by a BDT score of 0.3 while the loose WP is defined by a BDT score of 0.1. The tight WP is chosen such that it provides a background rejection 1/100 in order to reduce the backgrounds from Z + jets and $t\bar{t}$ events. The LPC contains a relatively large number of events from processes with zero or one b quark and is used to select background-enriched samples in the search. Reconstructed $a \rightarrow b\bar{b}$ candidates in the LPC and HPC are defined as identified $a \rightarrow b\bar{b}$ candidates and are used in this search. The signal efficiency of the two WPs vary with the mass of the a boson since mass-dependent variables are used in the training.

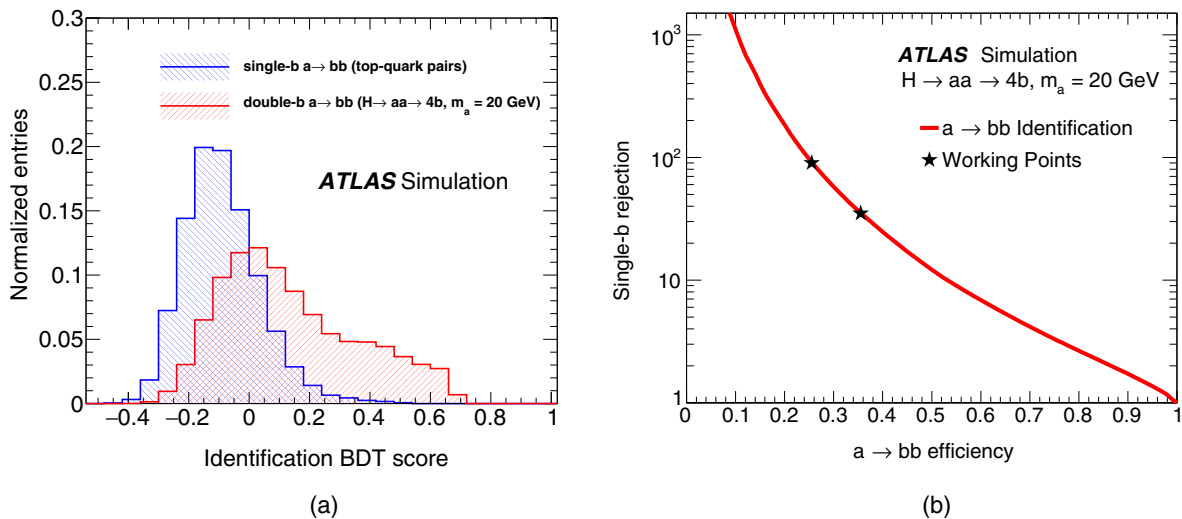


FIG. 2. (a) Identification BDT score distributions for signal and background $a \rightarrow b\bar{b}$ candidates and (b) signal efficiency as a function of the inverse of the $t\bar{t}$ background efficiency (rejection). For the signal $H \rightarrow aa \rightarrow (b\bar{b})(b\bar{b})$ sample with $m_a = 20$ GeV, both b quarks are required to lie within the reconstructed candidate, while for the background $t\bar{t}$ sample the reconstructed candidate contains a single b quark. In panel (b), the left and right stars indicate the tight and the loose WPs, respectively, which are used to define, as described in the text, the HPC and LPC.

The efficiency of the $a \rightarrow b\bar{b}$ identification is measured in data by selecting a multijet sample enriched in gluon decays into b quarks, $g \rightarrow b\bar{b}$. In order to measure the efficiency of the identification criterion for both signal and background, $a \rightarrow b\bar{b}$ candidates are categorized according to the flavor of the track jets that are reconstructed with the $\text{Ex}k_t^{(2)}$ algorithm, while the $\text{Ex}k_t^{(3)}$ track jets are used exclusively for identification purposes. All b and c hadrons present in the event simulation with $p_T > 5$ GeV are matched to the track jets using the ghost-association method. The track jets are assigned different flavor tags B, C, or L (light flavor) as follows. If a track jet has at least one simulated b hadron matched to it, it is classified as B. If it does not contain a simulated b hadron, but has a simulated c hadron matched to it, it is classified as C. Otherwise it is classified as L. The flavor of an $a \rightarrow b\bar{b}$ candidate is determined by the flavor of the two $\text{Ex}k_t^{(2)}$ jets. Most signal $a \rightarrow b\bar{b}$ candidates are BB candidates, while most background candidates are BL candidates. A signal candidate can be classified as BL when the two b quarks decay inside the same track jet or when they have $p_T \leq 5$ GeV. The identification efficiencies for BB and BL $a \rightarrow b\bar{b}$ candidates are measured separately in data for three transverse momentum ranges: $30 \text{ GeV} \leq p_T^{a \rightarrow b\bar{b}} < 90 \text{ GeV}$, $90 \text{ GeV} \leq p_T^{a \rightarrow b\bar{b}} < 140 \text{ GeV}$, and $p_T^{a \rightarrow b\bar{b}} \geq 140 \text{ GeV}$. These three ranges were chosen based on the $p_T^{a \rightarrow b\bar{b}}$ spectrum in signal samples and on the number of events in the multijet data sample used for the efficiency measurement. The complete procedure described below is applied independently in each transverse momentum range.

B. Efficiency measurement of $a \rightarrow b\bar{b}$ identification

The strategy for the efficiency measurement in data closely follows that used in the measurement of the

identification efficiency for boosted 125 GeV Higgs boson decays into a pair of b quarks [62]. A multijet sample is selected from a suite of single-jet triggers that differ by their jet p_T threshold. Only a small fraction of the events identified by the triggers with low p_T threshold are recorded. The choice of which jet events to keep is random and results in an effective integrated luminosity smaller than the total recorded by the ATLAS experiment, but does not introduce any selection bias. The fraction of events kept is known as the trigger prescale fraction. Triggers with a prescale fraction less than one are called prescaled triggers. The lowest jet p_T threshold for which all events are kept is 300 GeV. When comparing events recorded with prescaled and unprescaled triggers, each event is weighted by the inverse of the prescale fraction of the corresponding trigger used to record it.

The $a \rightarrow b\bar{b}$ reconstruction described in Sec. VA is applied to the multijet sample. The events recorded by the multijet triggers are dominated by LL candidates. Since muons are often produced in semileptonic decays of b hadrons, a sample with a larger fraction of BB and BL candidates is selected by requiring exactly one muon matched to one of the $\text{Ex}k_t^{(2)}$ track jets. The track jet matched to the muon is called the muon-matched track jet, while the other one is called the non-muon-matched track jet. The selected events are compared with simulated multijet events. In order to account for possible mismodeling of the flavor fractions in simulation relative to those in data, a correction is applied to the simulated event sample. The correction is described in detail in Ref. [62] and only a brief summary is given here. The simulated jet sample is split into subsamples depending on the flavor classification of the $a \rightarrow b\bar{b}$ candidate: BB, BL, CC, CL, and LL. The selected BC fraction in the multijet sample is negligible.

The fraction of each subsample is corrected by fitting the distribution of the signed transverse impact parameter significance $S_{d0}^{\text{jet}} = d_0/\sigma(d_0)$ of the two $\text{Ex}k_t^{(2)}$ track jets to data. The S_{d0}^{jet} of a track jet is defined as the average of the three largest signed transverse impact parameter significances S_{d0}^{trk} of its constituent tracks, since this observable is used to identify the long lifetime of b and c hadrons. The average is used to minimize the impact of misreconstructed tracks on this observable. The track impact parameter d_0^{trk} is calculated using the vector from the primary vertex to the point of closest approach of the track. The absolute value of d_0^{trk} is the norm of the projection of this vector in the transverse plane, while the sign depends on the angle between this vector and the track jet \vec{p}_T . If this angle is less than $\pi/2$, d_0^{trk} is taken as positive. For angles larger than $\pi/2$, the track impact parameter is considered negative. Large negative impact parameters are often obtained from interactions with the detector material and not from a long-lived b - or c -hadron decay, since the direction of the decay is not correlated with the jet axis.

A total of four flavor correction factors that scale the BB, BL, CC, and CL subsamples are determined from a Poisson likelihood fit to data. The scale parameter for the LL subsample is determined implicitly by requiring that the total number of candidates in simulation is the same as in data. The covariance matrix of these four parameters is determined from the statistical uncertainties and correlations, but also from the limited knowledge of the jet energy scale, and from the uncertainty in the impact parameter resolution following the method described in Ref. [62]. Figure 3 shows the result of this fit to data for the transverse momentum range $30 \text{ GeV} \leq p_T^{a \rightarrow b\bar{b}} < 90 \text{ GeV}$.

After the flavor correction is applied, the $a \rightarrow b\bar{b}$ identification BDT is used to select events in both the HPC and LPC. Once the identification criteria are used, only the BB and the BL subsamples contribute significantly. Any residual disagreement in these regions is the result of a difference in the $a \rightarrow b\bar{b}$ identification efficiency between data and simulation. A scale factor (SF) is defined as the ratio of the two efficiencies, $\text{SF} = \varepsilon_{\text{DATA}}/\varepsilon_{\text{MC}}$, for each flavor subsample. Only the BB and BL SFs are measured for both the HPC and LPC. All other flavors are subleading after applying the identification criterion, and for these the efficiency in data is considered the same as in simulation. In order to measure the BB and BL SFs, in both the HPC and LPC, a second Poisson likelihood fit of the S_{d0}^{jet} distribution to data is performed after using the identification BDT to select events in both simulation and data. The four SFs measured in each of the three $p_T^{a \rightarrow b\bar{b}}$ ranges constitute 12 parameters in total. The complete list of uncertainties is described in Sec. V C. Figure 4 shows the measured efficiencies in both data and simulation, for BB and BL candidates. The bottom panel in the same figure shows the SF as defined above.

C. Systematic uncertainties in the $a \rightarrow b\bar{b}$ identification

Several sources of uncertainty are considered when building the covariance matrix of the 12 SFs. The statistical uncertainties and correlations are interpreted directly from the likelihood fit to data. The impact of systematic uncertainties is considered by varying the appropriate quantity in the simulated event samples within $\pm 1\sigma$ for each source separately. The impact of each systematic

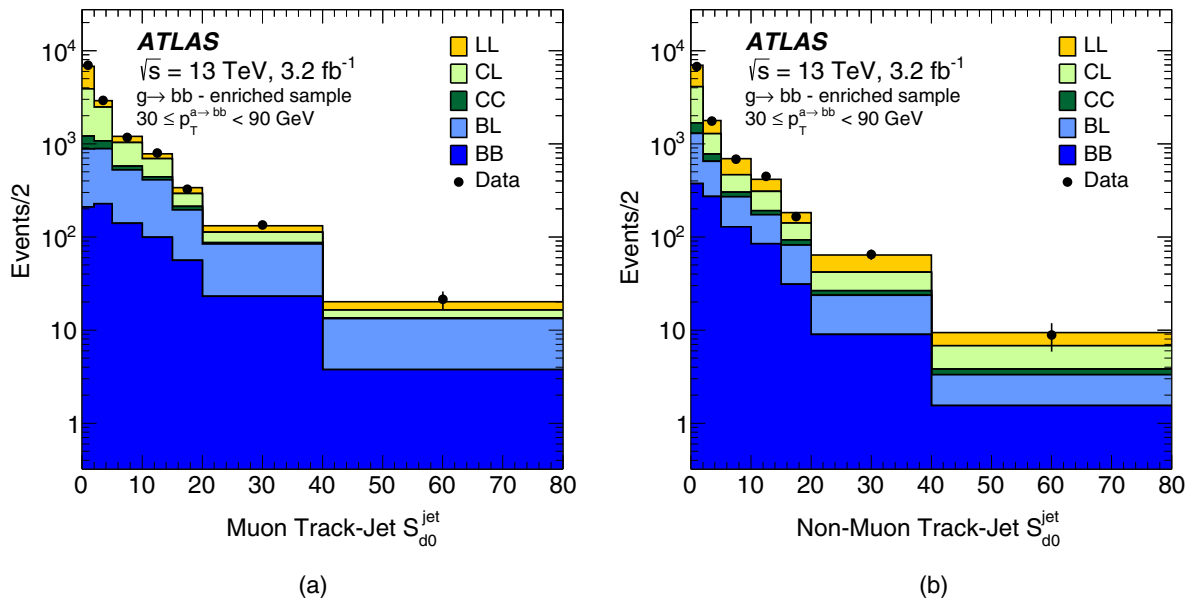


FIG. 3. Averaged signed impact parameter significance S_{d0}^{jet} distributions of the track jet (a) with a muon inside and (b) without a muon, after performing the fit of the flavor fractions to data. The total simulation yield is scaled to the same number of events observed in data. The fit is performed separately in $p_T^{a \rightarrow b\bar{b}}$ ranges. The figure shows the $30 \text{ GeV} \leq p_T^{a \rightarrow b\bar{b}} < 90 \text{ GeV}$ range of $a \rightarrow b\bar{b}$ candidates.

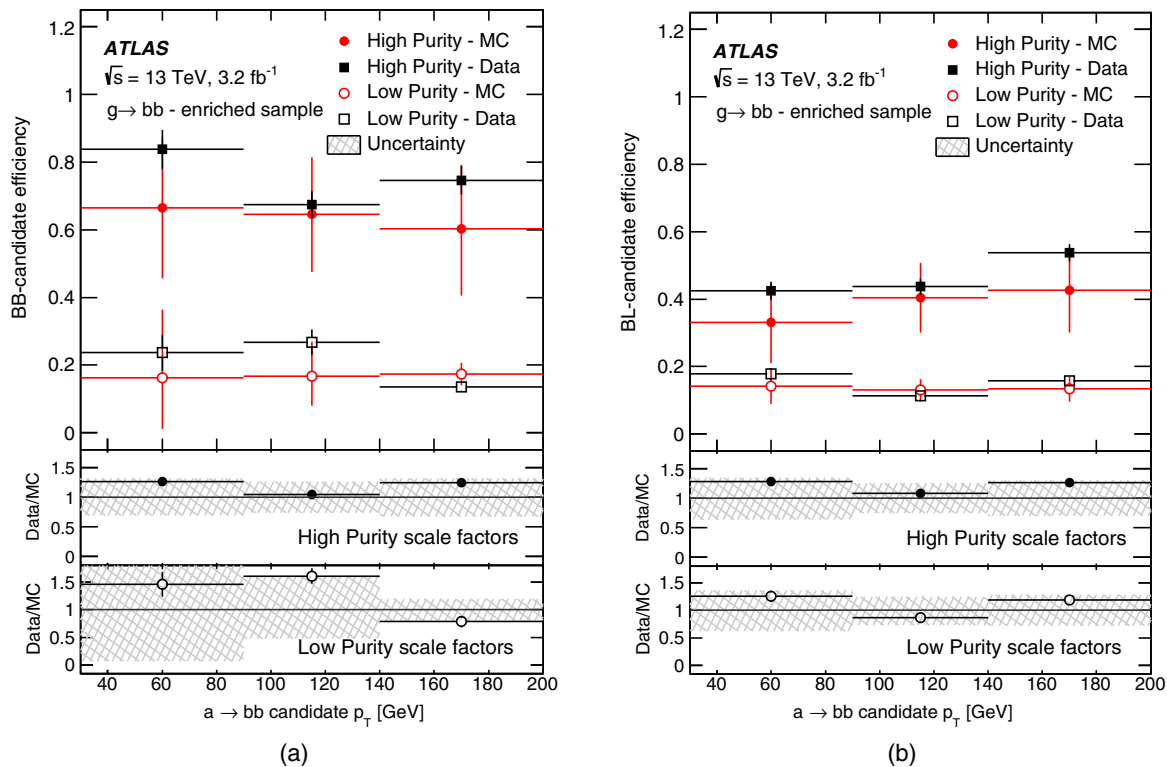


FIG. 4. Efficiency of the $a \rightarrow b\bar{b}$ identification criteria measured in data and simulated multijet events. The efficiency is measured in three transverse momentum ranges, separately for (a) BB and (b) BL candidates in both the HPC and LPC. The ratio of the measured values in data and simulation (bottom panels) are SFs used in the analysis when comparing simulation with data. The error bars in the top panels are statistical only, while the hashed bands on the ratios in the bottom panels include the full systematic uncertainties.

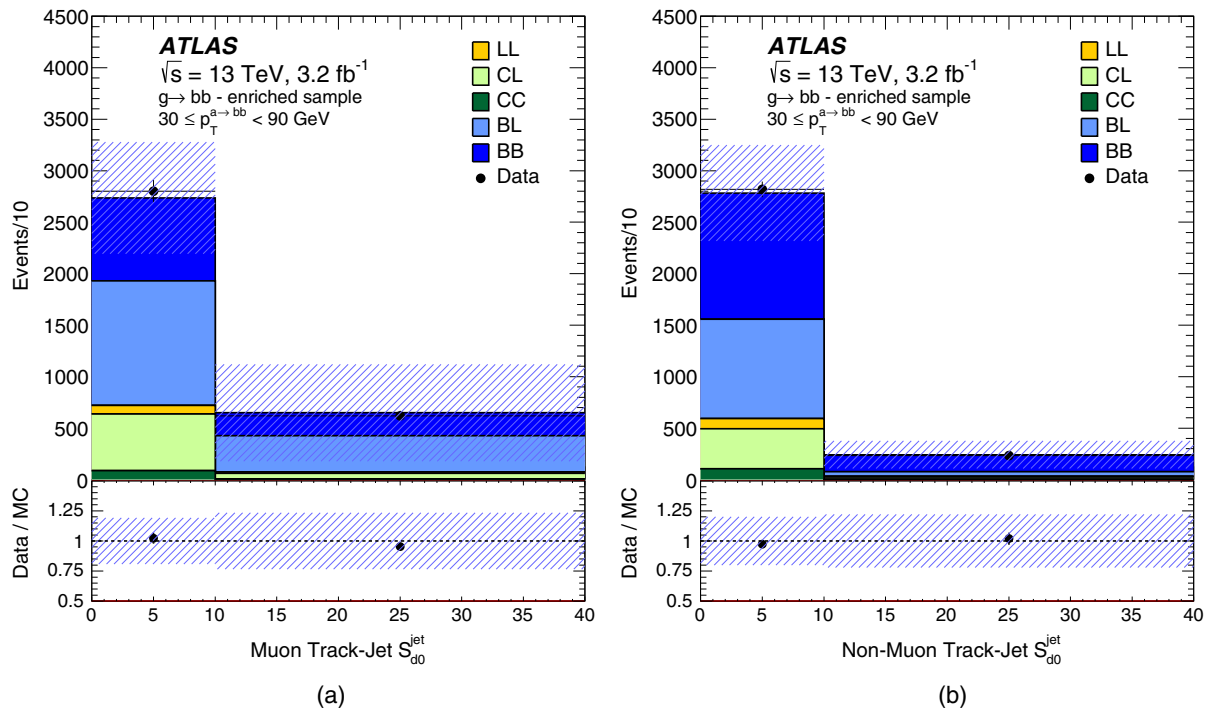


FIG. 5. Averaged signed impact parameter significance S_{d0}^{jet} distributions of the track jet (a) with a muon inside and (b) without a muon, in the $30 \text{ GeV} \leq p_T^{a \rightarrow b\bar{b}} < 90 \text{ GeV}$ range of $a \rightarrow b\bar{b}$ candidates in the HPC. The hashed area represents the total uncertainty in the predicted yields.

uncertainty is assessed as the difference in the measured SF when fitting the nominal sample and the one with the corresponding source variation. The covariance matrix from the four flavor-fraction corrections described in Sec. VB is propagated to the SF covariance matrix. The impact of the limited knowledge of the jet energy scale is, once again, considered in the covariance matrix. The uncertainty arising from the choice of hadronization model is included through its effect on the MV2 scores and propagated to the SF covariance matrix. This uncertainty changes the MV2 score by 5–10% depending on the track jet p_T [63] and has a minor impact on the SFs.

Two additional sources of uncertainty are considered. First, there is a possible mismodeling of the efficiency for candidates with flavors other than BB or BL. These components are highly suppressed by the BDT selection. An uncertainty of 50% in the efficiency of other flavor components is propagated to the covariance matrix, with negligible impact. The chosen value of 50% is based on the level of agreement between the S_{d0}^{jet} distribution in data and simulation, after the BDT criteria are applied, but before the SF fit. Second, there is a possible bias from the selection of $a \rightarrow b\bar{b}$ candidates with muons. In order to assess it, the measurement is repeated by selecting $a \rightarrow b\bar{b}$ candidates with two muons, one inside each track jet, and comparing the result with the one obtained above. The sample with two muons contains a negligible number of BL candidates and it is only possible to measure the BB SFs. The difference between the SF measured with the one-muon sample and the one measured with the two-muon sample is taken as an estimate of the systematic uncertainty due to a possible bias in the procedure. The same uncertainty is applied to the BL SFs. This uncertainty varies in each $p_T^{a \rightarrow b\bar{b}}$ range, but it is approximately 20% and is the dominant uncertainty in the p_T ranges with a large number of candidates. Figure 5 shows the S_{d0}^{jet} distribution in the $30 \text{ GeV} \leq p_T^{a \rightarrow b\bar{b}} < 90 \text{ GeV}$ range, for the HPC, after fitting for both the BB and BL SFs and including all the uncertainties described here.

These SFs are used when comparing simulated signal and background events with data. For the selected background events, the distributions of the variables used for the $a \rightarrow b\bar{b}$ identification are similar to the ones in $g \rightarrow b\bar{b}$ events. However, for the signal, due to the nonzero mass of the a boson, the distributions can be quite different, especially for the variables that are sensitive to the mass of the particle. The method presented here relies on the fact that any residual disagreement accounted for by the SFs is independent of the a -boson mass. In order to test this hypothesis, the efficiency measurement is repeated replacing data with a pseudodata built using the same multijet simulated sample used to obtain the S_{d0}^{jet} templates but where gluons were replaced by a spin-0 a boson with mass $m_a = 20 \text{ GeV}$ before the decay to two b quarks. Figure 6 shows the results of using this pseudodata in each of the

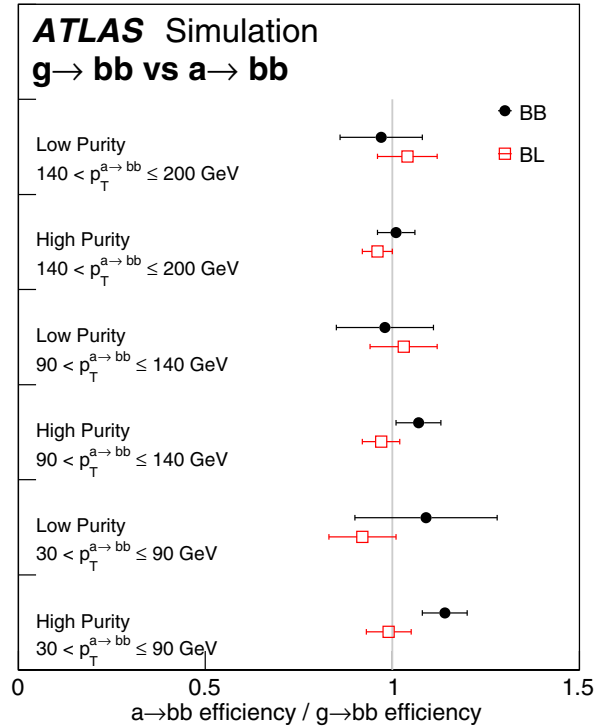


FIG. 6. Efficiency measured using a simulated multijet pseudodata where $g \rightarrow b\bar{b}$ decays are replaced by $a \rightarrow b\bar{b}$ decays with mass $m_a = 20 \text{ GeV}$. The efficiency is measured separately for BB and BL samples in the same p_T ranges used in the data-to-simulation SF measurement. The values can be interpreted as the ratio between the SFs for a particle with mass $m_a = 20 \text{ GeV}$ and the ones for a massless gluon. Only the statistical uncertainties are indicated.

categories considered above, which can be interpreted as the ratio between the SF for a particle with mass $m_a = 20 \text{ GeV}$ and the one for a massless gluon. The overall distribution is consistent with unity within the statistical uncertainty of the simulated event sample.

VI. ANALYSIS STRATEGY

The analysis strategy targets events where a Higgs boson is produced in association with a Z boson. The candidate events are required to be consistent with a ZH event, where the Z boson decays into electrons or muons and the Higgs boson decays into two a bosons each of which decays into a b -quark pair. Events are selected using triggers that require at least one electron or muon. The event is further required to have two oppositely charged electrons or two oppositely charged muons and two reconstructed $a \rightarrow b\bar{b}$ candidates. The leading electron or muon is required to have $p_T > 27 \text{ GeV}$ and be matched to the lepton candidate reconstructed by the trigger algorithms. The lepton momentum requirement and trigger matching are used so that all events have at least one lepton with p_T above the trigger thresholds. The dilepton mass must be consistent with the

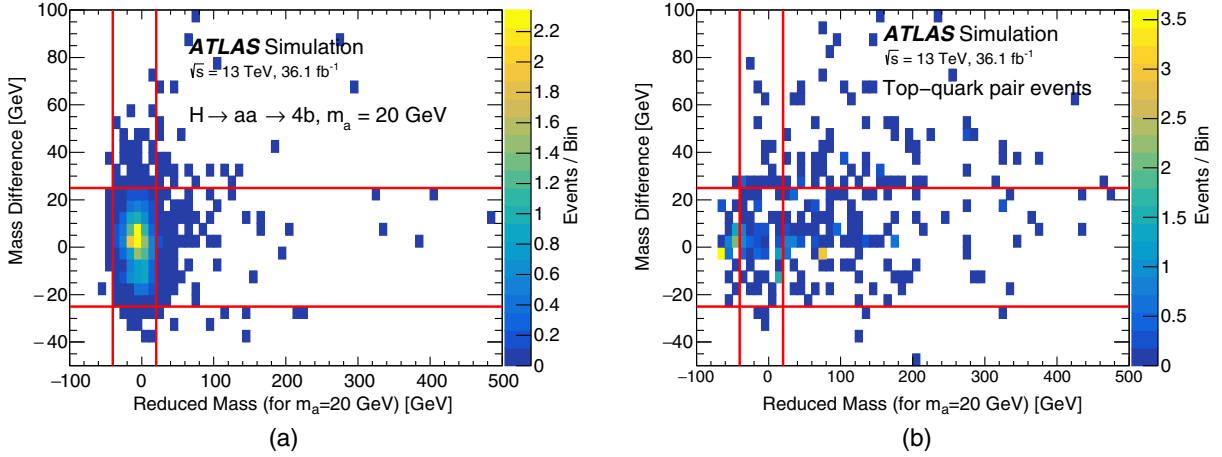


FIG. 7. Distribution of (a) expected signal events and (b) top-quark pair background in a plane defined by the two mass requirements described in the text, m_{red} and $\Delta m^{a \rightarrow b\bar{b}}$. The mass requirements aim at selecting events where the two $a \rightarrow b\bar{b}$ candidates have similar reconstructed masses and the mass of the pair of $a \rightarrow b\bar{b}$ candidates is consistent with the Higgs boson mass. The signal events correspond to ZH , $H \rightarrow aa \rightarrow (b\bar{b})(b\bar{b})$ with $m_a = 20$ GeV and are normalized to the SM $pp \rightarrow ZH$ cross section.

Z-boson mass and is required to be in the range $85 \text{ GeV} < m_{\ell\ell} < 100 \text{ GeV}$. Both $a \rightarrow b\bar{b}$ candidates are required to satisfy $p_T > 30 \text{ GeV}$ and $|\eta| < 2.0$.

Two mass requirements are imposed to select events consistent with a cascade decay $H \rightarrow aa \rightarrow (b\bar{b})(b\bar{b})$. First, the mass difference $\Delta m^{a \rightarrow b\bar{b}} = m^{a_1} - m^{a_2}$ between the two $a \rightarrow b\bar{b}$ candidates is required to satisfy $-25 \text{ GeV} < \Delta m^{a \rightarrow b\bar{b}} < 25 \text{ GeV}$. The ordering of $a \rightarrow b\bar{b}$ candidates is based on their transverse momenta, with a_1 corresponding to the higher- p_T $a \rightarrow b\bar{b}$ candidate. Second, the mass of the pair of $a \rightarrow b\bar{b}$ candidates is required to be consistent with the Higgs boson mass. The compatibility is assessed with the reduced mass:

$$m_{\text{red}} = (m^{a_1, a_2} - m_H) - (m^{a_1} + m^{a_2} - 2m_a),$$

which probes the difference between the invariant mass of the two $a \rightarrow b\bar{b}$ candidates, m^{a_1, a_2} , and the Higgs boson mass $m_H = 125 \text{ GeV}$. It should be noted that m_a is the mass hypothesis for the a boson.

The reduced mass is required to satisfy $-40 \text{ GeV} < m_{\text{red}} < 20 \text{ GeV}$, ensuring that the selection is highly efficient. The presence of m_a in the event selection means that different events are used to search for different mass hypotheses. No conditions on the individual values of m^{a_1} and m^{a_2} are imposed. The selected mass window, as a function of mass difference and reduced mass, is shown in Fig. 7 for signal events with $m_a = 20 \text{ GeV}$ and top-quark pair events.

Two signal-enriched regions are defined for this search. One requires the two reconstructed $a \rightarrow b\bar{b}$ candidates to be identified in the HPC, while the other requires one $a \rightarrow b\bar{b}$ candidate identified in the HPC and one in the LPC. The two main sources of background for this search are top-quark pair and Z-boson events produced in association with

additional quarks or gluons. In this search, the normalizations of these two backgrounds are measured in dedicated control regions which are selected to be enriched in the specific background. Three regions dominated by top-quark pair events are selected by requiring the dilepton mass to be outside the Z-boson mass window, i.e., $m_{\ell\ell} \leq 85 \text{ GeV}$ or $m_{\ell\ell} \geq 100 \text{ GeV}$. These three control regions differ by the identification of the two $a \rightarrow b\bar{b}$ candidates, with one requiring both to be in the HPC, a second requiring one $a \rightarrow b\bar{b}$ candidate in the HPC and one in

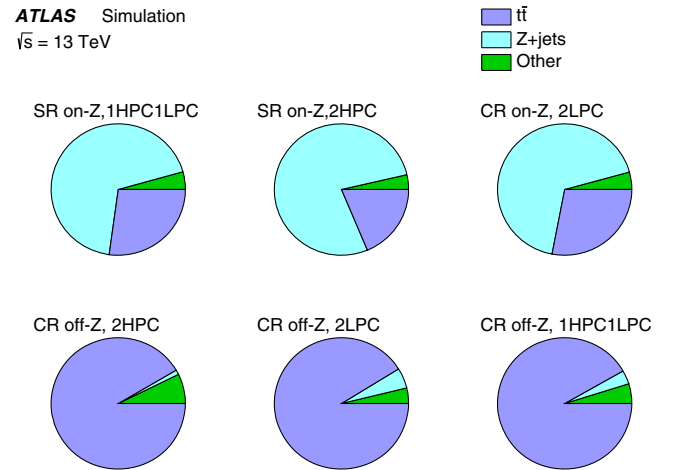


FIG. 8. Expected composition of events in each signal region (SR) and control region (CR) defined for the search. CRs have a negligible expected yield for the signal. Definitions of the regions are based on the dilepton mass and the purity of the two $a \rightarrow b\bar{b}$ candidates. Regions labeled “on-Z” require the dilepton mass to be in the range $85 \text{ GeV} < m_{\ell\ell} < 100 \text{ GeV}$, while regions “off-Z” require the dilepton mass to be outside this window. For $a \rightarrow b\bar{b}$ candidates, the HPC and LPC are defined using ranges of the identification BDT score, as described in Sec. V.

the LPC and, finally, the third requiring the two $a \rightarrow b\bar{b}$ candidates to be identified in the LPC. The three control regions probe $t\bar{t}$ events produced in association with different numbers of heavy-flavor jets. A dedicated control region for Z -boson events is formed by requiring the dilepton mass to be consistent with the Z -boson mass and the two $a \rightarrow b\bar{b}$ candidates in the LPC. Figure 8 shows the expected background yield fractions in each of the regions described here.

VII. SYSTEMATIC UNCERTAINTIES

Several sources of systematic uncertainty are considered. The identification efficiency for leptons is measured in Z -boson data events using a tag-and-probe method [47,49]. Small residual disagreements between efficiencies in simulation and those measured in data are corrected as a function of the lepton p_T and η . The uncertainties in these corrections are propagated through this search. Uncertainties in the lepton momentum scale and resolution are similarly considered.

Uncertainties associated with jets arise from their reconstruction and identification efficiencies. These are due to the uncertainty in the jet energy scale (JES), mass scale, energy resolution and the efficiency of the JVT requirement that is meant to remove jets from pileup. The JES and its uncertainty are derived by combining information from test-beam data, LHC collision data and simulation [53].

The identification efficiency for $a \rightarrow b\bar{b}$ candidates in simulation is also corrected by using the SFs measured with the methods described in Sec. V. The full covariance matrix for the 12 SFs is propagated after diagonalization in order to obtain uncorrelated sources of systematic uncertainty. Only $a \rightarrow b\bar{b}$ candidates with BB and BL flavors have their identification efficiency corrected in simulation. Candidates with flavors other than BB and BL represent a subleading fraction of candidates selected in this analysis, mostly from BC candidates. In this case, an uncertainty of 50% per candidate is applied, similarly to the uncertainty used when measuring the identification efficiency.

Several sources of systematic uncertainty affecting the modeling of the relative normalization of the background sources in control and signal regions are considered. Since the $Z + \text{jets}$ background normalization is measured in a region with two $a \rightarrow b\bar{b}$ candidates in the LPC, where a larger fraction of the candidates do not contain two b quarks, an uncertainty of 50% in the fraction of events which have two or more associated b hadrons is applied. This uncertainty is derived by comparing the level of agreement between data and simulation for $m_{\text{red}} < -40$ GeV calculated with $m_a = 20$ GeV. Similarly, for the top-quark pair background, three uncorrelated relative uncertainties of 50% are assigned to events with one associated b hadron, to events with two or more associated b hadrons, and to events with associated c hadrons. The number of associated hadrons in each event is determined following the procedure described in Ref. [64]. These

uncertainties are derived from a comparison of the $t\bar{t} + \text{heavy-flavor}$ production cross sections predicted by POWHEG+PYTHIA and by SHERPA+OPENLOOPS at NLO [64].

Beyond the uncertainties associated with heavy-flavor fractions, several sources of systematic uncertainty affecting the relative normalization between control and signal regions are considered. The procedure closely follows the description in Ref. [17]. For the $t\bar{t}$ background, it includes systematic uncertainties from variations of the factorization and renormalization scales, the PDF set used for simulation, α_s , the value of the top-quark mass, the choice of generator, the choice of parton shower and hadronization models, and the effects of initial- and final-state radiation. For the $Z + \text{jets}$ backgrounds, additional relative uncertainties are based on variations of the factorization and renormalization scales and of the parameters used in matching the matrix element to the parton showers in the SHERPA simulation.

Uncertainties in secondary background sources are also considered, affecting their normalization in both the signal and control regions. A 50% normalization uncertainty in the diboson background is assumed [65]. The uncertainties in the $t\bar{t}W$ and $t\bar{t}Z$ NLO cross-section predictions are 13% and 12%, respectively [66,67], and are treated as uncorrelated between the two processes. An additional modeling uncertainty for $t\bar{t}W$ and $t\bar{t}Z$, related to the choice of event generator, parton shower and hadronization models, is derived from comparisons of the nominal samples with alternative ones generated with SHERPA.

Several sources of systematic uncertainty affect the theoretical modeling of the signal. Uncertainties originate from the choice of PDFs, the factorization and renormalization scales, and the parton shower, hadronization and underlying-event models. The combined uncertainty in the expected signal yield from these sources is approximately 8%. Higher-order corrections to the decay of the a boson are small compared to the Higgs boson production uncertainties and, therefore, no additional uncertainty is included.

VIII. RESULTS

The results are obtained from a binned maximum-likelihood fit to the data using the two signal regions and four control regions. The likelihood function is constructed from the product of Poisson probabilities in each region. The parameter of interest (POI) scales the signal $H \rightarrow aa \rightarrow (b\bar{b})(b\bar{b})$ yield. The overall normalizations of the $Z + \text{jets}$ and $t\bar{t}$ backgrounds are modeled as unconstrained nuisance parameters. Simulation is used to determine the relative yields of $Z + \text{jets}$ and $t\bar{t}$ backgrounds in each signal and control region. Systematic uncertainties described in Sec. VII are incorporated as nuisance parameters with Gaussian priors with a standard deviation equal to the value of the uncertainty, and these nuisance parameters multiply the product of Poisson probabilities. Uncertainties arising from the finite number of simulated

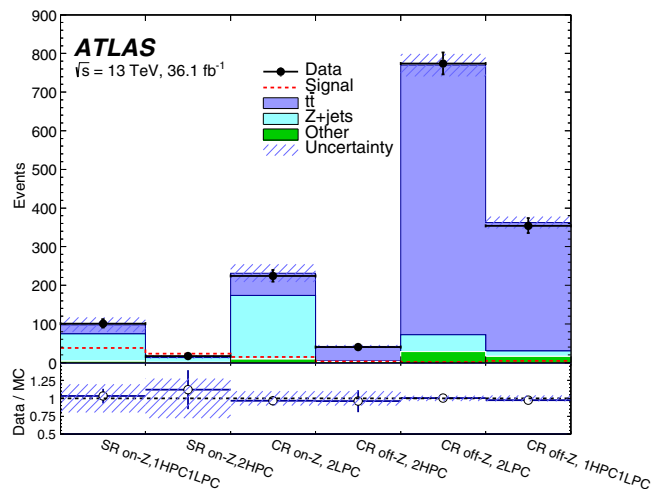


FIG. 9. Expected yields for the different background components in each signal region (SR) and control region (CR) after the profile likelihood fit to data. The expected yield for signal with $m_a = 20$ GeV is calculated before the profile likelihood fit and normalized to the observed limit in the cross section times the branching ratio for $ZH, H \rightarrow aa \rightarrow (b\bar{b})(b\bar{b})$. The data observed in each region is included for comparison. The hashed area represents the total uncertainty in the background.

events are modeled using gamma distribution priors [68]. Gamma distributions are used as a generalization of the Poisson distribution since the expected yield predicted in simulated event samples may not be an integer number. Figure 9 and Table I show a comparison of data and simulation when the nuisance parameters have the values that maximize the likelihood function and only the SM background processes are considered, i.e., the POI is fixed at zero. The data in all regions agrees with the prediction within one standard deviation.

Limits on the production cross section of $ZH, H \rightarrow aa \rightarrow (b\bar{b})(b\bar{b})$ events are calculated using the test statistic $t_\mu = -2 \ln(\mathcal{L}(\mu, \hat{\theta}_\mu) / \mathcal{L}(\hat{\mu}, \hat{\theta}))$, where \mathcal{L} is the likelihood described above, μ is the single POI and θ is the vector of nuisance parameters (NPs). In addition, $\hat{\mu}$ and $\hat{\theta}$ are the values which maximize the likelihood function, and $\hat{\theta}_\mu$ are

the values of the NPs which maximize the likelihood function for a given value of μ [17]. Upper limits at 95% C.L. on the production cross section as a function of the mass hypothesis are determined using the asymptotic distribution for t_μ [69–71].

The impact of systematic uncertainties on the upper limits is evaluated by varying the corresponding NP when building the Asimov data set [69] used to estimate the asymptotic distribution for t_μ . The NPs are varied by the value of their uncertainties in the fit performed to obtain $\mathcal{L}(\hat{\mu}, \hat{\theta})$. In order to partially account for the correlation between the fitted values of the NPs, the variations are performed after diagonalizing the correlation matrix obtained in the same fit. The diagonalization is performed in blocks of NPs that share a similar origin and that may have large correlations. The impact is defined as the relative variation of the expected upper limit when the modified asymptotic distribution is used. Variations in each block are summed in quadrature and the results are shown in Table II. The number of events in each of the four control regions is the main factor in determining the impact from the unconstrained nuisance parameters that model the normalization of the $Z + \text{jets}$ and $t\bar{t}$ backgrounds and, therefore, their values are highly correlated. Since they are individually important for the modeling of the background yields, their impacts are reported separately. A correlation of 44% is observed between the two unconstrained nuisance parameters. The impact of the statistical uncertainty is defined as the 1σ uncertainty in the expected upper limit after removing all nuisance parameters, both constrained and unconstrained, from the profile likelihood.

Figure 10 shows the exclusion limits for the production cross section times the branching ratio for $ZH, H \rightarrow aa \rightarrow (b\bar{b})(b\bar{b})$ as a function of the a -boson mass hypothesis. For comparison, the SM next-to-NLO (NNLO) cross section for $pp \rightarrow ZH$ is $\sigma_{\text{SM}}(pp \rightarrow ZH) = 0.88$ pb [66]. The figure also includes the expected exclusion limit calculated from an Asimov data set when all the constrained nuisance parameters are fixed to their expected values and the unconstrained nuisance parameters that scale the $Z + \text{jets}$

TABLE I. Expected yields and total uncertainty for the different background components in each signal and control region after the profile likelihood fit to data. The expected yield for signal with $m_a = 20$ GeV is calculated before the profile likelihood fit and normalized to the total ZH cross section [$\mathcal{B}(H \rightarrow aa \rightarrow (b\bar{b})(b\bar{b})) = 1$]. The data observed in each region is included for comparison.

	Signal regions		Control regions			
	on-Z, 1HPC1LPC	on-Z, 2HPC	on-Z, 2LPC	off-Z, 2HPC	off-Z, 2LPC	off-Z, 1HPC1LPC
$t\bar{t}$	23.5 ± 4.5	2.5 ± 0.8	57.8 ± 6.9	38.3 ± 4.0	698 ± 21	332 ± 14
$Z + \text{jets}$	71 ± 19	12.2 ± 4.1	164 ± 22	0.5 ± 0.6	44 ± 19	14.0 ± 6.0
Others	3.5 ± 0.6	0.4 ± 0.2	9.2 ± 1.1	2.8 ± 0.8	28.3 ± 2.4	16.2 ± 1.8
Total	98 ± 19	15.2 ± 4.2	231 ± 23	41.6 ± 4.2	770 ± 29	362 ± 15
Data	101	17	224	40	774	354
Signal	47 ± 27	28 ± 11	18 ± 18	3.2 ± 1.2	2.1 ± 2.1	5.2 ± 3.0

TABLE II. Impact of groups of systematic uncertainties on the expected upper limits for $m_a = 20$ GeV. For comparison, the statistical uncertainty impact, defined as the 1σ uncertainty of the expected upper limit after removing all nuisance parameters from the profile likelihood, is also shown.

Source	Impact on expected upper limit
Systematic uncertainties	
Objects	
$a \rightarrow b\bar{b}$ reconstruction and identification efficiency	18%
$a \rightarrow b\bar{b}$ energy scale and resolution	13%
Lepton reconstruction and identification efficiency	1.3%
Lepton energy scale and resolution	0.5%
Other experimental	
Pileup	6.5%
Luminosity	2.5%
Background	
$t\bar{t}$ normalization	2.0%
$t\bar{t}$ modeling	7.6%
Z + jets normalization	13%
Z + jets modeling	11%
Other backgrounds	0.8%
Signal	
Production modeling	3.2%
Statistical uncertainty	43%

and $t\bar{t}$ backgrounds are fixed to one. For $m_a = 20$ GeV, an upper limit of 0.71 pb ($0.52^{+0.31}_{-0.14}$ pb) is observed (expected) at 95% C.L. The reduced sensitivity for heavier a -boson mass hypotheses is due to a lower acceptance caused by the increased separation of the b jets, while the reduced sensitivity for lighter a -boson mass hypotheses is due to a lower efficiency to identify the two b jets inside an $a \rightarrow b\bar{b}$

candidate. The figure includes the results from a previous analysis targeting the higher range of m_a [17].

IX. CONCLUSION

A search for Higgs bosons decaying into a pair of new spin-0 particles that subsequently decay into a final state with four b quarks was presented. The search used 36 fb^{-1} of 13 TeV proton-proton collision data collected by the ATLAS detector at the LHC. A dedicated strategy for reconstruction and identification of $a \rightarrow b\bar{b}$ candidates in the mass range $15 \text{ GeV} \leq m_a \leq 30 \text{ GeV}$ was introduced. The measurement of the acceptance and efficiency of this strategy was described in detail and used to compare data with simulated events in regions with two $a \rightarrow b\bar{b}$ candidates consistent with the cascade decay $H \rightarrow aa \rightarrow (b\bar{b})(b\bar{b})$. The dominant background sources were measured in control regions defined by relaxing some of the identification criteria. No excess of data events consistent with $H \rightarrow aa \rightarrow (b\bar{b})(b\bar{b})$ was observed, and upper limits at 95% C.L. on the production cross section $\sigma_{ZH}\mathcal{B}(H \rightarrow aa \rightarrow (b\bar{b})(b\bar{b}))$ were obtained as a function of the a -boson mass hypothesis. This novel search improves the expected limit on $\sigma_{ZH}\mathcal{B}(H \rightarrow aa \rightarrow (b\bar{b})(b\bar{b}))$ for a mass hypothesis of $m_a = 20$ GeV by a factor of 2.5 when compared with the previous ATLAS result which uses the same integrated luminosity.

ACKNOWLEDGMENTS

We thank CERN for the very successful operation of the LHC, as well as the support staff from our institutions without whom ATLAS could not be operated efficiently.

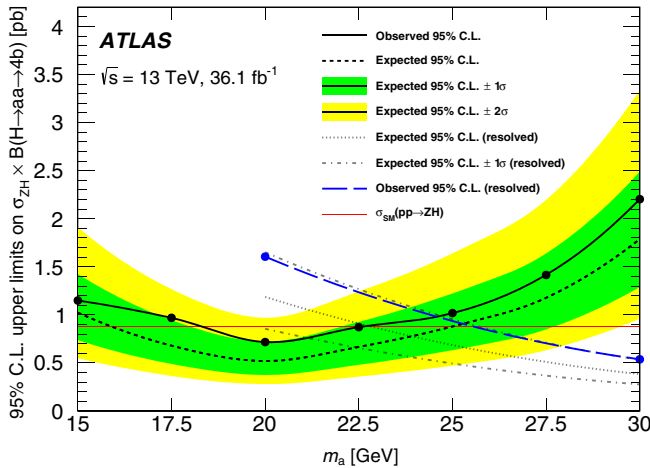


FIG. 10. Summary of the 95% C.L. upper limits on $\sigma_{ZH}\mathcal{B}(H \rightarrow aa \rightarrow (b\bar{b})(b\bar{b}))$ from this result and a previous search targeting the higher masses, labeled “(resolved)” [17]. The observed limits are shown together with the expected limits. In the case of the expected limits, one- and two-standard-deviation uncertainty bands are also displayed. The SM NNLO cross section for $pp \rightarrow ZH$ of 0.88 pb [66] is also shown.

We acknowledge the support of ANPCyT, Argentina; YerPhI, Armenia; ARC, Australia; BMWFW and FWF, Austria; ANAS, Azerbaijan; SSTC, Belarus; CNPq and FAPESP, Brazil; NSERC, NRC and CFI, Canada; CERN; ANID, Chile; CAS, MOST and NSFC, China; COLCIENCIAS, Colombia; MSMT CR, MPO CR and VSC CR, Czech Republic; DNRF and DNSRC, Denmark; IN2P3-CNRS and CEA-DRF/IRFU, France; SRNSFG, Georgia; BMBF, HGF and MPG, Germany; GSRT, Greece; RGC and Hong Kong SAR, China; ISF and Benozio Center, Israel; INFN, Italy; MEXT and JSPS, Japan; CNRST, Morocco; NWO, Netherlands; RCN, Norway; MNiSW and NCN, Poland; FCT, Portugal; MNE/IFA, Romania; MES of Russia and NRC KI, Russia Federation; JINR; MESTD, Serbia; MSSR, Slovakia; ARRS and MIZŠ, Slovenia; DST/NRF, South Africa; MICINN, Spain; SRC and Wallenberg Foundation, Sweden; SERI, SNSF and Cantons of Bern and Geneva, Switzerland; MOST, Taiwan; TAEK, Turkey; STFC, United Kingdom; DOE and NSF, United States of America. In addition, individual groups and members have received support from BCKDF, CANARIE, Compute

Canada and CRC, Canada; ERC, ERDF, Horizon 2020, Marie Skłodowska-Curie Actions and COST, European Union; Investissements d’Avenir Labex, Investissements d’Avenir IDEX and ANR, France; DFG and AvH Foundation, Germany; Herakleitos, Thales and Aristeia programmes co-financed by EU-ESF and the Greek NSRF, Greece; BSF-NSF and GIF, Israel; La Caixa Banking Foundation, CERCA Programme Generalitat de Catalunya and PROMETEO and GenT Programmes Generalitat Valenciana, Spain; Göran Gustafssons Stiftelse, Sweden; The Royal Society and Leverhulme Trust, United Kingdom. The crucial computing support from all WLCG partners is acknowledged gratefully, in particular from CERN, the ATLAS Tier-1 facilities at TRIUMF (Canada), NDGF (Denmark, Norway, Sweden), CC-IN2P3 (France), KIT/GridKA (Germany), INFN-CNAF (Italy), NL-T1 (Netherlands), PIC (Spain), ASGC (Taiwan), RAL (UK) and BNL (USA), the Tier-2 facilities worldwide and large non-WLCG resource providers. Major contributors of computing resources are listed in Ref. [72].

-
- [1] D. Curtin *et al.*, Exotic decays of the 125 GeV Higgs Boson, *Phys. Rev. D* **90**, 075004 (2014).
- [2] B. A. Dobrescu and K. T. Matchev, Light axion within the next-to-minimal Supersymmetric Standard Model, *J. High Energy Phys.* **09** (2000) 031.
- [3] U. Ellwanger, J. F. Gunion, C. Hugonie, and S. Moretti, Towards a no-lose theorem for NMSSM Higgs discovery at the LHC, [arXiv:hep-ph/0305109](https://arxiv.org/abs/hep-ph/0305109).
- [4] R. Dermisek and J. F. Gunion, Escaping the Large Fine-Tuning and Little Hierarchy Problems in the Next to Minimal Supersymmetric Model and $h \rightarrow aa$ Decays, *Phys. Rev. Lett.* **95**, 041801 (2005).
- [5] S. Chang, R. Dermisek, J. F. Gunion, and N. Weiner, Nonstandard Higgs boson decays, *Annu. Rev. Nucl. Part. Sci.* **58**, 75 (2008).
- [6] D. E. Morrissey and A. Pierce, Modified Higgs boson phenomenology from gauge or gaugino mediation in the next-to-minimal supersymmetric standard model, *Phys. Rev. D* **78**, 075029 (2008).
- [7] S. Profumo, M. J. Ramsey-Musolf, and G. Shaughnessy, Singlet Higgs phenomenology and the electroweak phase transition, *J. High Energy Phys.* **08** (2007) 010.
- [8] N. Blinov, J. Kozaczuk, D. E. Morrissey, and C. Tamarit, Electroweak baryogenesis from exotic electroweak symmetry breaking, *Phys. Rev. D* **92**, 035012 (2015).
- [9] V. Silveira and A. Zee, Scalar phantoms, *Phys. Lett.* **161B**, 136 (1985).
- [10] M. Pospelov, A. Ritz, and M. B. Voloshin, Secluded WIMP dark matter, *Phys. Lett. B* **662**, 53 (2008).
- [11] P. Draper, T. Liu, C. E. M. Wagner, L.-T. Wang, and H. Zhang, Dark Light-Higgs Bosons, *Phys. Rev. Lett.* **106**, 121805 (2011).
- [12] S. Ipek, D. McKeen, and A. E. Nelson, Renormalizable model for the Galactic Center gamma-ray excess from dark matter annihilation, *Phys. Rev. D* **90**, 055021 (2014).
- [13] A. Martin, J. Shelton, and J. Unwin, Fitting the Galactic Center gamma-ray excess with cascade annihilations, *Phys. Rev. D* **90**, 103513 (2014).
- [14] ATLAS Collaboration, Observation of a new particle in the search for the Standard Model Higgs boson with the ATLAS detector at the LHC, *Phys. Lett. B* **716**, 1 (2012).
- [15] CMS Collaboration, Observation of a new boson at a mass of 125 GeV with the CMS experiment at the LHC, *Phys. Lett. B* **716**, 30 (2012).
- [16] ATLAS Collaboration, Combined measurements of Higgs boson production and decay using up to 80 fb⁻¹ of proton-proton collision data at $\sqrt{s} = 13$ TeV collected with the ATLAS experiment, *Phys. Rev. D* **101**, 012002 (2020).
- [17] ATLAS Collaboration, Search for the Higgs boson produced in association with a vector boson and decaying into two spin-zero particles in the $H \rightarrow aa \rightarrow 4b$ channel in pp collisions at $\sqrt{s} = 13$ TeV with the ATLAS detector, *J. High Energy Phys.* **10** (2018) 031.
- [18] ATLAS Collaboration, The ATLAS Experiment at the CERN large hadron collider, *J. Instrum.* **3**, S08003 (2008).
- [19] ATLAS Collaboration, ATLAS insertable B-layer technical design report, ATLAS-TDR-19; CERN-LHCC-2010-013, 2010, <https://cds.cern.ch/record/1291633>.

- [20] B. Abbott *et al.*, Production and integration of the ATLAS Insertable B-Layer, *J. Instrum.* **13**, T05008 (2018).
- [21] ATLAS Collaboration, Luminosity determination in pp collisions at $\sqrt{s} = 8$ TeV using the ATLAS detector at the LHC, *Eur. Phys. J. C* **76**, 653 (2016).
- [22] G. Avoni *et al.*, The new LUCID-2 detector for luminosity measurement and monitoring in ATLAS, *J. Instrum.* **13**, P07017 (2018).
- [23] ATLAS Collaboration, Performance of the ATLAS trigger system in 2015, *Eur. Phys. J. C* **77**, 317 (2017).
- [24] ATLAS Collaboration, The ATLAS simulation infrastructure, *Eur. Phys. J. C* **70**, 823 (2010).
- [25] S. Agostinelli *et al.*, GEANT4—A simulation toolkit, *Nucl. Instrum. Methods Phys. Res., Sect. A* **506**, 250 (2003).
- [26] T. Sjöstrand, S. Mrenna, and P. Z. Skands, A brief introduction to PYTHIA 8.1, *Comput. Phys. Commun.* **178**, 852 (2008).
- [27] ATLAS Collaboration, Summary of ATLAS PYTHIA 8 tunes, ATL-PHYS-PUB-2012-003 (2012), <https://cds.cern.ch/record/1474107>.
- [28] A. D. Martin, W. J. Stirling, R. S. Thorne, and G. Watt, Parton distributions for the LHC, *Eur. Phys. J. C* **63**, 189 (2009).
- [29] D. J. Lange, The EvtGen particle decay simulation package, *Nucl. Instrum. Methods Phys. Res., Sect. A* **462**, 152 (2001).
- [30] T. Gleisberg, S. Höche, F. Krauss, M. Schönherr, S. Schumann, F. Siegert, and J. Winter, Event generation with SHERPA 1.1, *J. High Energy Phys.* **02** (2009) 007.
- [31] P. Nason, A new method for combining NLO QCD with shower Monte Carlo algorithms, *J. High Energy Phys.* **11** (2004) 040.
- [32] S. Frixione, P. Nason, and G. Ridolfi, A Positive-weight next-to-leading-order Monte Carlo for heavy flavour hadroproduction, *J. High Energy Phys.* **09** (2007) 126.
- [33] S. Frixione, P. Nason, and C. Oleari, Matching NLO QCD computations with parton shower simulations: The POWHEG method, *J. High Energy Phys.* **11** (2007) 070.
- [34] S. Alioli, P. Nason, C. Oleari, and E. Re, A general framework for implementing NLO calculations in shower Monte Carlo programs: The POWHEG BOX, *J. High Energy Phys.* **06** (2010) 043.
- [35] H.-L. Lai, M. Guzzi, J. Huston, Z. Li, P. M. Nadolsky, J. Pumplin, and C.-P. Yuan, New parton distributions for collider physics, *Phys. Rev. D* **82**, 074024 (2010).
- [36] ATLAS Collaboration, ATLAS PYTHIA 8 tunes to 7 TeV data, ATL-PHYS-PUB-2014-021 (2014), <http://cdsweb.cern.ch/record/1966419>.
- [37] J. M. Campbell, R. K. Ellis, P. Nason, and E. Re, Top-pair production and decay at NLO matched with parton showers, *J. High Energy Phys.* **04** (2015) 114.
- [38] T. Sjöstrand, S. Ask, J. R. Christiansen, R. Corke, N. Desai, P. Ilten, S. Mrenna, S. Prestel, C. O. Rasmussen, and P. Z. Skands, An introduction to PYTHIA 8.2, *Comput. Phys. Commun.* **191**, 159 (2015).
- [39] F. Cascioli, P. Maierhofer, N. Moretti, S. Pozzorini, and F. Siegert, NLO matching for $t\bar{t}b\bar{b}$ production with massive b -quarks, *Phys. Lett. B* **734**, 210 (2014).
- [40] F. Cascioli, P. Maierhofer, and S. Pozzorini, Scattering Amplitudes with Open Loops, *Phys. Rev. Lett.* **108**, 111601 (2012).
- [41] ATLAS Collaboration, Search for the Standard Model Higgs boson produced in association with top quarks and decaying into $b\bar{b}$ in pp collisions at $\sqrt{s} = 8$ TeV with the ATLAS detector, *Eur. Phys. J. C* **75**, 349 (2015).
- [42] S. Schumann and F. Krauss, A parton shower algorithm based on Catani-Seymour dipole factorisation, *J. High Energy Phys.* **03** (2008) 038.
- [43] ATLAS Collaboration, Monte Carlo generators for the production of a W or Z/γ^* boson in association with jets at ATLAS in Run 2, ATL-PHYS-PUB-2016-003, 2016, <https://cds.cern.ch/record/2120133>.
- [44] T. Gleisberg and S. Höche, Comix, a new matrix element generator, *J. High Energy Phys.* **12** (2008) 039.
- [45] S. Höche, F. Krauss, M. Schönherr, and F. Siegert, QCD matrix elements + parton showers: The NLO case, *J. High Energy Phys.* **04** (2013) 027.
- [46] ATLAS Collaboration, Multi-boson simulation for 13 TeV ATLAS analyses, ATL-PHYS-PUB-2016-002 (2016), <https://cds.cern.ch/record/2119986>.
- [47] ATLAS Collaboration, Electron reconstruction and identification in the ATLAS experiment using the 2015 and 2016 LHC proton–proton collision data at $\sqrt{s} = 13$ TeV, *Eur. Phys. J. C* **79**, 639 (2019).
- [48] ATLAS Collaboration, Electron efficiency measurements with the ATLAS detector using the 2015 LHC proton–proton collision data, ATLAS-CONF-2016-024, 2016, <https://cds.cern.ch/record/2157687>.
- [49] ATLAS Collaboration, Muon reconstruction performance of the ATLAS detector in proton–proton collision data at $\sqrt{s} = 13$ TeV, *Eur. Phys. J. C* **76**, 292 (2016).
- [50] ATLAS Collaboration, Topological cell clustering in the ATLAS calorimeters and its performance in LHC Run 1, *Eur. Phys. J. C* **77**, 490 (2017).
- [51] M. Cacciari, G. P. Salam, and G. Soyez, The anti- k_t jet clustering algorithm, *J. High Energy Phys.* **04** (2008) 063.
- [52] M. Cacciari, G. P. Salam, and G. Soyez, FastJet user manual, *Eur. Phys. J. C* **72**, 1896 (2012).
- [53] ATLAS Collaboration, Jet energy scale measurements and their systematic uncertainties in proton–proton collisions at $\sqrt{s} = 13$ TeV with the ATLAS detector, *Phys. Rev. D* **96**, 072002 (2017).
- [54] ATLAS Collaboration, Selection of jets produced in 13 TeV proton–proton collisions with the ATLAS detector, ATLAS-CONF-2015-029, 2015, <https://cds.cern.ch/record/2037702>.
- [55] ATLAS Collaboration, Tagging and suppression of pileup jets with the ATLAS detector, ATLASCONF-2014-018, 2014, <https://cds.cern.ch/record/1700870>.
- [56] ATLAS Collaboration, Optimisation of the ATLAS b -tagging performance for the 2016 LHC Run, ATL-PHYS-PUB-2016-012 (2016), <https://cds.cern.ch/record/2160731>.
- [57] ATLAS Collaboration, Performance of b -jet identification in the ATLAS experiment, *J. Instrum.* **11**, P04008 (2016).
- [58] B. Nachman, P. Nef, A. Schwartzman, M. Swiatlowski, and C. Wanotayaroj, Jets from jets: Reclustering as a tool for

- large radius jet reconstruction and grooming at the LHC, *J. High Energy Phys.* **02** (2015) 075.
- [59] M. Cacciari and G. P. Salam, Pileup subtraction using jet areas, *Phys. Lett. B* **659**, 119 (2008).
- [60] S. Catani, Y. L. Dokshitzer, M. H. Seymour, and B. R. Webber, Longitudinally-invariant k_{\perp} -clustering algorithms for hadron-hadron collisions, *Nucl. Phys.* **B406**, 187 (1993).
- [61] G. P. Salam, Towards jetography, *Eur. Phys. J. C* **67**, 637 (2010).
- [62] ATLAS Collaboration, Identification of boosted Higgs bosons decaying into b-quark pairs with the ATLAS detector at 13 TeV, *Eur. Phys. J. C* **79**, 836 (2019).
- [63] ATLAS Collaboration, Monte Carlo to Monte Carlo scale factors for flavour tagging efficiency calibration, ATLAS-PHYS-PUB-2020-009, 2020, <https://cds.cern.ch/record/2718610>.
- [64] ATLAS Collaboration, Search for the Standard Model Higgs boson produced in association with top quarks and decaying into a $b\bar{b}$ pair in pp collisions at $\sqrt{s} = 13$ TeV with the ATLAS detector, *Phys. Rev. D* **97**, 072016 (2018).
- [65] ATLAS Collaboration, Multi-boson simulation for 13 TeV ATLAS analyses, ATLAS-PHYS-PUB-2016-002, 2016, <https://cds.cern.ch/record/2119986>.
- [66] LHC Higgs Cross Section Working Group, Handbook of LHC Higgs Cross Sections: 4. Deciphering the nature of the Higgs sector, [arXiv:1610.07922](https://arxiv.org/abs/1610.07922).
- [67] J. M. Campbell and R. K. Ellis, $t\bar{t}W^{\pm}$ production and decay at NLO, *J. High Energy Phys.* **07** (2012) 052.
- [68] R. J. Barlow and C. Beeston, Fitting using finite Monte Carlo samples, *Comput. Phys. Commun.* **77**, 219 (1993).
- [69] G. Cowan, K. Cranmer, E. Gross, and O. Vitells, Asymptotic formulae for likelihood-based tests of new physics, *Eur. Phys. J. C* **71**, 1554 (2011); Erratum, *Eur. Phys. J. C* **73**, 2501 (2013).
- [70] A. L. Read, Presentation of search results: The CLs technique, *J. Phys. G* **28**, 2693 (2002).
- [71] T. Junk, Confidence level computation for combining searches with small statistics, *Nucl. Instrum. Methods Phys. Res., Sect. A* **434**, 435 (1999).
- [72] ATLAS Collaboration, ATLAS computing acknowledgements, ATLAS-SOFT-PUB-2020-001, <https://cds.cern.ch/record/2717821>.

G. Aad,¹⁰² B. Abbott,¹²⁸ D. C. Abbott,¹⁰³ A. Abed Abud,³⁶ K. Abeling,⁵³ D. K. Abhayasinghe,⁹⁴ S. H. Abidi,¹⁶⁶ O. S. AbouZeid,⁴⁰ N. L. Abraham,¹⁵⁵ H. Abramowicz,¹⁶⁰ H. Abreu,¹⁵⁹ Y. Abulaiti,⁶ B. S. Acharya,^{67a,67b,b} B. Achkar,⁵³ L. Adam,¹⁰⁰ C. Adam Bourdarios,⁵ L. Adamczyk,^{84a} L. Adamek,¹⁶⁶ J. Adelman,¹²¹ M. Adersberger,¹¹⁴ A. Adiguzel,^{12c} S. Adorni,⁵⁴ T. Adye,¹⁴³ A. A. Affolder,¹⁴⁵ Y. Afik,¹⁵⁹ C. Agapopoulou,⁶⁵ M. N. Agaras,³⁸ A. Aggarwal,¹¹⁹ C. Agheorghiesei,^{27c} J. A. Aguilar-Saavedra,^{139f,139a,c} A. Ahmad,³⁶ F. Ahmadov,⁸⁰ W. S. Ahmed,¹⁰⁴ X. Ai,¹⁸ G. Aielli,^{74a,74b} S. Akatsuka,⁸⁶ M. Akbiyik,¹⁰⁰ T. P. A. Åkesson,⁹⁷ E. Akilli,⁵⁴ A. V. Akimov,¹¹¹ K. Al Khoury,⁶⁵ G. L. Alberghi,^{23b,23a} J. Albert,¹⁷⁵ M. J. Alconada Verzini,¹⁶⁰ S. Alderweireldt,³⁶ M. Aleksa,³⁶ I. N. Aleksandrov,⁸⁰ C. Alexa,^{27b} T. Alexopoulos,¹⁰ A. Alfonsi,¹²⁰ F. Alfonsi,^{23b,23a} M. Alhroob,¹²⁸ B. Ali,¹⁴¹ S. Ali,¹⁵⁷ M. Aliev,¹⁶⁵ G. Alimonti,^{69a} C. Allaire,³⁶ B. M. M. Allbrooke,¹⁵⁵ B. W. Allen,¹³¹ P. P. Allport,²¹ A. Aloisio,^{70a,70b} F. Alonso,⁸⁹ C. Alpigiani,¹⁴⁷ E. Alunno Camelia,^{74a,74b} M. Alvarez Estevez,⁹⁹ M. G. Alvigi,^{70a,70b} Y. Amaral Coutinho,^{81b} A. Ambler,¹⁰⁴ L. Ambroz,¹³⁴ C. Amelung,²⁶ D. Amidei,¹⁰⁶ S. P. Amor Dos Santos,^{139a} S. Amoroso,⁴⁶ C. S. Amrouche,⁵⁴ F. An,⁷⁹ C. Anastopoulos,¹⁴⁸ N. Andari,¹⁴⁴ T. Andeen,¹¹ J. K. Anders,²⁰ S. Y. Andrean,^{45a,45b} A. Andreatta,^{69a,69b} V. Andrei,^{61a} C. R. Anelli,¹⁷⁵ S. Angelidakis,⁹ A. Angerami,³⁹ A. V. Anisenkov,^{122b,122a} A. Annovi,^{72a} C. Antel,⁵⁴ M. T. Anthony,¹⁴⁸ E. Antipov,¹²⁹ M. Antonelli,⁵¹ D. J. A. Antrim,¹⁷⁰ F. Anulli,^{73a} M. Aoki,⁸² J. A. Aparisi Pozo,¹⁷³ M. A. Aparo,¹⁵⁵ L. Aperio Bella,⁴⁶ N. Aranzabal,³⁶ V. Araujo Ferraz,^{81a} R. Araujo Pereira,^{81b} C. Arcangeletti,⁵¹ A. T. H. Arce,⁴⁹ F. A. Arduh,⁸⁹ J.-F. Arguin,¹¹⁰ S. Argyropoulos,⁵² J.-H. Arling,⁴⁶ A. J. Armbruster,³⁶ A. Armstrong,¹⁷⁰ O. Arnaez,¹⁶⁶ H. Arnold,¹²⁰ Z. P. Arrubarrena Tame,¹¹⁴ G. Artoni,¹³⁴ K. Asai,¹²⁶ S. Asai,¹⁶² T. Asawatavonvanich,¹⁶⁴ N. Asbah,⁵⁹ E. M. Asimakopoulou,¹⁷¹ L. Asquith,¹⁵⁵ J. Assahsah,^{35d} K. Assamagan,²⁹ R. Astalos,^{28a} R. J. Atkin,^{33a} M. Atkinson,¹⁷² N. B. Atlay,¹⁹ H. Atmani,⁶⁵ K. Augsten,¹⁴¹ V. A. Austrup,¹⁸¹ G. Avolio,³⁶ M. K. Ayoub,^{15a} G. Azuelos,^{110,d} H. Bachacou,¹⁴⁴ K. Bachas,¹⁶¹ M. Backes,¹³⁴ F. Backman,^{45a,45b} P. Bagnaia,^{73a,73b} M. Bahmani,⁸⁵ H. Bahrasemani,¹⁵¹ A. J. Bailey,¹⁷³ V. R. Bailey,¹⁷² J. T. Baines,¹⁴³ C. Bakalis,¹⁰ O. K. Baker,¹⁸² P. J. Bakker,¹²⁰ E. Bakos,¹⁶ D. Bakshi Gupta,⁸ S. Balaji,¹⁵⁶ E. M. Baldin,^{122b,122a} P. Balek,¹⁷⁹ F. Balli,¹⁴⁴ W. K. Balunas,¹³⁴ J. Balz,¹⁰⁰ E. Banas,⁸⁵ M. Bandieramonte,¹³⁸ A. Bandyopadhyay,²⁴ Sw. Banerjee,^{180,e} L. Barak,¹⁶⁰ W. M. Barbe,³⁸ E. L. Barberio,¹⁰⁵ D. Barberis,^{55b,55a} M. Barbero,¹⁰² G. Barbour,⁹⁵ T. Barillari,¹¹⁵ M.-S. Barisits,³⁶ J. Barkeloo,¹³¹ T. Barklow,¹⁵² R. Barnea,¹⁵⁹ B. M. Barnett,¹⁴³ R. M. Barnett,¹⁸ Z. Barnovska-Blenessy,^{60a} A. Baroncelli,^{60a} G. Barone,²⁹ A. J. Barr,¹³⁴ L. Barranco Navarro,^{45a,45b} F. Barreiro,⁹⁹ J. Barreiro Guimarães da Costa,^{15a} U. Barron,¹⁶⁰ S. Barsov,¹³⁷ F. Bartels,^{61a} R. Bartoldus,¹⁵² G. Bartolini,¹⁰² A. E. Barton,⁹⁰ P. Bartos,^{28a} A. Basalaeu,⁴⁶ A. Basan,¹⁰⁰ A. Bassalat,^{65,f} M. J. Basso,¹⁶⁶ R. L. Bates,⁵⁷ S. Batlamous,^{35e} J. R. Batley,³² B. Batool,¹⁵⁰ M. Battaglia,¹⁴⁵ M. Bauce,^{73a,73b} F. Bauer,¹⁴⁴ K. T. Bauer,¹⁷⁰ P. Bauer,²⁴ H. S. Bawa,³¹ A. Bayirli,^{12c}

J. B. Beacham,⁴⁹ T. Beau,¹³⁵ P. H. Beauchemin,¹⁶⁹ F. Becherer,⁵² P. Bechtle,²⁴ H. C. Beck,⁵³ H. P. Beck,^{20,g} K. Becker,¹⁷⁷ C. Becot,⁴⁶ A. Beddall,^{12d} A. J. Beddall,^{12a} V. A. Bednyakov,⁸⁰ M. Bedognetti,¹²⁰ C. P. Bee,¹⁵⁴ T. A. Beermann,¹⁸¹ M. Begalli,^{81b} M. Begel,²⁹ A. Behera,¹⁵⁴ J. K. Behr,⁴⁶ F. Beisiegel,²⁴ M. Belfkir,⁵ A. S. Bell,⁹⁵ G. Bella,¹⁶⁰ L. Bellagamba,^{23b} A. Bellerive,³⁴ P. Bellos,⁹ K. Beloborodov,^{122b,122a} K. Belotskiy,¹¹² N. L. Belyaev,¹¹² D. Benckekroun,^{35a} N. Benekos,¹⁰ Y. Benhammou,¹⁶⁰ D. P. Benjamin,⁶ M. Benoit,⁵⁴ J. R. Bensinger,²⁶ S. Bentvelsen,¹²⁰ L. Beresford,¹³⁴ M. Beretta,⁵¹ D. Berge,¹⁹ E. Bergeaas Kuutmann,¹⁷¹ N. Berger,⁵ B. Bergmann,¹⁴¹ L. J. Bergsten,²⁶ J. Beringer,¹⁸ S. Berlendis,⁷ G. Bernardi,¹³⁵ C. Bernius,¹⁵² F. U. Bernlochner,²⁴ T. Berry,⁹⁴ P. Berta,¹⁰⁰ C. Bertella,^{15a} A. Berthold,⁴⁸ I. A. Bertram,⁹⁰ O. Bessidskaia Bylund,¹⁸¹ N. Besson,¹⁴⁴ A. Bethani,¹⁰¹ S. Bethke,¹¹⁵ A. Betti,⁴² A. J. Bevan,⁹³ J. Beyer,¹¹⁵ D. S. Bhattacharya,¹⁷⁶ P. Bhattarai,²⁶ V. S. Bhopatkar,⁶ R. Bi,¹³⁸ R. M. Bianchi,¹³⁸ O. Biebel,¹¹⁴ D. Biedermann,¹⁹ R. Bielski,³⁶ K. Bierwagen,¹⁰⁰ N. V. Biesuz,^{72a,72b} M. Biglietti,^{75a} T. R. V. Billoud,¹¹⁰ M. Bindi,⁵³ A. Bingul,^{12d} C. Bini,^{73a,73b} S. Biondi,^{23b,23a} C. J. Birch-sykes,¹⁰¹ M. Birman,¹⁷⁹ T. Bisanz,⁵³ J. P. Biswal,³ D. Biswas,^{180,e} A. Bitadze,¹⁰¹ C. Bittrich,⁴⁸ K. Bjørke,¹³³ T. Blazek,^{28a} I. Bloch,⁴⁶ C. Blocker,²⁶ A. Blue,⁵⁷ U. Blumenschein,⁹³ G. J. Bobbink,¹²⁰ V. S. Bobrovnikov,^{122b,122a} S. S. Bocchetta,⁹⁷ D. Bogavac,¹⁴ A. G. Bogdanchikov,^{122b,122a} C. Bohm,^{45a} V. Boisvert,⁹⁴ P. Bokan,^{53,171,53} T. Bold,^{84a} A. E. Bolz,^{61b} M. Bomben,¹³⁵ M. Bona,⁹³ J. S. Bonilla,¹³¹ M. Boonekamp,¹⁴⁴ C. D. Booth,⁹⁴ A. G. Borbély,⁵⁷ H. M. Borecka-Bielska,⁹¹ L. S. Borgna,⁹⁵ A. Borisov,¹²³ G. Borissoy,⁹⁰ D. Bortoletto,¹³⁴ D. Boscherini,^{23b} M. Bosman,¹⁴ J. D. Bossio Sola,¹⁰⁴ K. Bouaouda,^{35a} J. Boudreau,¹³⁸ E. V. Bouhova-Thacker,⁹⁰ D. Boumediene,³⁸ S. K. Boutle,⁵⁷ A. Boveia,¹²⁷ J. Boyd,³⁶ D. Boye,^{33c} I. R. Boyko,⁸⁰ A. J. Bozson,⁹⁴ J. Bracinik,²¹ N. Brahimi,^{60d} G. Brandt,¹⁸¹ O. Brandt,³² F. Braren,⁴⁶ B. Brau,¹⁰³ J. E. Brau,¹³¹ W. D. Breaden Madden,⁵⁷ K. Brendlinger,⁴⁶ R. Brenner,¹⁵⁹ L. Brenner,³⁶ R. Brenner,¹⁷¹ S. Bressler,¹⁷⁹ B. Brickwedde,¹⁰⁰ D. L. Briglin,²¹ D. Britton,⁵⁷ D. Britzger,¹¹⁵ I. Brock,²⁴ R. Brock,¹⁰⁷ G. Brooijmans,³⁹ W. K. Brooks,^{146d} E. Brost,²⁹ P. A. Bruckman de Renstrom,⁸⁵ B. Brüers,⁴⁶ D. Bruncko,^{28b} A. Bruni,^{23b} G. Bruni,^{23b} L. S. Bruni,¹²⁰ S. Bruno,^{74a,74b} M. Bruschi,^{23b} N. Brusino,^{73a,73b} L. Bryngemark,¹⁵² T. Buanes,¹⁷ Q. Buat,¹⁵⁴ P. Buchholz,¹⁵⁰ A. G. Buckley,⁵⁷ I. A. Budagov,⁸⁰ M. K. Bugge,¹³³ F. Bühner,⁵² O. Bulekov,¹¹² B. A. Bullard,⁵⁹ T. J. Burch,¹²¹ S. Burdin,⁹¹ C. D. Burgard,¹²⁰ A. M. Burger,¹²⁹ B. Burghgrave,⁸ J. T. P. Burr,⁴⁶ C. D. Burton,¹¹ J. C. Burzynski,¹⁰³ V. Büscher,¹⁰⁰ E. Buschmann,⁵³ P. J. Bussey,⁵⁷ J. M. Butler,²⁵ C. M. Buttar,⁵⁷ J. M. Butterworth,⁹⁵ P. Butti,³⁶ W. Buttinger,³⁶ C. J. Buxo Vazquez,¹⁰⁷ A. Buzatu,¹⁵⁷ A. R. Buzykaev,^{122b,122a} G. Cabras,^{23b,23a} S. Cabrera Urbán,¹⁷³ D. Caforio,⁵⁶ H. Cai,¹³⁸ V. M. M. Cairo,¹⁵² O. Cakir,^{4a} N. Calace,³⁶ P. Calafiura,¹⁸ G. Calderini,¹³⁵ P. Calfayan,⁶⁶ G. Callea,⁵⁷ L. P. Caloba,^{81b} A. Caltabiano,^{74a,74b} S. Calvente Lopez,⁹⁹ D. Calvet,³⁸ S. Calvet,³⁸ T. P. Calvet,¹⁰² M. Calvetti,^{72a,72b} R. Camacho Toro,¹³⁵ S. Camarda,³⁶ D. Camarero Munoz,⁹⁹ P. Camarri,^{74a,74b} M. T. Camerlingo,^{75a,75b} D. Cameron,¹³³ C. Camincher,³⁶ S. Campana,³⁶ M. Campanelli,⁹⁵ A. Camplani,⁴⁰ V. Canale,^{70a,70b} A. Canesse,¹⁰⁴ M. Cano Bret,⁷⁸ J. Cantero,¹²⁹ T. Cao,¹⁶⁰ Y. Cao,¹⁷² M. D. M. Capeans Garrido,³⁶ M. Capua,^{41b,41a} R. Cardarelli,^{74a} F. Cardillo,¹⁴⁸ G. Carducci,^{41b,41a} I. Carli,¹⁴² T. Carli,³⁶ G. Carlino,^{70a} B. T. Carlson,¹³⁸ E. M. Carlson,^{175,167a} L. Carminati,^{69a,69b} R. M. D. Carney,¹⁵² S. Caron,¹¹⁹ E. Carquin,^{146d} S. Carrá,⁴⁶ G. Carratta,^{23b,23a} J. W. S. Carter,¹⁶⁶ T. M. Carter,⁵⁰ M. P. Casado,^{14,h} A. F. Casha,¹⁶⁶ F. L. Castillo,¹⁷³ L. Castillo Garcia,¹⁴ V. Castillo Gimenez,¹⁷³ N. F. Castro,^{139a,139e} A. Catinaccio,³⁶ J. R. Catmore,¹³³ A. Cattai,³⁶ V. Cavaliere,²⁹ V. Cavasinni,^{72a,72b} E. Celebi,^{12b} F. Celli,¹³⁴ K. Cerny,¹³⁰ A. S. Cerqueira,^{81a} A. Cerri,¹⁵⁵ L. Cerrito,^{74a,74b} F. Cerutti,¹⁸ A. Cervelli,^{23b,23a} S. A. Cetin,^{12b} Z. Chadi,^{35a} D. Chakraborty,¹²¹ J. Chan,¹⁸⁰ W. S. Chan,¹²⁰ W. Y. Chan,⁹¹ J. D. Chapman,³² B. Chargeishvili,^{158b} D. G. Charlton,²¹ T. P. Charman,⁹³ C. C. Chau,³⁴ S. Che,¹²⁷ S. Chekanov,⁶ S. V. Chekulaev,^{167a} G. A. Chelkov,^{80,i} B. Chen,⁷⁹ C. Chen,^{60a} C. H. Chen,⁷⁹ H. Chen,²⁹ J. Chen,^{60a} J. Chen,³⁹ J. Chen,²⁶ S. Chen,¹³⁶ S. J. Chen,^{15c} X. Chen,^{15b} Y. Chen,^{60a} Y.-H. Chen,⁴⁶ H. C. Cheng,^{63a} H. J. Cheng,^{15a} A. Cheplakov,⁸⁰ E. Cheremushkina,¹²³ R. Cherkaoui El Moursli,^{35e} E. Cheu,⁷ K. Cheung,⁶⁴ T. J. A. Chevalérias,¹⁴⁴ L. Chevalier,¹⁴⁴ V. Chiarella,⁵¹ G. Chiarelli,^{72a} G. Chiodini,^{68a} A. S. Chisholm,²¹ A. Chitan,^{27b} I. Chiu,¹⁶² Y. H. Chiu,¹⁷⁵ M. V. Chizhov,⁸⁰ K. Choi,¹¹ A. R. Chomont,^{73a,73b} Y. S. Chow,¹²⁰ L. D. Christopher,^{33e} M. C. Chu,^{63a} X. Chu,^{15a,15d} J. Chudoba,¹⁴⁰ J. J. Chwastowski,⁸⁵ L. Chytka,¹³⁰ D. Cieri,¹¹⁵ K. M. Ciesla,⁸⁵ D. Cinca,⁴⁷ V. Cindro,⁹² I. A. Cioară,^{27b} A. Ciocio,¹⁸ F. Ciotto,^{70a,70b} Z. H. Citron,^{179,j} M. Citterio,^{69a} D. A. Ciubotaru,^{27b} B. M. Ciungu,¹⁶⁶ A. Clark,⁵⁴ M. R. Clark,³⁹ P. J. Clark,⁵⁰ S. E. Clawson,¹⁰¹ C. Clement,^{45a,45b} Y. Coadou,¹⁰² M. Cobal,^{67a,67c} A. Coccaro,^{55b} J. Cochran,⁷⁹ R. Coelho Lopes De Sa,¹⁰³ H. Cohen,¹⁶⁰ A. E. C. Coimbra,³⁶ B. Cole,³⁹ A. P. Colijn,¹²⁰ J. Collot,⁵⁸ P. Conde Muiño,^{139a,139h} S. H. Connell,^{33c} I. A. Connelly,⁵⁷ S. Constantinescu,^{27b} F. Conventi,^{70a,k} A. M. Cooper-Sarkar,¹³⁴ F. Cormier,¹⁷⁴ K. J. R. Cormier,¹⁶⁶ L. D. Corpe,⁹⁵ M. Corradi,^{73a,73b} E. E. Corrigan,⁹⁷ F. Corriveau,^{104,l} M. J. Costa,¹⁷³ F. Costanza,⁵ D. Costanzo,¹⁴⁸ G. Cowan,⁹⁴ J. W. Cowley,³² J. Crane,¹⁰¹ K. Cranmer,¹²⁵ R. A. Creager,¹³⁶ S. Crépe-Renaudin,⁵⁸ F. Crescioli,¹³⁵ M. Cristinziani,²⁴ V. Croft,¹⁶⁹ G. Crosetti,^{41b,41a}

A. Cueto,⁵ T. Cuhadar Donszelmann,¹⁷⁰ H. Cui,^{15a,15d} A. R. Cukierman,¹⁵² W. R. Cunningham,⁵⁷ S. Czekierda,⁸⁵ P. Czodrowski,³⁶ M. M. Czurylo,^{61b} M. J. Da Cunha Sargedas De Sousa,^{60b} J. V. Da Fonseca Pinto,^{81b} C. Da Via,¹⁰¹ W. Dabrowski,^{84a} F. Dachs,³⁶ T. Dado,⁴⁷ S. Dahbi,^{33c} T. Dai,¹⁰⁶ C. Dallapiccola,¹⁰³ M. Dam,⁴⁰ G. D'amen,²⁹ V. D'Amico,^{75a,75b} J. Damp,¹⁰⁰ J. R. Dandoy,¹³⁶ M. F. Daneri,³⁰ M. Danninger,¹⁵¹ V. Dao,³⁶ G. Darbo,^{55b} O. Dartsis,⁵ A. Dattagupta,¹³¹ T. Daubney,⁴⁶ S. D'Auria,^{69a,69b} C. David,^{167b} T. Davidek,¹⁴² D. R. Davis,⁴⁹ I. Dawson,¹⁴⁸ K. De,⁸ R. De Asmundis,^{70a} M. De Beurs,¹²⁰ S. De Castro,^{23b,23a} N. De Groot,¹¹⁹ P. de Jong,¹²⁰ H. De la Torre,¹⁰⁷ A. De Maria,^{15c} D. De Pedis,^{73a} A. De Salvo,^{73a} U. De Sanctis,^{74a,74b} M. De Santis,^{74a,74b} A. De Santo,¹⁵⁵ J. B. De Vivie De Regie,⁶⁵ C. Debenedetti,¹⁴⁵ D. V. Dedovich,⁸⁰ A. M. Deiana,⁴² J. Del Peso,⁹⁹ Y. Delabat Diaz,⁴⁶ D. Delgove,⁶⁵ F. Deliot,¹⁴⁴ C. M. Delitzsch,⁷ M. Della Pietra,^{70a,70b} D. Della Volpe,⁵⁴ A. Dell'Acqua,³⁶ L. Dell'Asta,^{74a,74b} M. Delmastro,⁵ C. Delporte,⁶⁵ P. A. Delsart,⁵⁸ D. A. DeMarco,¹⁶⁶ S. Demers,¹⁸² M. Demichev,⁸⁰ G. Demontigny,¹¹⁰ S. P. Denisov,¹²³ L. D'Eramo,¹²¹ D. Derendarz,⁸⁵ J. E. Derkaoui,^{35d} F. Derue,¹³⁵ P. Dervan,⁹¹ K. Desch,²⁴ K. Dette,¹⁶⁶ C. Deutsch,²⁴ M. R. Devesa,³⁰ P. O. Deviveiros,³⁶ F. A. Di Bello,^{73a,73b} A. Di Ciaccio,^{74a,74b} L. Di Ciaccio,⁵ W. K. Di Clemente,¹³⁶ C. Di Donato,^{70a,70b} A. Di Girolamo,³⁶ G. Di Gregorio,^{72a,72b} B. Di Micco,^{75a,75b} R. Di Nardo,^{75a,75b} K. F. Di Petrillo,⁵⁹ R. Di Sipio,¹⁶⁶ C. Diaconu,¹⁰² F. A. Dias,¹²⁰ T. Dias Do Vale,^{139a} M. A. Diaz,^{146a} F. G. Diaz Capriles,²⁴ J. Dickinson,¹⁸ M. Didenko,¹⁶⁵ E. B. Diehl,¹⁰⁶ J. Dietrich,¹⁹ S. Díez Cornell,⁴⁶ C. Díez Pardos,¹⁵⁰ A. Dimitrievska,¹⁸ W. Ding,^{15b} J. Dingfelder,²⁴ S. J. Dittmeier,^{61b} F. Dittus,³⁶ F. Djama,¹⁰² T. Djobava,^{158b} J. I. Djuvsland,¹⁷ M. A. B. Do Vale,^{81c} M. Dobre,^{27b} D. Dodsworth,²⁶ C. Doglioni,⁹⁷ J. Dolejsi,¹⁴² Z. Dolezal,¹⁴² M. Donadelli,^{81d} B. Dong,^{60c} J. Donini,³⁸ A. D'Onofrio,^{15c} M. D'Onofrio,⁹¹ J. Dopke,¹⁴³ A. Doria,^{70a} M. T. Dova,⁸⁹ A. T. Doyle,⁵⁷ E. Drechsler,¹⁵¹ E. Dreyer,¹⁵¹ T. Dreyer,⁵³ A. S. Drobac,¹⁶⁹ D. Du,^{60b} T. A. du Pree,¹²⁰ Y. Duan,^{60d} F. Dubinin,¹¹¹ M. Dubovsky,^{28a} A. Dubreuil,⁵⁴ E. Duchovni,¹⁷⁹ G. Duckeck,¹¹⁴ O. A. Ducu,³⁶ D. Duda,¹¹⁵ A. Dudarev,³⁶ A. C. Dudder,¹⁰⁰ E. M. Duffield,¹⁸ M. D'uffizi,¹⁰¹ L. Duflot,⁶⁵ M. Dührssen,³⁶ C. Dülsen,¹⁸¹ M. Dumancic,¹⁷⁹ A. E. Dumitriu,^{27b} M. Dunford,^{61a} A. Duperrin,¹⁰² H. Duran Yildiz,^{4a} M. Düren,⁵⁶ A. Durglishvili,^{158b} D. Duschinger,⁴⁸ B. Dutta,⁴⁶ D. Duvnjak,¹ G. I. Dyckes,¹³⁶ M. Dyndal,³⁶ S. Dysch,¹⁰¹ B. S. Dziedzic,⁸⁵ M. G. Eggleston,⁴⁹ T. Eifert,⁸ G. Eigen,¹⁷ K. Einsweiler,¹⁸ T. Ekelof,¹⁷¹ H. El Jarrari,^{35e} V. Ellajosyula,¹⁷¹ M. Ellert,¹⁷¹ F. Ellinghaus,¹⁸¹ A. A. Elliot,⁹³ N. Ellis,³⁶ J. Elmsheuser,²⁹ M. Elsing,³⁶ D. Emelianov,¹⁴³ A. Emerman,³⁹ Y. Enari,¹⁶² M. B. Epland,⁴⁹ J. Erdmann,⁴⁷ A. Ereditato,²⁰ P. A. Erland,⁸⁵ M. Errenst,¹⁸¹ M. Escalier,⁶⁵ C. Escobar,¹⁷³ O. Estrada Pastor,¹⁷³ E. Etzion,¹⁶⁰ H. Evans,⁶⁶ M. O. Evans,¹⁵⁵ A. Ezhilov,¹³⁷ F. Fabbri,⁵⁷ L. Fabbri,^{23b,23a} V. Fabiani,¹¹⁹ G. Facini,¹⁷⁷ R. M. Fakhruddinov,¹²³ S. Falciano,^{73a} P. J. Falke,²⁴ S. Falke,³⁶ J. Faltova,¹⁴² Y. Fang,^{15a} Y. Fang,^{15a} G. Fanourakis,⁴⁴ M. Fanti,^{69a,69b} M. Faraj,^{67a,67c,m} A. Farbin,⁸ A. Farilla,^{75a} E. M. Farina,^{71a,71b} T. Farooque,¹⁰⁷ S. M. Farrington,⁵⁰ P. Farthouat,³⁶ F. Fassi,^{35e} P. Fassnacht,³⁶ D. Fassouliotis,⁹ M. Fauci Giannelli,⁵⁰ W. J. Fawcett,³² L. Fayard,⁶⁵ O. L. Fedin,^{137,n} W. Fedorko,¹⁷⁴ A. Fehr,²⁰ M. Feickert,¹⁷² L. Feligioni,¹⁰² A. Fell,¹⁴⁸ C. Feng,^{60b} M. Feng,⁴⁹ M. J. Fenton,¹⁷⁰ A. B. Fenyuk,¹²³ S. W. Ferguson,⁴³ J. Ferrando,⁴⁶ A. Ferrante,¹⁷² A. Ferrari,¹⁷¹ P. Ferrari,¹²⁰ R. Ferrari,^{71a} D. E. Ferreira de Lima,^{61b} A. Ferrer,¹⁷³ D. Ferrere,⁵⁴ C. Ferretti,¹⁰⁶ F. Fiedler,¹⁰⁰ A. Filipčič,⁹² F. Filthaut,¹¹⁹ K. D. Finelli,²⁵ M. C. N. Fiolhais,^{139a,139c,o} L. Fiorini,¹⁷³ F. Fischer,¹¹⁴ J. Fischer,¹⁰⁰ W. C. Fisher,¹⁰⁷ T. Fitschen,²¹ I. Fleck,¹⁵⁰ P. Fleischmann,¹⁰⁶ T. Flick,¹⁸¹ B. M. Flierl,¹¹⁴ L. Flores,¹³⁶ L. R. Flores Castillo,^{63a} F. M. Follega,^{76a,76b} N. Fomin,¹⁷ J. H. Foo,¹⁶⁶ G. T. Forcolin,^{76a,76b} B. C. Forland,⁶⁶ A. Formica,¹⁴⁴ F. A. Förster,¹⁴ A. C. Forti,¹⁰¹ E. Fortin,¹⁰² M. G. Foti,¹³⁴ D. Fournier,⁶⁵ H. Fox,⁹⁰ P. Francavilla,^{72a,72b} S. Francescato,^{73a,73b} M. Franchini,^{23b,23a} S. Franchino,^{61a} D. Francis,³⁶ L. Franco,⁵ L. Franconi,²⁰ M. Franklin,⁵⁹ G. Frattari,^{73a,73b} A. N. Fray,⁹³ P. M. Freeman,²¹ B. Freund,¹¹⁰ W. S. Freund,^{181b} E. M. Freundlich,⁴⁷ D. C. Frizzell,¹²⁸ D. Froidevaux,³⁶ J. A. Frost,¹³⁴ M. Fujimoto,¹²⁶ C. Fukunaga,¹⁶³ E. Fullana Torregrosa,¹⁷³ T. Fusayasu,¹¹⁶ J. Fuster,¹⁷³ A. Gabrielli,^{23b,23a} A. Gabrielli,³⁶ S. Gadatsch,⁵⁴ P. Gadow,¹¹⁵ G. Gagliardi,^{55b,55a} L. G. Gagnon,¹¹⁰ G. E. Gallardo,¹³⁴ E. J. Gallas,¹³⁴ B. J. Gallop,¹⁴³ R. Gamboa Goni,⁹³ K. K. Gan,¹²⁷ S. Ganguly,¹⁷⁹ J. Gao,^{60a} Y. Gao,⁵⁰ Y. S. Gao,^{31,p} F. M. Garay Walls,^{146a} C. García,¹⁷³ J. E. García Navarro,¹⁷³ J. A. García Pascual,^{15a} C. Garcia-Argos,⁵² M. Garcia-Sciveres,¹⁸ R. W. Gardner,³⁷ N. Garelli,¹⁵² S. Gargiulo,⁵² C. A. Garner,¹⁶⁶ V. Garonne,¹³³ S. J. Gasiorowski,¹⁴⁷ P. Gaspar,^{81b} A. Gaudiello,^{55b,55a} G. Gaudio,^{71a} I. L. Gavrilenko,¹¹¹ A. Gavriluk,¹²⁴ C. Gay,¹⁷⁴ G. Gaycken,⁴⁶ E. N. Gazis,¹⁰ A. A. Geanta,^{27b} C. M. Gee,¹⁴⁵ C. N. P. Gee,¹⁴³ J. Geisen,⁹⁷ M. Geisen,¹⁰⁰ C. Gemme,^{55b} M. H. Genest,⁵⁸ C. Geng,¹⁰⁶ S. Gentile,^{73a,73b} S. George,⁹⁴ T. Gerialis,⁴⁴ L. O. Gerlach,⁵³ P. Gessinger-Befurt,¹⁰⁰ G. Gessner,⁴⁷ S. Ghasemi,¹⁵⁰ M. Ghasemi Bostanabad,¹⁷⁵ M. Ghneimat,¹⁵⁰ A. Ghosh,⁶⁵ A. Ghosh,⁷⁸ B. Giacobbe,^{23b} S. Giagu,^{73a,73b} N. Giangiacomini,^{23b,23a} P. Giannetti,^{72a} A. Giannini,^{70a,70b} G. Giannini,¹⁴ S. M. Gibson,⁹⁴ M. Gignac,¹⁴⁵ D. T. Gil,^{84b} B. J. Gilbert,³⁹ D. Gillberg,³⁴ G. Gilles,¹⁸¹ D. M. Gingrich,^{3,d} M. P. Giordani,^{67a,67c} P. F. Giraud,¹⁴⁴ G. Giugliarelli,^{67a,67c} D. Giugni,^{69a} F. Giulii,^{74a,74b} S. Gkaitatzis,¹⁶¹ I. Gkialas,^{9,q} E. L. Gkougkousis,¹⁴

P. Gkoutoumis,¹⁰ L. K. Gladilin,¹¹³ C. Glasman,⁹⁹ J. Glatzer,¹⁴ P. C. F. Glaysheer,⁴⁶ A. Glazov,⁴⁶ G. R. Gledhill,¹³¹
 I. Gnesi,^{41b,r} M. Goblirsch-Kolb,²⁶ D. Godin,¹¹⁰ S. Goldfarb,¹⁰⁵ T. Golling,⁵⁴ D. Golubkov,¹²³ A. Gomes,^{139a,139b}
 R. Goncalves Gama,⁵³ R. Gonçalo,^{139a,139c} G. Gonella,¹³¹ L. Gonella,²¹ A. Gongadze,⁸⁰ F. Gonnella,²¹ J. L. Gonski,³⁹
 S. González de la Hoz,¹⁷³ S. Gonzalez Fernandez,¹⁴ R. Gonzalez Lopez,⁹¹ C. Gonzalez Renteria,¹⁸ R. Gonzalez Suarez,¹⁷¹
 S. Gonzalez-Sevilla,⁵⁴ G. R. Gonzalvo Rodriguez,¹⁷³ L. Goossens,³⁶ N. A. Gorasia,²¹ P. A. Gorbounov,¹²⁴ H. A. Gordon,²⁹
 B. Gorini,³⁶ E. Gorini,^{68a,68b} A. Gorišek,⁹² A. T. Goshaw,⁴⁹ M. I. Gostkin,⁸⁰ C. A. Gottardo,¹¹⁹ M. Goughri,^{35b}
 A. G. Goussiou,¹⁴⁷ N. Govender,^{33c} C. Goy,⁵ I. Grabowska-Bold,^{84a} E. C. Graham,⁹¹ J. Gramling,¹⁷⁰ E. Gramstad,¹³³
 S. Grancagnolo,¹⁹ M. Grandi,¹⁵⁵ V. Gratchev,¹³⁷ P. M. Gravila,^{27f} F. G. Gravili,^{68a,68b} C. Gray,⁵⁷ H. M. Gray,¹⁸ C. Grefe,²⁴
 K. Gregersen,⁹⁷ I. M. Gregor,⁴⁶ P. Grenier,¹⁵² K. Grevtsov,⁴⁶ C. Grieco,¹⁴ N. A. Grieser,¹²⁸ A. A. Grillo,¹⁴⁵ K. Grimm,^{31,s}
 S. Grinstein,^{14,t} J.-F. Grivaz,⁶⁵ S. Groh,¹⁰⁰ E. Gross,¹⁷⁹ J. Grosse-Knetter,⁵³ Z. J. Grout,⁹⁵ C. Grud,¹⁰⁶ A. Grummer,¹¹⁸
 J. C. Grundy,¹³⁴ L. Guan,¹⁰⁶ W. Guan,¹⁸⁰ C. Gubbels,¹⁷⁴ J. Guenther,³⁶ A. Guerguichon,⁶⁵ J. G. R. Guerrero Rojas,¹⁷³
 F. Guescini,¹¹⁵ D. Guest,¹⁷⁰ R. Gugel,¹⁰⁰ A. Guida,⁴⁶ T. Guillemin,⁵ S. Guindon,³⁶ U. Gul,⁵⁷ J. Guo,^{60c} W. Guo,¹⁰⁶ Y. Guo,^{60a}
 Z. Guo,¹⁰² R. Gupta,⁴⁶ S. Gurbuz,^{12c} G. Gustavino,¹²⁸ M. Guth,⁵² P. Gutierrez,¹²⁸ C. Gutschow,⁹⁵ C. Guyot,¹⁴⁴
 C. Gwenlan,¹³⁴ C. B. Gwilliam,⁹¹ E. S. Haaland,¹³³ A. Haas,¹²⁵ C. Haber,¹⁸ H. K. Hadavand,⁸ A. Hadeef,^{60a} M. Haleem,¹⁷⁶
 J. Haley,¹²⁹ J. J. Hall,¹⁴⁸ G. Halladjian,¹⁰⁷ G. D. Hallowell,¹⁰² K. Hamano,¹⁷⁵ H. Hamdaoui,^{35e} M. Hamer,²⁴ G. N. Hamity,⁵⁰
 K. Han,^{60a,u} L. Han,^{60a} S. Han,¹⁸ Y. F. Han,¹⁶⁶ K. Hanagaki,^{82,v} M. Hance,¹⁴⁵ D. M. Handl,¹¹⁴ M. D. Hank,³⁷ R. Hankache,¹³⁵
 E. Hansen,⁹⁷ J. B. Hansen,⁴⁰ J. D. Hansen,⁴⁰ M. C. Hansen,²⁴ P. H. Hansen,⁴⁰ E. C. Hanson,¹⁰¹ K. Hara,¹⁶⁸ T. Harenberg,¹⁸¹
 S. Harkusha,¹⁰⁸ P. F. Harrison,¹⁷⁷ N. M. Hartman,¹⁵² N. M. Hartmann,¹¹⁴ Y. Hasegawa,¹⁴⁹ A. Hasib,⁵⁰ S. Hassani,¹⁴⁴
 S. Haug,²⁰ R. Hauser,¹⁰⁷ L. B. Havener,³⁹ M. Havranek,¹⁴¹ C. M. Hawkes,²¹ R. J. Hawkings,³⁶ S. Hayashida,¹¹⁷
 D. Hayden,¹⁰⁷ C. Hayes,¹⁰⁶ R. L. Hayes,¹⁷⁴ C. P. Hays,¹³⁴ J. M. Hays,⁹³ H. S. Hayward,⁹¹ S. J. Haywood,¹⁴³ F. He,^{60a}
 Y. He,¹⁶⁴ M. P. Heath,⁵⁰ V. Hedberg,⁹⁷ S. Heer,²⁴ A. L. Heggelund,¹³³ C. Heidegger,⁵² K. K. Heidegger,⁵² W. D. Heidorn,⁷⁹
 J. Heilman,³⁴ S. Heim,⁴⁶ T. Heim,¹⁸ B. Heinemann,^{46,w} J. G. Heinlein,¹³⁶ J. J. Heinrich,¹³¹ L. Heinrich,³⁶ J. Hejbal,¹⁴⁰
 L. Helary,⁴⁶ A. Held,¹²⁵ S. Hellesund,¹³³ C. M. Helling,¹⁴⁵ S. Hellman,^{45a,45b} C. Helsen,³⁶ R. C. W. Henderson,⁹⁰
 Y. Heng,¹⁸⁰ L. Henkelmann,³² A. M. Henriques Correia,³⁶ H. Herde,²⁶ Y. Hernández Jiménez,^{33e} H. Herr,¹⁰⁰
 M. G. Herrmann,¹¹⁴ T. Herrmann,⁴⁸ G. Herten,⁵² R. Hertenberger,¹¹⁴ L. Hervas,³⁶ T. C. Herwig,¹³⁶ G. G. Hesketh,⁹⁵
 N. P. Hesse,^{167a} H. Hibi,⁸³ A. Higashida,¹⁶² S. Higashino,⁸² E. Higón-Rodríguez,¹⁷³ K. Hildebrand,³⁷ J. C. Hill,³²
 K. K. Hill,²⁹ K. H. Hiller,⁴⁶ S. J. Hillier,²¹ M. Hils,⁴⁸ I. Hinchliffe,¹⁸ F. Hinterkeuser,²⁴ M. Hirose,¹³² S. Hirose,⁵²
 D. Hirschbuehl,¹⁸¹ B. Hiti,⁹² O. Hladik,¹⁴⁰ D. R. Hlaluku,^{33e} J. Hobbs,¹⁵⁴ N. Hod,¹⁷⁹ M. C. Hodgkinson,¹⁴⁸ A. Hoecker,³⁶
 D. Hohn,⁵² D. Hohov,⁶⁵ T. Holm,²⁴ T. R. Holmes,³⁷ M. Holzbock,¹¹⁴ L. B. A. H. Hommels,³² T. M. Hong,¹³⁸ J. C. Honig,⁵²
 A. Hönle,¹¹⁵ B. H. Hooberman,¹⁷² W. H. Hopkins,⁶ Y. Horii,¹¹⁷ P. Horn,⁴⁸ L. A. Horyn,³⁷ S. Hou,¹⁵⁷ A. Hoummada,^{35a}
 J. Howarth,⁵⁷ J. Hoya,⁸⁹ M. Hrabovsky,¹³⁰ J. Hrdinka,⁷⁷ J. Hrivnac,⁶⁵ A. Hrynevich,¹⁰⁹ T. Hryn'ova,⁵ P. J. Hsu,⁶⁴
 S.-C. Hsu,¹⁴⁷ Q. Hu,²⁹ S. Hu,^{60c} Y. F. Hu,^{15a,15d,x} D. P. Huang,⁹⁵ Y. Huang,^{60a} Y. Huang,^{15a} Z. Hubacek,¹⁴¹ F. Hubaut,¹⁰²
 M. Huebner,²⁴ F. Huegging,²⁴ T. B. Huffman,¹³⁴ M. Huhtinen,³⁶ R. Hulsken,⁵⁸ R. F. H. Hunter,³⁴ P. Huo,¹⁵⁴ N. Huseynov,^{80,y}
 J. Huston,¹⁰⁷ J. Huth,⁵⁹ R. Hyneman,¹⁵² S. Hyrych,^{28a} G. Iacobucci,⁵⁴ G. Iakovidis,²⁹ I. Ibragimov,¹⁵⁰
 L. Iconomidou-Fayard,⁶⁵ P. Iengo,³⁶ R. Ignazzi,⁴⁰ O. Igonkina,^{120,a,z} R. Iguchi,¹⁶² T. Iizawa,⁵⁴ Y. Ikegami,⁸² M. Ikeno,⁸²
 N. Ilic,^{119,166,1} F. Iltzsche,⁴⁸ H. Imam,^{35a} G. Introzzi,^{71a,71b} M. Iodice,^{75a} K. Iordanidou,^{167a} V. Ippolito,^{73a,73b} M. F. Isacson,¹⁷¹
 M. Ishino,¹⁶² W. Islam,¹²⁹ C. Issever,^{19,46} S. Istin,¹⁵⁹ F. Ito,¹⁶⁸ J. M. Iturbe Ponce,^{63a} R. Iuppa,^{76a,76b} A. Ivina,¹⁷⁹ H. Iwasaki,⁸²
 J. M. Izen,⁴³ V. Izzo,^{70a} P. Jacka,¹⁴⁰ P. Jackson,¹ R. M. Jacobs,⁴⁶ B. P. Jaeger,¹⁵¹ V. Jain,² G. Jäkel,¹⁸¹ K. B. Jakobi,¹⁰⁰
 K. Jakobs,⁵² T. Jakoubek,¹⁷⁹ J. Jamieson,⁵⁷ K. W. Janas,^{84a} R. Jansky,⁵⁴ M. Janus,⁵³ P. A. Janus,^{84a} G. Jarlskog,⁹⁷
 A. E. Jaspán,⁹¹ N. Javadov,^{80,y} T. Javůrek,³⁶ M. Javurkova,¹⁰³ F. Jeanneau,¹⁴⁴ L. Jeanty,¹³¹ J. Jejelava,^{158a} P. Jenni,^{52,aa}
 N. Jeong,⁴⁶ S. Jézéquel,⁵ H. Ji,¹⁸⁰ J. Jia,¹⁵⁴ H. Jiang,⁷⁹ Y. Jiang,^{60a} Z. Jiang,¹⁵² S. Jiggins,⁵² F. A. Jimenez Morales,³⁸
 J. Jimenez Pena,¹¹⁵ S. Jin,^{15c} A. Jinaru,^{27b} O. Jinnouchi,¹⁶⁴ H. Jivan,^{33e} P. Johansson,¹⁴⁸ K. A. Johns,⁷ C. A. Johnson,⁶⁶
 R. W. L. Jones,⁹⁰ S. D. Jones,¹⁵⁵ T. J. Jones,⁹¹ J. Jongmanns,^{61a} J. Jovicevic,³⁶ X. Ju,¹⁸ J. J. Junggeburth,¹¹⁵
 A. Juste Rozas,^{14,t} A. Kaczmarska,⁸⁵ M. Kado,^{73a,73b} H. Kagan,¹²⁷ M. Kagan,¹⁵² A. Kahn,³⁹ C. Kahra,¹⁰⁰ T. Kaji,¹⁷⁸
 E. Kajomovitz,¹⁵⁹ C. W. Kalderon,²⁹ A. Kaluza,¹⁰⁰ A. Kamenshchikov,¹²³ M. Kaneda,¹⁶² N. J. Kang,¹⁴⁵ S. Kang,⁷⁹
 Y. Kano,¹¹⁷ J. Kanzaki,⁸² L. S. Kaplan,¹⁸⁰ D. Kar,^{33e} K. Karava,¹³⁴ M. J. Kareem,^{167b} I. Karkanias,¹⁶¹ S. N. Karpov,⁸⁰
 Z. M. Karpova,⁸⁰ V. Kartvelishvili,⁹⁰ A. N. Karyukhin,¹²³ E. Kasimi,¹⁶¹ A. Kastanas,^{45a,45b} C. Kato,^{60d,60c} J. Katzy,⁴⁶
 K. Kawade,¹⁴⁹ K. Kawagoe,⁸⁸ T. Kawaguchi,¹¹⁷ T. Kawamoto,¹⁴⁴ G. Kawamura,⁵³ E. F. Kay,¹⁷⁵ S. Kazakos,¹⁴
 V. F. Kazanin,^{122b,122a} R. Keeler,¹⁷⁵ R. Kehoe,⁴² J. S. Keller,³⁴ E. Kellermann,⁹⁷ D. Kelsey,¹⁵⁵ J. J. Kempster,²¹ J. Kendrick,²¹

K. E. Kennedy,³⁹ O. Kepka,¹⁴⁰ S. Kersten,¹⁸¹ B. P. Kerševan,⁹² S. Ketabchi Haghghat,¹⁶⁶ M. Khader,¹⁷² F. Khalil-Zada,¹³ M. Khandoga,¹⁴⁴ A. Khanov,¹²⁹ A. G. Kharlamov,^{122b,122a} T. Kharlamova,^{122b,122a} E. E. Khoda,¹⁷⁴ A. Khodinov,¹⁶⁵ T. J. Khoo,⁵⁴ G. Khoraiuli,¹⁷⁶ E. Khramov,⁸⁰ J. Khubua,^{158b} S. Kido,⁸³ M. Kiehn,³⁶ C. R. Kilby,⁹⁴ E. Kim,¹⁶⁴ Y. K. Kim,³⁷ N. Kimura,⁹⁵ A. Kirchhoff,⁵³ D. Kirchmeier,⁴⁸ J. Kirk,¹⁴³ A. E. Kiryunin,¹¹⁵ T. Kishimoto,¹⁶² D. P. Kisliuk,¹⁶⁶ V. Kitalli,⁴⁶ C. Kitsaki,¹⁰ O. Kivernyk,²⁴ T. Klapdor-Kleingrothaus,⁵² M. Klassen,^{61a} C. Klein,³⁴ M. H. Klein,¹⁰⁶ M. Klein,⁹¹ U. Klein,⁹¹ K. Kleinknecht,¹⁰⁰ P. Klimek,¹²¹ A. Klimentov,²⁹ T. Klingl,²⁴ T. Klioutchnikova,³⁶ F. F. Klitzner,¹¹⁴ P. Kluit,¹²⁰ S. Kluth,¹¹⁵ E. Kneringer,⁷⁷ E. B. F. G. Knoops,¹⁰² A. Knue,⁵² D. Kobayashi,⁸⁸ M. Kobel,⁴⁸ M. Kocian,¹⁵² T. Kodama,¹⁶² P. Kodys,¹⁴² D. M. Koeck,¹⁵⁵ P. T. Koenig,²⁴ T. Koffas,³⁴ N. M. Köhler,³⁶ M. Kolb,¹⁴⁴ I. Koletsou,⁵ T. Komarek,¹³⁰ T. Kondo,⁸² K. Köneke,⁵² A. X. Y. Kong,¹ A. C. König,¹¹⁹ T. Kono,¹²⁶ V. Konstantinides,⁹⁵ N. Konstantinidis,⁹⁵ B. Konya,⁹⁷ R. Kopeliainsky,⁶⁶ S. Koperny,^{84a} K. Korcyl,⁸⁵ K. Kordas,¹⁶¹ G. Koren,¹⁶⁰ A. Korn,⁹⁵ I. Korolkov,¹⁴ E. V. Korolkova,¹⁴⁸ N. Korotkova,¹¹³ O. Kortner,¹¹⁵ S. Kortner,¹¹⁵ V. V. Kostyukhin,^{148,165} A. Kotskechagia,⁶⁵ A. Kotwal,⁴⁹ A. Koulouris,¹⁰ A. Kourkoulis-Charalampidi,^{71a,71b} C. Kourkoulis,⁹ E. Kourlitis,⁶ V. Kouskoura,²⁹ R. Kowalewski,¹⁷⁵ W. Kozanecki,¹⁰¹ A. S. Kozhin,¹²³ V. A. Kramarenko,¹¹³ G. Kramberger,⁹² D. Krasnopevtsev,^{60a} M. W. Krasny,¹³⁵ A. Krasznahorkay,³⁶ D. Krauss,¹¹⁵ J. A. Kremer,¹⁰⁰ J. Kretzschmar,⁹¹ P. Krieger,¹⁶⁶ F. Krieter,¹¹⁴ A. Krishnan,^{61b} M. Krivos,¹⁴² K. Krizka,¹⁸ K. Kroeninger,⁴⁷ H. Kroha,¹¹⁵ J. Kroll,¹⁴⁰ J. Kroll,¹³⁶ K. S. Krowpman,¹⁰⁷ U. Kruchonak,⁸⁰ H. Krüger,²⁴ N. Krumnack,⁷⁹ M. C. Kruse,⁴⁹ J. A. Krzysiak,⁸⁵ A. Kubota,¹⁶⁴ O. Kuchinskaia,¹⁶⁵ S. Kuday,^{4b} D. Kuechler,⁴⁶ J. T. Kuechler,⁴⁶ S. Kuehn,³⁶ T. Kuhl,⁴⁶ V. Kukhtin,⁸⁰ Y. Kulchitsky,^{108,bb} S. Kuleshov,^{146b} Y. P. Kulinich,¹⁷² M. Kuna,⁵⁸ T. Kunigo,⁸⁶ A. Kupco,¹⁴⁰ T. Kupfer,⁴⁷ O. Kuprash,⁵² H. Kurashige,⁸³ L. L. Kurchaninov,^{167a} Y. A. Kurochkin,¹⁰⁸ A. Kurova,¹¹² M. G. Kurth,^{15a,15d} E. S. Kuwertz,³⁶ M. Kuze,¹⁶⁴ A. K. Kvam,¹⁴⁷ J. Kvitka,¹³⁰ T. Kwan,¹⁰⁴ F. La Ruffa,^{41b,41a} C. Lacasta,¹⁷³ F. Lacava,^{73a,73b} D. P. J. Lack,¹⁰¹ H. Lacker,¹⁹ D. Lacour,¹³⁵ E. Ladygin,⁸⁰ R. Lafaye,⁵ B. Laforge,¹³⁵ T. Lagouri,^{146c} S. Lai,⁵³ I. K. Lakomicz,^{84a} J. E. Lambert,¹²⁸ S. Lammers,⁶⁶ W. Lampl,⁷ C. Lampoudis,¹⁶¹ E. Lançon,²⁹ U. Landgraf,⁵² M. P. J. Landon,⁹³ M. C. Lanfermann,⁵⁴ V. S. Lang,⁵² J. C. Lange,⁵³ R. J. Langenberg,¹⁰³ A. J. Lankford,¹⁷⁰ F. Lanni,²⁹ K. Lantzsich,²⁴ A. Lanza,^{71a} A. Lapertosa,^{55b,55a} J. F. Laporte,¹⁴⁴ T. Lari,^{69a} F. Lasagni Manghi,^{23b,23a} M. Lassnig,³⁶ T. S. Lau,^{63a} A. Laudrain,⁶⁵ A. Laurier,³⁴ M. Lavorgna,^{70a,70b} S. D. Lawlor,⁹⁴ M. Lazzaroni,^{69a,69b} B. Le,¹⁰¹ E. Le Guirrec,¹⁰² A. Lebedev,⁷⁹ M. LeBlanc,⁷ T. LeCompte,⁶ F. Ledroit-Guillon,⁵⁸ A. C. A. Lee,⁹⁵ C. A. Lee,²⁹ G. R. Lee,¹⁷ L. Lee,⁵⁹ S. C. Lee,¹⁵⁷ S. Lee,⁷⁹ B. Lefebvre,^{167a} H. P. Lefebvre,⁹⁴ M. Lefebvre,¹⁷⁵ C. Leggett,¹⁸ K. Lehmann,¹⁵¹ N. Lehmann,²⁰ G. Lehmann Miotto,³⁶ W. A. Leight,⁴⁶ A. Leisos,^{161,cc} M. A. L. Leite,^{81d} C. E. Leitgeb,¹¹⁴ R. Leitner,¹⁴² D. Lellouch,^{179,a} K. J. C. Leney,⁴² T. Lenz,²⁴ S. Leone,^{72a} C. Leonidopoulos,⁵⁰ A. Leopold,¹³⁵ C. Leroy,¹¹⁰ R. Les,¹⁰⁷ C. G. Lester,³² M. Levchenko,¹³⁷ J. Levêque,⁵ D. Levin,¹⁰⁶ L. J. Levinson,¹⁷⁹ D. J. Lewis,²¹ B. Li,^{15b} B. Li,¹⁰⁶ C-Q. Li,^{60a} F. Li,^{60c} H. Li,^{60a} H. Li,^{60b} J. Li,^{60c} K. Li,¹⁴⁷ L. Li,^{60c} M. Li,^{15a,15d} Q. Li,^{15a,15d} Q. Y. Li,^{60a} S. Li,^{60d,60c} X. Li,⁴⁶ Y. Li,⁴⁶ Z. Li,^{60b} Z. Li,¹³⁴ Z. Li,¹⁰⁴ Z. Liang,^{15a} M. Liberatore,⁴⁶ B. Liberti,^{74a} A. Liblong,¹⁶⁶ K. Lie,^{63c} S. Lim,²⁹ C. Y. Lin,³² K. Lin,¹⁰⁷ R. A. Linck,⁶⁶ R. E. Lindley,⁷ J. H. Lindon,²¹ A. Linss,⁴⁶ A. L. Lioni,⁵⁴ E. Lipeles,¹³⁶ A. Lipniacka,¹⁷ T. M. Liss,^{172,dd} A. Lister,¹⁷⁴ J. D. Little,⁸ B. Liu,⁷⁹ B. L. Liu,²⁹ H. B. Liu,^{60a} J. K. K. Liu,³⁷ K. Liu,^{60d} M. Liu,^{60a} P. Liu,^{15a} X. Liu,^{60a} Y. Liu,⁴⁶ Y. Liu,^{15a,15d} Y. L. Liu,¹⁰⁶ Y. W. Liu,^{60a} M. Livan,^{71a,71b} A. Lleres,⁵⁸ J. Llorente Merino,¹⁵¹ S. L. Lloyd,⁹³ C. Y. Lo,^{63b} E. M. Lobodzinska,⁴⁶ P. Loch,⁷ S. Loffredo,^{74a,74b} T. Lohse,¹⁹ K. Lohwasser,¹⁴⁸ M. Lokajicek,¹⁴⁰ J. D. Long,¹⁷² R. E. Long,⁹⁰ I. Longarini,^{73a,73b} L. Longo,³⁶ K. A. Looper,¹²⁷ I. Lopez Paz,¹⁰¹ A. Lopez Solis,¹⁴⁸ J. Lorenz,¹¹⁴ N. Lorenzo Martinez,⁵ A. M. Lory,¹¹⁴ P. J. Lösel,¹¹⁴ A. Lösle,⁵² X. Lou,⁴⁶ X. Lou,^{15a} A. Lounis,⁶⁵ J. Love,⁶ P. A. Love,⁹⁰ J. J. Lozano Bahilo,¹⁷³ M. Lu,^{60a} Y. J. Lu,⁶⁴ H. J. Lubatti,¹⁴⁷ C. Luci,^{73a,73b} F. L. Lucio Alves,^{15c} A. Lucotte,⁵⁸ F. Luehring,⁶⁶ I. Luise,¹³⁵ L. Luminari,^{73a} B. Lund-Jensen,¹⁵³ M. S. Lutz,¹⁶⁰ D. Lynn,²⁹ H. Lyons,⁹¹ R. Lysak,¹⁴⁰ E. Lytken,⁹⁷ F. Lyu,^{15a} V. Lyubushkin,⁸⁰ T. Lyubushkina,⁸⁰ H. Ma,²⁹ L. L. Ma,^{60b} Y. Ma,⁹⁵ D. M. Mac Donell,¹⁷⁵ G. Maccarrone,⁵¹ A. Macchiolo,¹¹⁵ C. M. Macdonald,¹⁴⁸ J. C. MacDonald,¹⁴⁸ J. Machado Miguens,¹³⁶ D. Madaffari,¹⁷³ R. Madar,³⁸ W. F. Mader,⁴⁸ M. Madugoda Ralalage Don,¹²⁹ N. Madysa,⁴⁸ J. Maeda,⁸³ T. Maeno,²⁹ M. Maerker,⁴⁸ V. Magerl,⁵² N. Magini,⁷⁹ J. Magro,^{67a,67c,m} D. J. Mahon,³⁹ C. Maidantchik,^{81b} T. Maier,¹¹⁴ A. Maio,^{139a,139b,139d} K. Maj,^{84a} O. Majersky,^{28a} S. Majewski,¹³¹ Y. Makida,⁸² N. Makovec,⁶⁵ B. Malaescu,¹³⁵ Pa. Malecki,⁸⁵ V. P. Maleev,¹³⁷ F. Malek,⁵⁸ D. Malito,^{41b,41a} U. Mallik,⁷⁸ D. Malon,⁶ C. Malone,³² S. Maltezos,¹⁰ S. Malyukov,⁸⁰ J. Mamuzic,¹⁷³ G. Mancini,^{70a,70b} I. Mandić,⁹² L. Manhaes de Andrade Filho,^{81a} I. M. Maniatis,¹⁶¹ J. Manjarres Ramos,⁴⁸ K. H. Mankinen,⁹⁷ A. Mann,¹¹⁴ A. Manousos,⁷⁷ B. Mansoulie,¹⁴⁴ I. Manthos,¹⁶¹ S. Manzoni,¹²⁰ A. Marantis,¹⁶¹ G. Marceca,³⁰ L. Marchese,¹³⁴ G. Marchiori,¹³⁵ M. Marcisovsky,¹⁴⁰ L. Marcoccia,^{74a,74b} C. Marcon,⁹⁷ C. A. Marin Tobon,³⁶ M. Marjanovic,¹²⁸ Z. Marshall,¹⁸ M. U. F. Martensson,¹⁷¹ S. Marti-Garcia,¹⁷³ C. B. Martin,¹²⁷ T. A. Martin,¹⁷⁷ V. J. Martin,⁵⁰ B. Martin dit Latour,¹⁷

L. Martinelli,^{75a,75b} M. Martinez,^{14,t} P. Martinez Agullo,¹⁷³ V. I. Martinez Outschoorn,¹⁰³ S. Martin-Haugh,¹⁴³
V. S. Martoiu,^{27b} A. C. Martyniuk,⁹⁵ A. Marzin,³⁶ S. R. Maschek,¹¹⁵ L. Masetti,¹⁰⁰ T. Mashimo,¹⁶² R. Mashinistov,¹¹¹
J. Masik,¹⁰¹ A. L. Maslennikov,^{122b,122a} L. Massa,^{23b,23a} P. Massarotti,^{70a,70b} P. Mastrandrea,^{72a,72b} A. Mastroberardino,^{41b,41a}
T. Masubuchi,¹⁶² D. Matakias,²⁹ A. Matic,¹¹⁴ N. Matsuzawa,¹⁶² P. Mättig,²⁴ J. Maurer,^{27b} B. Maček,⁹²
D. A. Maximov,^{122b,122a} R. Mazini,¹⁵⁷ I. Maznas,¹⁶¹ S. M. Mazza,¹⁴⁵ J. P. Mc Gowan,¹⁰⁴ S. P. Mc Kee,¹⁰⁶ T. G. McCarthy,¹¹⁵
W. P. McCormack,¹⁸ E. F. McDonald,¹⁰⁵ J. A. MCFayden,³⁶ G. Mchedlidze,^{158b} M. A. McKay,⁴² K. D. McLean,¹⁷⁵
S. J. McMahon,¹⁴³ P. C. McNamara,¹⁰⁵ C. J. McNicol,¹⁷⁷ R. A. McPherson,^{175,1} J. E. Mdhului,^{33e} Z. A. Meadows,¹⁰³
S. Meehan,³⁶ T. Megy,³⁸ S. Mehlhase,¹¹⁴ A. Mehta,⁹¹ B. Meirose,⁴³ D. Melini,¹⁵⁹ B. R. Mellado Garcia,^{33e}
J. D. Mellenthin,⁵³ M. Melo,^{28a} F. Meloni,⁴⁶ A. Melzer,²⁴ E. D. Mendes Gouveia,^{139a,139e} L. Meng,³⁶ X. T. Meng,¹⁰⁶
S. Menke,¹¹⁵ E. Meoni,^{41b,41a} S. Mergelmeyer,¹⁹ S. A. M. Merkt,¹³⁸ C. Merlassino,¹³⁴ P. Mermod,⁵⁴ L. Merola,^{70a,70b}
C. Meroni,^{69a} G. Merz,¹⁰⁶ O. Meshkov,^{113,111} J. K. R. Meshreki,¹⁵⁰ J. Metcalfe,⁶ A. S. Mete,⁶ C. Meyer,⁶⁶ J-P. Meyer,¹⁴⁴
M. Michetti,¹⁹ R. P. Middleton,¹⁴³ L. Mijović,⁵⁰ G. Mikenberg,¹⁷⁹ M. Mikestikova,¹⁴⁰ M. Mikuz,⁹² H. Mildner,¹⁴⁸
A. Milic,¹⁶⁶ C. D. Milke,⁴² D. W. Miller,³⁷ A. Milov,¹⁷⁹ D. A. Milstead,^{45a,45b} R. A. Mina,¹⁵² A. A. Minaenko,¹²³
I. A. Minashvili,^{158b} A. I. Mincer,¹²⁵ B. Mindur,^{84a} M. Mineev,⁸⁰ Y. Minegishi,¹⁶² L. M. Mir,¹⁴ M. Mironova,¹³⁴
A. Mirto,^{68a,68b} K. P. Mistry,¹³⁶ T. Mitani,¹⁷⁸ J. Mitrevski,¹¹⁴ V. A. Mitsou,¹⁷³ M. Mittal,^{60c} O. Miu,¹⁶⁶ A. Miucci,²⁰
P. S. Miyagawa,⁹³ A. Mizukami,⁸² J. U. Mjörnmark,⁹⁷ T. Mkrtychyan,^{61a} M. Mlynarikova,¹⁴² T. Moa,^{45a,45b} S. Mobius,⁵³
K. Mochizuki,¹¹⁰ P. Mogg,¹¹⁴ S. Mohapatra,³⁹ R. Moles-Valls,²⁴ K. Mönig,⁴⁶ E. Monnier,¹⁰² A. Montalbano,¹⁵¹
J. Montejo Berlingen,³⁶ M. Montella,⁹⁵ F. Monticelli,⁸⁹ S. Monzani,^{69a} N. Morange,⁶⁵ A. L. Moreira De Carvalho,^{139a}
D. Moreno,^{22a} M. Moreno Llácer,¹⁷³ C. Moreno Martinez,¹⁴ P. Morettini,^{55b} M. Morgenstern,¹⁵⁹ S. Morgenstern,⁴⁸
D. Mori,¹⁵¹ M. Morii,⁵⁹ M. Morinaga,¹⁷⁸ V. Morisbak,¹³³ A. K. Morley,³⁶ G. Mornacchi,³⁶ A. P. Morris,⁹⁵ L. Morvaj,¹⁵⁴
P. Moschovakos,³⁶ B. Moser,¹²⁰ M. Mosidze,^{158b} T. Moskalets,¹⁴⁴ J. Moss,^{31,ee} E. J. W. Moyse,¹⁰³ S. Muanza,¹⁰²
J. Mueller,¹³⁸ R. S. P. Mueller,¹¹⁴ D. Muenstermann,⁹⁰ G. A. Mullier,⁹⁷ D. P. Mungo,^{69a,69b} J. L. Munoz Martinez,¹⁴
F. J. Munoz Sanchez,¹⁰¹ P. Murin,^{28b} W. J. Murray,^{177,143} A. Murrone,^{69a,69b} J. M. Muse,¹²⁸ M. Muškinja,¹⁸ C. Mwewa,^{33a}
A. G. Myagkov,^{123,i} A. A. Myers,¹³⁸ G. Myers,⁶⁶ J. Myers,¹³¹ M. Myska,¹⁴¹ B. P. Nachman,¹⁸ O. Nackenhorst,⁴⁷
A. Nag Nag,⁴⁸ K. Nagai,¹³⁴ K. Nagano,⁸² Y. Nagasaka,⁶² J. L. Nagle,²⁹ E. Nagy,¹⁰² A. M. Nairz,³⁶ Y. Nakahama,¹¹⁷
K. Nakamura,⁸² T. Nakamura,¹⁶² H. Nanjo,¹³² F. Napolitano,^{61a} R. F. Naranjo Garcia,⁴⁶ R. Narayan,⁴² I. Naryshkin,¹³⁷
T. Naumann,⁴⁶ G. Navarro,^{22a} P. Y. Nechaeva,¹¹¹ F. Nechansky,⁴⁶ T. J. Neep,²¹ A. Negri,^{71a,71b} M. Negrini,^{23b} C. Nellist,¹¹⁹
C. Nelson,¹⁰⁴ M. E. Nelson,^{45a,45b} S. Nemecek,¹⁴⁰ M. Nessi,^{36,ff} M. S. Neubauer,¹⁷² F. Neuhaus,¹⁰⁰ M. Neumann,¹⁸¹
R. Newhouse,¹⁷⁴ P. R. Newman,²¹ C. W. Ng,¹³⁸ Y. S. Ng,¹⁹ Y. W. Y. Ng,¹⁷⁰ B. Ngair,^{35e} H. D. N. Nguyen,¹⁰²
T. Nguyen Manh,¹¹⁰ E. Nibigira,³⁸ R. B. Nickerson,¹³⁴ R. Nicolaidou,¹⁴⁴ D. S. Nielsen,⁴⁰ J. Nielsen,¹⁴⁵ M. Niemeyer,⁵³
N. Nikiforou,¹¹ V. Nikolaenko,^{123,i} I. Nikolic-Audit,¹³⁵ K. Nikolopoulos,²¹ P. Nilsson,²⁹ H. R. Nindhito,⁵⁴ Y. Ninomiya,⁸²
A. Nisati,^{73a} N. Nishu,^{60c} R. Nisius,¹¹⁵ I. Nitsche,⁴⁷ T. Nitta,¹⁷⁸ T. Nobe,¹⁶² D. L. Noel,³² Y. Noguchi,⁸⁶ I. Nomidis,¹³⁵
M. A. Nomura,²⁹ M. Nordberg,³⁶ J. Novak,⁹² T. Novak,⁹² O. Novgorodova,⁴⁸ R. Novotny,¹⁴¹ L. Nozka,¹³⁰ K. Ntekas,¹⁷⁰
E. Nurse,⁹⁵ F. G. Oakham,^{34,d} H. Oberlack,¹¹⁵ J. Ocariz,¹³⁵ A. Ochi,⁸³ I. Ochoa,³⁹ J. P. Ochoa-Ricoux,^{146a} K. O'Connor,²⁶
S. Oda,⁸⁸ S. Odaka,⁸² S. Oerdek,⁵³ A. Ogrodnik,^{84a} A. Oh,¹⁰¹ C. C. Ohm,¹⁵³ H. Oide,¹⁶⁴ M. L. Ojeda,¹⁶⁶ H. Okawa,¹⁶⁸
Y. Okazaki,⁸⁶ M. W. O'Keefe,⁹¹ Y. Okumura,¹⁶² T. Okuyama,⁸² A. Olariu,^{27b} L. F. Oleiro Seabra,^{139a} S. A. Olivares Pino,^{146a}
D. Oliveira Damazio,²⁹ J. L. Oliver,¹ M. J. R. Olsson,¹⁷⁰ A. Olszewski,⁸⁵ J. Olszowska,⁸⁵ Ö. O. Öncel,²⁴ D. C. O'Neil,¹⁵¹
A. P. O'neil,¹³⁴ A. Onofre,^{139a,139e} P. U. E. Onyisi,¹¹ H. Oppen,¹³³ R. G. Oreamuno Madriz,¹²¹ M. J. Oreglia,³⁷
G. E. Orellana,⁸⁹ D. Orestano,^{75a,75b} N. Orlando,¹⁴ R. S. Orr,¹⁶⁶ V. O'Shea,⁵⁷ R. Ospanov,^{60a} G. Otero y Garzon,³⁰
H. Otono,⁸⁸ P. S. Ott,^{61a} G. J. Ottino,¹⁸ M. Ouchrif,^{35d} J. Ouellette,²⁹ F. Ould-Saada,¹³³ A. Ouraou,¹⁴⁴ Q. Ouyang,^{15a}
M. Owen,⁵⁷ R. E. Owen,¹⁴³ V. E. Ozcan,^{12c} N. Ozturk,⁸ J. Pacalt,¹³⁰ H. A. Pacey,³² K. Pachal,⁴⁹ A. Pacheco Pages,¹⁴
C. Padilla Aranda,¹⁴ S. Pagan Griso,¹⁸ G. Palacino,⁶⁶ S. Palazzo,⁵⁰ S. Palestini,³⁶ M. Palka,^{84b} P. Palni,^{84a} C. E. Pandini,⁵⁴
J. G. Panduro Vazquez,⁹⁴ P. Pani,⁴⁶ G. Panizzo,^{67a,67c} L. Paolozzi,⁵⁴ C. Papadatos,¹¹⁰ K. Papageorgiou,^{9,q} S. Parajuli,⁴²
A. Paramonov,⁶ C. Paraskevopoulos,¹⁰ D. Paredes Hernandez,^{63b} S. R. Paredes Saenz,¹³⁴ B. Parida,¹⁷⁹ T. H. Park,¹⁶⁶
A. J. Parker,³¹ M. A. Parker,³² F. Parodi,^{55b,55a} E. W. Parrish,¹²¹ J. A. Parsons,³⁹ U. Parzefall,⁵² L. Pascual Dominguez,¹³⁵
V. R. Pascuzzi,¹⁸ J. M. P. Pasner,¹⁴⁵ F. Pasquali,¹²⁰ E. Pasqualucci,^{73a} S. Passaggio,^{55b} F. Pastore,⁹⁴ P. Pasuwan,^{45a,45b}
S. Patariaia,¹⁰⁰ J. R. Pater,¹⁰¹ A. Pathak,^{180,e} J. Patton,⁹¹ T. Pauly,³⁶ J. Pearkes,¹⁵² B. Pearson,¹¹⁵ M. Pedersen,¹³³
L. Pedraza Diaz,¹¹⁹ R. Pedro,^{139a} T. Peiffer,⁵³ S. V. Peleganchuk,^{122b,122a} O. Penc,¹⁴⁰ H. Peng,^{60a} B. S. Peralva,^{81a}
M. M. Perego,⁶⁵ A. P. Pereira Peixoto,^{139a} L. Pereira Sanchez,^{45a,45b} D. V. Perepelitsa,²⁹ E. Perez Codina,^{167a} F. Peri,¹⁹

L. Perini,^{69a,69b} H. Pernegger,³⁶ S. Perrella,³⁶ A. Perrevoort,¹²⁰ K. Peters,⁴⁶ R. F. Y. Peters,¹⁰¹ B. A. Petersen,³⁶ T. C. Petersen,⁴⁰ E. Petit,¹⁰² V. Petousis,¹⁴¹ A. Petridis,¹ C. Petridou,¹⁶¹ F. Petrucci,^{75a,75b} M. Pettee,¹⁸² N. E. Pettersson,¹⁰³ K. Petukhova,¹⁴² A. Peyaud,¹⁴⁴ R. Pezoa,^{146d} L. Pezzotti,^{71a,71b} T. Pham,¹⁰⁵ F. H. Phillips,¹⁰⁷ P. W. Phillips,¹⁴³ M. W. Phipps,¹⁷² G. Piacquadio,¹⁵⁴ E. Pianori,¹⁸ A. Picazio,¹⁰³ R. H. Pickles,¹⁰¹ R. Piegai,³⁰ D. Pietreanu,^{27b} J. E. Pilcher,³⁷ A. D. Pilkington,¹⁰¹ M. Pinamonti,^{67a,67c} J. L. Pinfold,³ C. Pitman Donaldson,⁹⁵ M. Pitt,¹⁶⁰ L. Pizzimento,^{74a,74b} A. Pizzini,¹²⁰ M.-A. Pleier,²⁹ V. Plesanovs,⁵² V. Pleskot,¹⁴² E. Plotnikova,⁸⁰ P. Podberezko,^{122b,122a} R. Poettgen,⁹⁷ R. Poggi,⁵⁴ L. Poggioli,¹³⁵ I. Pogrebnyak,¹⁰⁷ D. Pohl,²⁴ I. Pokharel,⁵³ G. Polesello,^{71a} A. Poley,^{151,167a} A. Policicchio,^{73a,73b} R. Polifka,¹⁴² A. Polini,^{23b} C. S. Pollard,⁴⁶ V. Polychronakos,²⁹ D. Ponomarenko,¹¹² L. Pontecorvo,³⁶ S. Popa,^{27a} G. A. Popeneciu,^{27d} L. Portales,⁵ D. M. Portillo Quintero,⁵⁸ S. Pospisil,¹⁴¹ K. Potamianos,⁴⁶ I. N. Potrap,⁸⁰ C. J. Potter,³² H. Potti,¹¹ T. Poulsen,⁹⁷ J. Poveda,¹⁷³ T. D. Powell,¹⁴⁸ G. Pownall,⁴⁶ M. E. Pozo Astigarraga,³⁶ P. Pralavorio,¹⁰² S. Prell,⁷⁹ D. Price,¹⁰¹ M. Primavera,^{68a} M. L. Proffitt,¹⁴⁷ N. Proklova,¹¹² K. Prokofiev,^{63c} F. Prokoshin,⁸⁰ S. Protopopescu,²⁹ J. Proudfoot,⁶ M. Przybycien,^{84a} D. Pudza,¹³⁷ A. Puri,¹⁷² P. Puzo,⁶⁵ D. Pyatiizbyantseva,¹¹² J. Qian,¹⁰⁶ Y. Qin,¹⁰¹ A. Quadt,⁵³ M. Queitsch-Maitland,³⁶ M. Racko,^{28a} F. Ragusa,^{69a,69b} G. Rahal,⁹⁸ J. A. Raine,⁵⁴ S. Rajagopalan,²⁹ A. Ramirez Morales,⁹³ K. Ran,^{15a,15d} D. M. Rauch,⁴⁶ F. Rauscher,¹¹⁴ S. Rave,¹⁰⁰ B. Ravina,¹⁴⁸ I. Ravinovitch,¹⁷⁹ J. H. Rawling,¹⁰¹ M. Raymond,³⁶ A. L. Read,¹³³ N. P. Readioff,¹⁴⁸ M. Reale,^{68a,68b} D. M. Rebuffi,^{71a,71b} G. Redlinger,²⁹ K. Reeves,⁴³ J. Reichert,¹³⁶ D. Reikher,¹⁶⁰ A. Reiss,¹⁰⁰ A. Rej,¹⁵⁰ C. Rembser,³⁶ A. Renardi,⁴⁶ M. Renda,^{27b} M. B. Rendel,¹¹⁵ A. G. Rennie,⁵⁷ S. Resconi,^{69a} E. D. Resseguie,¹⁸ S. Rettie,⁹⁵ B. Reynolds,¹²⁷ E. Reynolds,²¹ O. L. Rezanova,^{122b,122a} P. Reznicek,¹⁴² E. Ricci,^{76a,76b} R. Richter,¹¹⁵ S. Richter,⁴⁶ E. Richter-Was,^{84b} M. Ridel,¹³⁵ P. Rieck,¹¹⁵ O. Rifki,⁴⁶ M. Rijssenbeek,¹⁵⁴ A. Rimoldi,^{71a,71b} M. Rimoldi,⁴⁶ L. Rinaldi,^{23b} T. T. Rinn,¹⁷² G. Ripellino,¹⁵³ I. Riu,¹⁴ P. Rivadeneira,⁴⁶ J. C. Rivera Vergara,¹⁷⁵ F. Rizatdinova,¹²⁹ E. Rizvi,⁹³ C. Rizzi,³⁶ S. H. Robertson,^{104,1} M. Robin,⁴⁶ D. Robinson,³² C. M. Robles Gajardo,^{146d} M. Robles Manzano,¹⁰⁰ A. Robson,⁵⁷ A. Rocchi,^{74a,74b} E. Rocco,¹⁰⁰ C. Roda,^{72a,72b} S. Rodriguez Bosca,¹⁷³ A. M. Rodríguez Vera,^{167b} S. Roe,³⁶ J. Roggel,¹⁸¹ O. Røhne,¹³³ R. Röhrig,¹¹⁵ R. A. Rojas,^{146d} B. Roland,⁵² C. P. A. Roland,⁶⁶ J. Roloff,²⁹ A. Romaniouk,¹¹² M. Romano,^{23b,23a} N. Rompotis,⁹¹ M. Ronzani,¹²⁵ L. Roos,¹³⁵ S. Rosati,^{73a} G. Rosin,¹⁰³ B. J. Rosser,¹³⁶ E. Rossi,⁴⁶ E. Rossi,^{75a,75b} E. Rossi,^{70a,70b} L. P. Rossi,^{55b} L. Rossini,⁴⁶ R. Rosten,¹⁴ M. Rotaru,^{27b} B. Rottler,⁵² D. Rousseau,⁶⁵ G. Rovelli,^{71a,71b} A. Roy,¹¹ D. Roy,^{33e} A. Rozanov,¹⁰² Y. Rozen,¹⁵⁹ X. Ruan,^{33e} T. A. Ruggeri,¹ F. Rühr,⁵² A. Ruiz-Martinez,¹⁷³ A. Rummeler,³⁶ Z. Rurikova,⁵² N. A. Rusakovich,⁸⁰ H. L. Russell,¹⁰⁴ L. Rustige,^{38,47} J. P. Rutherford,⁷ E. M. Rüttinger,¹⁴⁸ M. Rybar,¹⁴² G. Rybkin,⁶⁵ E. B. Rye,¹³³ A. Ryzhov,¹²³ J. A. Sabater Iglesias,⁴⁶ P. Sabatini,⁵³ L. Sabetta,^{73a,73b} S. Sacerdoti,⁶⁵ H. F.-W. Sadrozinski,¹⁴⁵ R. Sadykov,⁸⁰ F. Safai Tehrani,^{73a} B. Safarzadeh Samani,¹⁵⁵ M. Safdari,¹⁵² P. Saha,¹²¹ S. Saha,¹⁰⁴ M. Sahinsoy,¹¹⁵ A. Sahu,¹⁸¹ M. Saimpert,³⁶ M. Saito,¹⁶² T. Saito,¹⁶² H. Sakamoto,¹⁶² D. Salamani,⁵⁴ G. Salamanna,^{75a,75b} A. Salnikov,¹⁵² J. Salt,¹⁷³ A. Salvador Salas,¹⁴ D. Salvatore,^{41b,41a} F. Salvatore,¹⁵⁵ A. Salvucci,^{63a,63b,63c} A. Salzburger,³⁶ J. Samarati,³⁶ D. Sammel,⁵² D. Sampsonidis,¹⁶¹ D. Sampsonidou,¹⁶¹ J. Sánchez,¹⁷³ A. Sanchez Pineda,^{67a,36,67c} H. Sandaker,¹³³ C. O. Sander,⁴⁶ I. G. Sanderswood,⁹⁰ M. Sandhoff,¹⁸¹ C. Sandoval,^{22b} D. P. C. Sankey,¹⁴³ M. Sannino,^{55b,55a} Y. Sano,¹¹⁷ A. Sansoni,⁵¹ C. Santoni,³⁸ H. Santos,^{139a,139b} S. N. Santpur,¹⁸ A. Santra,¹⁷³ K. A. Saoucha,¹⁴⁸ A. Saprnov,⁸⁰ J. G. Saraiva,^{139a,139d} O. Sasaki,⁸² K. Sato,¹⁶⁸ F. Sauerburger,⁵² E. Sauvan,⁵ P. Savard,^{166,d} R. Sawada,¹⁶² C. Sawyer,¹⁴³ L. Sawyer,^{96,gg} I. Sayago Galvan,¹⁷³ C. Sbarra,^{23b} A. Sbrizzi,^{67a,67c} T. Scanlon,⁹⁵ J. Schaarschmidt,¹⁴⁷ P. Schacht,¹¹⁵ D. Schaefer,³⁷ L. Schaefer,¹³⁶ S. Schaepe,³⁶ U. Schäfer,¹⁰⁰ A. C. Schaffer,⁶⁵ D. Schaile,¹¹⁴ R. D. Schamberger,¹⁵⁴ E. Schanet,¹¹⁴ C. Scharf,¹⁹ N. Scharmberg,¹⁰¹ V. A. Schegelsky,¹³⁷ D. Scheirich,¹⁴² F. Schenck,¹⁹ M. Schernau,¹⁷⁰ C. Schiavi,^{55b,55a} L. K. Schildgen,²⁴ Z. M. Schillaci,²⁶ E. J. Schioppa,^{68a,68b} M. Schioppa,^{41b,41a} K. E. Schleicher,⁵² S. Schlenker,³⁶ K. R. Schmidt-Sommerfeld,¹¹⁵ K. Schmieden,³⁶ C. Schmitt,¹⁰⁰ S. Schmitt,⁴⁶ J. C. Schmoeckel,⁴⁶ L. Schoeffel,¹⁴⁴ A. Schoening,^{61b} P. G. Scholer,⁵² E. Schopf,¹³⁴ M. Schott,¹⁰⁰ J. F. P. Schouwenberg,¹¹⁹ J. Schovancova,³⁶ S. Schramm,⁵⁴ F. Schroeder,¹⁸¹ A. Schulte,¹⁰⁰ H.-C. Schultz-Coulon,^{61a} M. Schumacher,⁵² B. A. Schumm,¹⁴⁵ Ph. Schune,¹⁴⁴ A. Schwartzman,¹⁵² T. A. Schwarz,¹⁰⁶ Ph. Schwemling,¹⁴⁴ R. Schwienhorst,¹⁰⁷ A. Sciandra,¹⁴⁵ G. Sciolla,²⁶ M. Scornajenghi,^{41b,41a} F. Scuri,^{72a} F. Scutti,¹⁰⁵ L. M. Scyboz,¹¹⁵ C. D. Sebastiani,⁹¹ P. Seema,¹⁹ S. C. Seidel,¹¹⁸ A. Seiden,¹⁴⁵ B. D. Seidlitz,²⁹ T. Seiss,³⁷ C. Seitz,⁴⁶ J. M. Seixas,^{81b} G. Sekhniaidze,^{70a} S. J. Sekula,⁴² N. Semprini-Cesari,^{23b,23a} S. Sen,⁴⁹ C. Serfon,²⁹ L. Serin,⁶⁵ L. Serkin,^{67a,67b} M. Sessa,^{60a} H. Severini,¹²⁸ S. Sevova,¹⁵² F. Sforza,^{55b,55a} A. Sfyrta,⁵⁴ E. Shabalina,⁵³ J. D. Shahinian,¹⁴⁵ N. W. Shaikh,^{45a,45b} D. Shaked Renous,¹⁷⁹ L. Y. Shan,^{15a} M. Shapiro,¹⁸ A. Sharma,¹³⁴ A. S. Sharma,¹ P. B. Shatalov,¹²⁴ K. Shaw,¹⁵⁵ S. M. Shaw,¹⁰¹ M. Shehade,¹⁷⁹ Y. Shen,¹²⁸ A. D. Sherman,²⁵ P. Sherwood,⁹⁵ L. Shi,⁹⁵ S. Shimizu,⁸² C. O. Shimmin,¹⁸² Y. Shimogama,¹⁷⁸ M. Shimojima,¹¹⁶ I. P. J. Shipsey,¹³⁴ S. Shirabe,¹⁶⁴ M. Shiyakova,^{80,hh} J. Shlomi,¹⁷⁹ A. Shmeleva,¹¹¹

M. J. Shochet,³⁷ J. Shojaii,¹⁰⁵ D. R. Shope,¹⁵³ S. Shrestha,¹²⁷ E. M. Shrif,^{33e} E. Shulga,¹⁷⁹ P. Sicho,¹⁴⁰ A. M. Sickles,¹⁷² E. Sideras Haddad,^{33e} O. Sidiropoulou,³⁶ A. Sidoti,^{23b,23a} F. Siegert,⁴⁸ Dj. Sijacki,¹⁶ M. Jr. Silva,¹⁸⁰ M. V. Silva Oliveira,³⁶ S. B. Silverstein,^{45a} S. Simion,⁶⁵ R. Simoniello,¹⁰⁰ C. J. Simpson-allsoy,²¹ S. Simsek,^{12b} P. Sinervo,¹⁶⁶ V. Sinetckii,¹¹³ S. Singh,¹⁵¹ M. Sioli,^{23b,23a} I. Siral,¹³¹ S. Yu. Sivoklov,¹¹³ J. Sjölin,^{45a,45b} A. Skaf,⁵³ E. Skorda,⁹⁷ P. Skubic,¹²⁸ M. Slawinska,⁸⁵ K. Sliwa,¹⁶⁹ R. Slovak,¹⁴² V. Smakhtin,¹⁷⁹ B. H. Smart,¹⁴³ J. Smiesko,^{28b} N. Smirnov,¹¹² S. Yu. Smirnov,¹¹² Y. Smirnov,¹¹² L. N. Smirnova,^{113,ii} O. Smirnova,⁹⁷ E. A. Smith,³⁷ H. A. Smith,¹³⁴ M. Smizanska,⁹⁰ K. Smolek,¹⁴¹ A. Smykiewicz,⁸⁵ A. A. Snesarev,¹¹¹ H. L. Snoek,¹²⁰ I. M. Snyder,¹³¹ S. Snyder,²⁹ R. Sobie,^{175,1} A. Soffer,¹⁶⁰ A. Søggaard,⁵⁰ F. Sohns,⁵³ C. A. Solans Sanchez,³⁶ E. Yu. Soldatov,¹¹² U. Soldevila,¹⁷³ A. A. Solodkov,¹²³ A. Soloshenko,⁸⁰ O. V. Solovyanov,¹²³ V. Solovyev,¹³⁷ P. Sommer,¹⁴⁸ H. Son,¹⁶⁹ W. Song,¹⁴³ W. Y. Song,^{167b} A. Sopczak,¹⁴¹ A. L. Soppio,⁹⁵ F. Sopkova,^{28b} S. Sottocornola,^{71a,71b} R. Soualah,^{67a,67c} A. M. Soukharev,^{122b,122a} D. South,⁴⁶ S. Spagnolo,^{68a,68b} M. Spalla,¹¹⁵ M. Spangenberg,¹⁷⁷ F. Spanò,⁹⁴ D. Sperlich,⁵² T. M. Spieker,^{61a} G. Spigo,³⁶ M. Spina,¹⁵⁵ D. P. Spiteri,⁵⁷ M. Spousta,¹⁴² A. Stabile,^{69a,69b} B. L. Stamas,¹²¹ R. Stamen,^{61a} M. Stamenkovic,¹²⁰ E. Stanecka,⁸⁵ B. Stanislaus,¹³⁴ M. M. Stanitzki,⁴⁶ M. Stankaityte,¹³⁴ B. Stapf,¹²⁰ E. A. Starchenko,¹²³ G. H. Stark,¹⁴⁵ J. Stark,⁵⁸ P. Staroba,¹⁴⁰ P. Starovoitov,^{61a} S. Storz,¹⁰⁴ R. Staszewski,⁸⁵ G. Stavropoulos,⁴⁴ M. Stegler,⁴⁶ P. Steinberg,²⁹ A. L. Steinhebel,¹³¹ B. Stelzer,^{151,167a} H. J. Stelzer,¹³⁸ O. Stelzer-Chilton,^{167a} H. Stenzel,⁵⁶ T. J. Stevenson,¹⁵⁵ G. A. Stewart,³⁶ M. C. Stockton,³⁶ G. Stoicea,^{27b} M. Stolarski,^{139a} S. Stonjek,¹¹⁵ A. Straessner,⁴⁸ J. Strandberg,¹⁵³ S. Strandberg,^{45a,45b} M. Strauss,¹²⁸ T. Strebler,¹⁰² P. Strizenec,^{28b} R. Ströhmer,¹⁷⁶ D. M. Strom,¹³¹ R. Stroynowski,⁴² A. Strubig,⁵⁰ S. A. Stucci,²⁹ B. Stugu,¹⁷ J. Stupak,¹²⁸ N. A. Styles,⁴⁶ D. Su,¹⁵² W. Su,^{60c,147} X. Su,^{60a} V. V. Sulin,¹¹¹ M. J. Sullivan,⁹¹ D. M. S. Sultan,⁵⁴ S. Sultansoy,^{4c} T. Sumida,⁸⁶ S. Sun,¹⁰⁶ X. Sun,¹⁰¹ K. Suruliz,¹⁵⁵ C. J. E. Suster,¹⁵⁶ M. R. Sutton,¹⁵⁵ S. Suzuki,⁸² M. Svatos,¹⁴⁰ M. Swiatlowski,^{167a} S. P. Swift,² T. Swirski,¹⁷⁶ A. Sydorenko,¹⁰⁰ I. Sykora,^{28a} M. Sykora,¹⁴² T. Sykora,¹⁴² D. Ta,¹⁰⁰ K. Tackmann,^{46,ij} J. Taenzer,¹⁶⁰ A. Taffard,¹⁷⁰ R. Tafirout,^{167a} E. Tagiev,¹²³ R. Takashima,⁸⁷ K. Takeda,⁸³ T. Takeshita,¹⁴⁹ E. P. Takeva,⁵⁰ Y. Takubo,⁸² M. Talby,¹⁰² A. A. Talyshev,^{122b,122a} K. C. Tam,^{63b} N. M. Tamir,¹⁶⁰ J. Tanaka,¹⁶² R. Tanaka,⁶⁵ S. Tapia Araya,¹⁷² S. Tapprogge,¹⁰⁰ A. Tarek Abouelfadl Mohamed,¹⁰⁷ S. Tarem,¹⁵⁹ K. Tariq,^{60b} G. Tarna,^{27b,kk} G. F. Tartarelli,^{69a} P. Tas,¹⁴² M. Tasevsky,¹⁴⁰ T. Tashiro,⁸⁶ E. Tassi,^{41b,41a} A. Tavares Delgado,^{139a} Y. Tayalati,^{35e} A. J. Taylor,⁵⁰ G. N. Taylor,¹⁰⁵ W. Taylor,^{167b} H. Teagle,⁹¹ A. S. Tee,⁹⁰ R. Teixeira De Lima,¹⁵² P. Teixeira-Dias,⁹⁴ H. Ten Kate,³⁶ J. J. Teoh,¹²⁰ S. Terada,⁸² K. Terashi,¹⁶² J. Terron,⁹⁹ S. Terzo,¹⁴ M. Testa,⁵¹ R. J. Teuscher,^{166,1} S. J. Thais,¹⁸² N. Themistokleous,⁵⁰ T. Theveneaux-Pelzer,⁴⁶ F. Thiele,⁴⁰ D. W. Thomas,⁹⁴ J. O. Thomas,⁴² J. P. Thomas,²¹ E. A. Thompson,⁴⁶ P. D. Thompson,²¹ E. Thomson,¹³⁶ E. J. Thorpe,⁹³ R. E. Ticse Torres,⁵³ V. O. Tikhomirov,^{111,li} Yu. A. Tikhonov,^{122b,122a} S. Timoshenko,¹¹² P. Tipton,¹⁸² S. Tisserant,¹⁰² K. Todome,^{23b,23a} S. Todorova-Nova,¹⁴² S. Todt,⁴⁸ J. Tojo,⁸⁸ S. Tokár,^{28a} K. Tokushuku,⁸² E. Tolley,¹²⁷ R. Tombs,³² K. G. Tomiwa,^{33e} M. Tomoto,¹¹⁷ L. Tompkins,¹⁵² P. Tornambe,¹⁰³ E. Torrence,¹³¹ H. Torres,⁴⁸ E. Torró Pastor,¹⁴⁷ C. Toscirì,¹³⁴ J. Toth,^{102,mm} D. R. Tovey,¹⁴⁸ A. Traet,¹⁷ C. J. Treado,¹²⁵ T. Trefzger,¹⁷⁶ F. Tresoldi,¹⁵⁵ A. Tricoli,²⁹ I. M. Trigger,^{167a} S. Trincaz-Duvoid,¹³⁵ D. A. Trischuk,¹⁷⁴ W. Trischuk,¹⁶⁶ B. Trocmé,⁵⁸ A. Trofymov,⁶⁵ C. Troncon,^{69a} F. Trovato,¹⁵⁵ L. Truong,^{33c} M. Trzebinski,⁸⁵ A. Trzupek,⁸⁵ F. Tsai,⁴⁶ J. C-L. Tseng,¹³⁴ P. V. Tsiarehka,^{108,bb} A. Tsirigotis,^{161,cc} V. Tsiskaridze,¹⁵⁴ E. G. Tskhadadze,^{158a} M. Tsopoulou,¹⁶¹ I. I. Tsukerman,¹²⁴ V. Tsulaia,¹⁸ S. Tsuno,⁸² D. Tsybychev,¹⁵⁴ Y. Tu,^{63b} A. Tudorache,^{27b} V. Tudorache,^{27b} T. T. Tulbure,^{27a} A. N. Tuna,⁵⁹ S. Turchikhin,⁸⁰ D. Turgeman,¹⁷⁹ I. Turk Cakir,^{4b,nn} R. J. Turner,²¹ R. Turra,^{69a} P. M. Tuts,³⁹ S. Tzamarias,¹⁶¹ E. Tzovara,¹⁰⁰ K. Uchida,¹⁶² F. Ukegawa,¹⁶⁸ G. Unal,³⁶ M. Unal,¹¹ A. Undrus,²⁹ G. Unel,¹⁷⁰ F. C. Ungaro,¹⁰⁵ Y. Unno,⁸² K. Uno,¹⁶² J. Urban,^{28b} P. Urquijo,¹⁰⁵ G. Usai,⁸ Z. Uysal,^{12d} V. Vacek,¹⁴¹ B. Vachon,¹⁰⁴ K. O. H. Vadla,¹³³ T. Vafeiadis,³⁶ A. Vaidya,⁹⁵ C. Valderanis,¹¹⁴ E. Valdes Santurio,^{45a,45b} M. Valente,⁵⁴ S. Valentinetti,^{23b,23a} A. Valero,¹⁷³ L. Valéry,⁴⁶ R. A. Vallance,²¹ A. Vallier,³⁶ J. A. Valls Ferrer,¹⁷³ T. R. Van Daalen,¹⁴ P. Van Gemmeren,⁶ S. Van Stroud,⁹⁵ I. Van Vulpen,¹²⁰ M. Vanadia,^{74a,74b} W. Vandelli,³⁶ M. Vandenbroucke,¹⁴⁴ E. R. Vandewall,¹²⁹ A. Vaniachine,¹⁶⁵ D. Vannicola,^{73a,73b} R. Vari,^{73a} E. W. Varnes,⁷ C. Varni,^{55b,55a} T. Varol,¹⁵⁷ D. Varouchas,⁶⁵ K. E. Varvell,¹⁵⁶ M. E. Vasile,^{27b} G. A. Vasquez,¹⁷⁵ F. Vazeille,³⁸ D. Vazquez Furelos,¹⁴ T. Vazquez Schroeder,³⁶ J. Veatch,⁵³ V. Vecchio,¹⁰¹ M. J. Veen,¹²⁰ L. M. Veloce,¹⁶⁶ F. Veloso,^{139a,139c} S. Veneziano,^{73a} A. Ventura,^{68a,68b} A. Verbytskyi,¹¹⁵ V. Vercesi,^{71a} M. Verducci,^{72a,72b} C. M. Vergel Infante,⁷⁹ C. Vergis,²⁴ W. Verkerke,¹²⁰ A. T. Vermeulen,¹²⁰ J. C. Vermeulen,¹²⁰ C. Vernieri,¹⁵² M. C. Vetterli,^{151,d} N. Viaux Maira,^{146d} T. Vickey,¹⁴⁸ O. E. Vickey Boeriu,¹⁴⁸ G. H. A. Viehhauser,¹³⁴ L. Vigani,^{61b} M. Villa,^{23b,23a} M. Villaplana Perez,³ E. M. Villhauer,⁵⁰ E. Vilucchi,⁵¹ M. G. Vincter,³⁴ G. S. Virdee,²¹ A. Vishwakarma,⁵⁰ C. Vittori,^{23b,23a} I. Vivarelli,¹⁵⁵ M. Vogel,¹⁸¹ P. Vokac,¹⁴¹ S. E. von Buddenbrock,^{33e} E. Von Toerne,²⁴ V. Vorobel,¹⁴² K. Vorobev,¹¹² M. Vos,¹⁷³ J. H. Vosseveld,⁹¹ M. Vozak,¹⁰¹ N. Vranjes,¹⁶ M. Vranjes Milosavljevic,¹⁶ V. Vrba,¹⁴¹ M. Vreeswijk,¹²⁰ R. Vuillermet,³⁶ I. Vukotic,³⁷ S. Wada,¹⁶⁸

P. Wagner,²⁴ W. Wagner,¹⁸¹ J. Wagner-Kuhr,¹¹⁴ S. Wahdan,¹⁸¹ H. Wahlberg,⁸⁹ R. Wakasa,¹⁶⁸ V. M. Walbrecht,¹¹⁵ J. Walder,¹⁴³ R. Walker,¹¹⁴ S. D. Walker,⁹⁴ W. Walkowiak,¹⁵⁰ V. Wallangen,^{45a,45b} A. M. Wang,⁵⁹ A. Z. Wang,¹⁸⁰ C. Wang,^{60a} C. Wang,^{60c} F. Wang,¹⁸⁰ H. Wang,¹⁸ H. Wang,³ J. Wang,^{63a} P. Wang,⁴² Q. Wang,¹²⁸ R.-J. Wang,¹⁰⁰ R. Wang,^{60a} R. Wang,⁶ S. M. Wang,¹⁵⁷ W. T. Wang,^{60a} W. Wang,^{15c} W. X. Wang,^{60a} Y. Wang,^{60a} Z. Wang,¹⁰⁶ C. Wanotayaroj,⁴⁶ A. Warburton,¹⁰⁴ C. P. Ward,³² D. R. Wardrope,⁹⁵ N. Warrack,⁵⁷ A. T. Watson,²¹ M. F. Watson,²¹ G. Watts,¹⁴⁷ B. M. Waugh,⁹⁵ A. F. Webb,¹¹ C. Weber,²⁹ M. S. Weber,²⁰ S. A. Weber,³⁴ S. M. Weber,^{61a} A. R. Weidberg,¹³⁴ J. Weingarten,⁴⁷ M. Weirich,¹⁰⁰ C. Weiser,⁵² P. S. Wells,³⁶ T. Wenaus,²⁹ B. Wendland,⁴⁷ T. Wengler,³⁶ S. Wenig,³⁶ N. Wermes,²⁴ M. Wessels,^{61a} T. D. Weston,²⁰ K. Whalen,¹³¹ A. M. Wharton,⁹⁰ A. S. White,¹⁰⁶ A. White,⁸ M. J. White,¹ D. Whiteson,¹⁷⁰ B. W. Whitmore,⁹⁰ W. Wiedenmann,¹⁸⁰ C. Wiel,⁴⁸ M. Wielers,¹⁴³ N. Wieseotte,¹⁰⁰ C. Wiglesworth,⁴⁰ L. A. M. Wiik-Fuchs,⁵² H. G. Wilkens,³⁶ L. J. Wilkins,⁹⁴ H. H. Williams,¹³⁶ S. Williams,³² S. Willocq,¹⁰³ P. J. Windischhofer,¹³⁴ I. Wingerter-Seez,⁵ E. Winkels,¹⁵⁵ F. Winklmeier,¹³¹ B. T. Winter,⁵² M. Wittgen,¹⁵² M. Wobisch,⁹⁶ A. Wolf,¹⁰⁰ R. Wölker,¹³⁴ J. Wollrath,⁵² M. W. Wolter,⁸⁵ H. Wolters,^{139a,139c} V. W. S. Wong,¹⁷⁴ N. L. Woods,¹⁴⁵ S. D. Worm,⁴⁶ B. K. Wosiek,⁸⁵ K. W. Woźniak,⁸⁵ K. Wraight,⁵⁷ S. L. Wu,¹⁸⁰ X. Wu,⁵⁴ Y. Wu,^{60a} J. Wuerzinger,¹³⁴ T. R. Wyatt,¹⁰¹ B. M. Wynne,⁵⁰ S. Xella,⁴⁰ L. Xia,¹⁷⁷ J. Xiang,^{63c} X. Xiao,¹⁰⁶ X. Xie,^{60a} I. Xiotidis,¹⁵⁵ D. Xu,^{15a} H. Xu,^{60a} H. Xu,^{60a} L. Xu,²⁹ T. Xu,¹⁴⁴ W. Xu,¹⁰⁶ Z. Xu,^{60b} Z. Xu,¹⁵² B. Yabsley,¹⁵⁶ S. Yacoob,^{33a} K. Yajima,¹³² D. P. Yallup,⁹⁵ N. Yamaguchi,⁸⁸ Y. Yamaguchi,¹⁶⁴ A. Yamamoto,⁸² M. Yamatani,¹⁶² T. Yamazaki,¹⁶² Y. Yamazaki,⁸³ J. Yan,^{60c} Z. Yan,²⁵ H. J. Yang,^{60c,60d} H. T. Yang,¹⁸ S. Yang,^{60a} T. Yang,^{63c} X. Yang,^{60b,58} Y. Yang,¹⁶² Z. Yang,^{60a} W.-M. Yao,¹⁸ Y. C. Yap,⁴⁶ Y. Yasu,⁸² E. Yatsenko,^{60c} H. Ye,^{15c} J. Ye,⁴² S. Ye,²⁹ I. Yeletsikh,⁸⁰ M. R. Yexley,⁹⁰ E. Yigitbasi,²⁵ P. Yin,³⁹ K. Yorita,¹⁷⁸ K. Yoshihara,⁷⁹ C. J. S. Young,³⁶ C. Young,¹⁵² J. Yu,⁷⁹ R. Yuan,^{60b,oo} X. Yue,^{61a} M. Zaazoua,^{35e} B. Zabinski,⁸⁵ G. Zacharis,¹⁰ E. Zaffaroni,⁵⁴ J. Zahreddine,¹³⁵ A. M. Zaitsev,^{123,i} T. Zakareishvili,^{158b} N. Zakharchuk,³⁴ S. Zambito,³⁶ D. Zanzi,³⁶ D. R. Zaripovas,⁵⁷ S. V. Zeiβner,⁴⁷ C. Zeitnitz,¹⁸¹ G. Zemaityte,¹³⁴ J. C. Zeng,¹⁷² O. Zenin,¹²³ T. Ženiš,^{28a} D. Zerwas,⁶⁵ M. Zgubič,¹³⁴ B. Zhang,^{15c} D. F. Zhang,^{15b} G. Zhang,^{15b} J. Zhang,⁶ Kaili. Zhang,^{15a} L. Zhang,^{15c} L. Zhang,^{60a} M. Zhang,¹⁷² R. Zhang,¹⁸⁰ S. Zhang,¹⁰⁶ X. Zhang,^{60c} X. Zhang,^{60b} Y. Zhang,^{15a,15d} Z. Zhang,^{63a} Z. Zhang,⁶⁵ P. Zhao,⁴⁹ Z. Zhao,^{60a} A. Zhemchugov,⁸⁰ Z. Zheng,¹⁰⁶ D. Zhong,¹⁷² B. Zhou,¹⁰⁶ C. Zhou,¹⁸⁰ H. Zhou,⁷ M. S. Zhou,^{15a,15d} M. Zhou,¹⁵⁴ N. Zhou,^{60c} Y. Zhou,⁷ C. G. Zhu,^{60b} C. Zhu,^{15a,15d} H. L. Zhu,^{60a} H. Zhu,^{15a} J. Zhu,¹⁰⁶ Y. Zhu,^{60a} X. Zhuang,^{15a} K. Zhukov,¹¹¹ V. Zhulanov,^{122b,122a} D. Ziemińska,⁶⁶ N. I. Zimine,⁸⁰ S. Zimmermann,⁵² Z. Zinonos,¹¹⁵ M. Ziolkowski,¹⁵⁰ L. Živković,¹⁶ G. Zobernig,¹⁸⁰ A. Zoccoli,^{23b,23a} K. Zoch,⁵³ T. G. Zorbas,¹⁴⁸ R. Zou,³⁷ and L. Zwalinski³⁶

(ATLAS Collaboration)

¹Department of Physics, University of Adelaide, Adelaide, Australia²Physics Department, SUNY Albany, Albany, New York, USA³Department of Physics, University of Alberta, Edmonton AB, Canada^{4a}Department of Physics, Ankara University, Ankara, Turkey^{4b}Istanbul Aydin University, Application and Research Center for Advanced Studies, Istanbul, Turkey^{4c}Division of Physics, TOBB University of Economics and Technology, Ankara, Turkey⁵LAPP, Université Grenoble Alpes, Université Savoie Mont Blanc, CNRS/IN2P3, Annecy, France⁶High Energy Physics Division, Argonne National Laboratory, Argonne, Illinois, USA⁷Department of Physics, University of Arizona, Tucson, Arizona, USA⁸Department of Physics, University of Texas at Arlington, Arlington, Texas, USA⁹Physics Department, National and Kapodistrian University of Athens, Athens, Greece¹⁰Physics Department, National Technical University of Athens, Zografou, Greece¹¹Department of Physics, University of Texas at Austin, Austin, Texas, USA^{12a}Bahcesehir University, Faculty of Engineering and Natural Sciences, Istanbul, Turkey^{12b}Istanbul Bilgi University, Faculty of Engineering and Natural Sciences, Istanbul, Turkey^{12c}Department of Physics, Bogazici University, Istanbul, Turkey^{12d}Department of Physics Engineering, Gaziantep University, Gaziantep, Turkey¹³Institute of Physics, Azerbaijan Academy of Sciences, Baku, Azerbaijan¹⁴Institut de Física d'Altes Energies (IFAE), Barcelona Institute of Science and Technology, Barcelona, Spain^{15a}Institute of High Energy Physics, Chinese Academy of Sciences, Beijing, China^{15b}Physics Department, Tsinghua University, Beijing, China^{15c}Department of Physics, Nanjing University, Nanjing, China

- ^{15d}University of Chinese Academy of Science (UCAS), Beijing, China
- ¹⁶Institute of Physics, University of Belgrade, Belgrade, Serbia
- ¹⁷Department for Physics and Technology, University of Bergen, Bergen, Norway
- ¹⁸Physics Division, Lawrence Berkeley National Laboratory and University of California, Berkeley, California, USA
- ¹⁹Institut für Physik, Humboldt Universität zu Berlin, Berlin, Germany
- ²⁰Albert Einstein Center for Fundamental Physics and Laboratory for High Energy Physics, University of Bern, Bern, Switzerland
- ²¹School of Physics and Astronomy, University of Birmingham, Birmingham, United Kingdom
- ^{22a}Facultad de Ciencias y Centro de Investigaciones, Universidad Antonio Nariño, Bogotá, Colombia
- ^{22b}Departamento de Física, Universidad Nacional de Colombia, Bogotá, Colombia, Colombia
- ^{23a}INFN Bologna and Università di Bologna, Dipartimento di Fisica, Italy
- ^{23b}INFN Sezione di Bologna, Italy
- ²⁴Physikalisches Institut, Universität Bonn, Bonn, Germany
- ²⁵Department of Physics, Boston University, Boston, Massachusetts, USA
- ²⁶Department of Physics, Brandeis University, Waltham, Massachusetts, USA
- ^{27a}Transilvania University of Brasov, Brasov, Romania
- ^{27b}Horia Hulubei National Institute of Physics and Nuclear Engineering, Bucharest, Romania
- ^{27c}Department of Physics, Alexandru Ioan Cuza University of Iasi, Iasi, Romania
- ^{27d}National Institute for Research and Development of Isotopic and Molecular Technologies, Physics Department, Cluj-Napoca, Romania
- ^{27e}University Politehnica Bucharest, Bucharest, Romania
- ^{27f}West University in Timisoara, Timisoara, Romania
- ^{28a}Faculty of Mathematics, Physics and Informatics, Comenius University, Bratislava, Slovak Republic
- ^{28b}Department of Subnuclear Physics, Institute of Experimental Physics of the Slovak Academy of Sciences, Kosice, Slovak Republic
- ²⁹Physics Department, Brookhaven National Laboratory, Upton, New York, USA
- ³⁰Departamento de Física, Universidad de Buenos Aires, Buenos Aires, Argentina
- ³¹California State University, California, USA
- ³²Cavendish Laboratory, University of Cambridge, Cambridge, United Kingdom
- ^{33a}Department of Physics, University of Cape Town, Cape Town, South Africa
- ^{33b}iThemba Labs, Western Cape, South Africa
- ^{33c}Department of Mechanical Engineering Science, University of Johannesburg, Johannesburg, South Africa
- ^{33d}University of South Africa, Department of Physics, Pretoria, South Africa
- ^{33e}School of Physics, University of the Witwatersrand, Johannesburg, South Africa
- ³⁴Department of Physics, Carleton University, Ottawa ON, Canada
- ^{35a}Faculté des Sciences Ain Chock, Réseau Universitaire de Physique des Hautes Energies—Université Hassan II, Casablanca, Morocco
- ^{35b}Faculté des Sciences, Université Ibn-Tofail, Kénitra, Morocco
- ^{35c}Faculté des Sciences Semlalia, Université Cadi Ayyad, LPHEA-Marrakech, Morocco
- ^{35d}Faculté des Sciences, Université Mohamed Premier and LPTPM, Oujda, Morocco
- ^{35e}Faculté des sciences, Université Mohammed V, Rabat, Morocco
- ³⁶CERN, Geneva, Switzerland
- ³⁷Enrico Fermi Institute, University of Chicago, Chicago, Illinois, USA
- ³⁸LPC, Université Clermont Auvergne, CNRS/IN2P3, Clermont-Ferrand, France
- ³⁹Nevis Laboratory, Columbia University, Irvington, New York, USA
- ⁴⁰Niels Bohr Institute, University of Copenhagen, Copenhagen, Denmark
- ^{41a}Dipartimento di Fisica, Università della Calabria, Rende, Italy
- ^{41b}INFN Gruppo Collegato di Cosenza, Laboratori Nazionali di Frascati, Italy
- ⁴²Physics Department, Southern Methodist University, Dallas, Texas, USA
- ⁴³Physics Department, University of Texas at Dallas, Richardson, Texas, USA
- ⁴⁴National Centre for Scientific Research “Demokritos”, Agia Paraskevi, Greece
- ^{45a}Department of Physics, Stockholm University, Sweden
- ^{45b}Oskar Klein Centre, Stockholm, Sweden
- ⁴⁶Deutsches Elektronen-Synchrotron DESY, Hamburg and Zeuthen, Germany
- ⁴⁷Lehrstuhl für Experimentelle Physik IV, Technische Universität Dortmund, Dortmund, Germany
- ⁴⁸Institut für Kern- und Teilchenphysik, Technische Universität Dresden, Dresden, Germany
- ⁴⁹Department of Physics, Duke University, Durham, North Carolina, USA
- ⁵⁰SUPA—School of Physics and Astronomy, University of Edinburgh, Edinburgh, United Kingdom

- ⁵¹*INFN e Laboratori Nazionali di Frascati, Frascati, Italy*
- ⁵²*Physikalisches Institut, Albert-Ludwigs-Universität Freiburg, Freiburg, Germany*
- ⁵³*II. Physikalisches Institut, Georg-August-Universität Göttingen, Göttingen, Germany*
- ⁵⁴*Département de Physique Nucléaire et Corpusculaire, Université de Genève, Genève, Switzerland*
- ^{55a}*Dipartimento di Fisica, Università di Genova, Genova, Italy*
- ^{55b}*INFN Sezione di Genova, Italy*
- ⁵⁶*II. Physikalisches Institut, Justus-Liebig-Universität Giessen, Giessen, Germany*
- ⁵⁷*SUPA—School of Physics and Astronomy, University of Glasgow, Glasgow, United Kingdom*
- ⁵⁸*LPSC, Université Grenoble Alpes, CNRS/IN2P3, Grenoble INP, Grenoble, France*
- ⁵⁹*Laboratory for Particle Physics and Cosmology, Harvard University, Cambridge, Massachusetts, USA*
- ^{60a}*Department of Modern Physics and State Key Laboratory of Particle Detection and Electronics, University of Science and Technology of China, Hefei, China*
- ^{60b}*Institute of Frontier and Interdisciplinary Science and Key Laboratory of Particle Physics and Particle Irradiation (MOE), Shandong University, Qingdao, China*
- ^{60c}*School of Physics and Astronomy, Shanghai Jiao Tong University, KLPPAC-MoE, SKLPPC, Shanghai, China*
- ^{60d}*Tsung-Dao Lee Institute, Shanghai, China*
- ^{61a}*Kirchhoff-Institut für Physik, Ruprecht-Karls-Universität Heidelberg, Heidelberg, Germany*
- ^{61b}*Physikalisches Institut, Ruprecht-Karls-Universität Heidelberg, Heidelberg, Germany*
- ⁶²*Faculty of Applied Information Science, Hiroshima Institute of Technology, Hiroshima, Japan*
- ^{63a}*Department of Physics, Chinese University of Hong Kong, Shatin, N.T., Hong Kong, China*
- ^{63b}*Department of Physics, University of Hong Kong, Hong Kong, China*
- ^{63c}*Department of Physics and Institute for Advanced Study, Hong Kong University of Science and Technology, Clear Water Bay, Kowloon, Hong Kong, China*
- ⁶⁴*Department of Physics, National Tsing Hua University, Hsinchu, Taiwan*
- ⁶⁵*IJCLab, Université Paris-Saclay, CNRS/IN2P3, 91405, Orsay, France*
- ⁶⁶*Department of Physics, Indiana University, Bloomington, Indiana, USA*
- ^{67a}*INFN Gruppo Collegato di Udine, Sezione di Trieste, Udine, Italy*
- ^{67b}*ICTP, Trieste, Italy*
- ^{67c}*Dipartimento Politecnico di Ingegneria e Architettura, Università di Udine, Udine, Italy*
- ^{68a}*INFN Sezione di Lecce, Italy*
- ^{68b}*Dipartimento di Matematica e Fisica, Università del Salento, Lecce, Italy*
- ^{69a}*INFN Sezione di Milano, Italy*
- ^{69b}*Dipartimento di Fisica, Università di Milano, Milano, Italy*
- ^{70a}*INFN Sezione di Napoli, Italy*
- ^{70b}*Dipartimento di Fisica, Università di Napoli, Napoli, Italy*
- ^{71a}*INFN Sezione di Pavia, Italy*
- ^{71b}*Dipartimento di Fisica, Università di Pavia, Pavia, Italy*
- ^{72a}*INFN Sezione di Pisa, Italy*
- ^{72b}*Dipartimento di Fisica E. Fermi, Università di Pisa, Pisa, Italy*
- ^{73a}*INFN Sezione di Roma, Italy*
- ^{73b}*Dipartimento di Fisica, Sapienza Università di Roma, Roma, Italy*
- ^{74a}*INFN Sezione di Roma Tor Vergata, Italy*
- ^{74b}*Dipartimento di Fisica, Università di Roma Tor Vergata, Roma, Italy*
- ^{75a}*INFN Sezione di Roma Tre, Italy*
- ^{75b}*Dipartimento di Matematica e Fisica, Università Roma Tre, Roma, Italy*
- ^{76a}*INFN-TIFPA, Italy*
- ^{76b}*Università degli Studi di Trento, Trento, Italy*
- ⁷⁷*Institut für Astro- und Teilchenphysik, Leopold-Franzens-Universität, Innsbruck, Austria*
- ⁷⁸*University of Iowa, Iowa City, Iowa, USA*
- ⁷⁹*Department of Physics and Astronomy, Iowa State University, Ames, Iowa, USA*
- ⁸⁰*Joint Institute for Nuclear Research, Dubna, Russia*
- ^{81a}*Departamento de Engenharia Elétrica, Universidade Federal de Juiz de Fora (UFJF), Juiz de Fora, Brazil*
- ^{81b}*Universidade Federal do Rio De Janeiro COPPE/EE/IF, Rio de Janeiro, Brazil*
- ^{81c}*Universidade Federal de São João del Rei (UFSJ), São João del Rei, Brazil*
- ^{81d}*Instituto de Física, Universidade de São Paulo, São Paulo, Brazil*
- ⁸²*KEK, High Energy Accelerator Research Organization, Tsukuba, Japan*
- ⁸³*Graduate School of Science, Kobe University, Kobe, Japan*

- ^{84a}AGH University of Science and Technology, Faculty of Physics and Applied Computer Science, Krakow, Poland
- ^{84b}Marian Smoluchowski Institute of Physics, Jagiellonian University, Krakow, Poland
- ⁸⁵Institute of Nuclear Physics Polish Academy of Sciences, Krakow, Poland
- ⁸⁶Faculty of Science, Kyoto University, Kyoto, Japan
- ⁸⁷Kyoto University of Education, Kyoto, Japan
- ⁸⁸Research Center for Advanced Particle Physics and Department of Physics, Kyushu University, Fukuoka, Japan
- ⁸⁹Instituto de Física La Plata, Universidad Nacional de La Plata and CONICET, La Plata, Argentina
- ⁹⁰Physics Department, Lancaster University, Lancaster, United Kingdom
- ⁹¹Oliver Lodge Laboratory, University of Liverpool, Liverpool, United Kingdom
- ⁹²Department of Experimental Particle Physics, Jožef Stefan Institute and Department of Physics, University of Ljubljana, Ljubljana, Slovenia
- ⁹³School of Physics and Astronomy, Queen Mary University of London, London, United Kingdom
- ⁹⁴Department of Physics, Royal Holloway University of London, Egham, United Kingdom
- ⁹⁵Department of Physics and Astronomy, University College London, London, United Kingdom
- ⁹⁶Louisiana Tech University, Ruston, Louisiana, USA
- ⁹⁷Fysiska institutionen, Lunds universitet, Lund, Sweden
- ⁹⁸Centre de Calcul de l'Institut National de Physique Nucléaire et de Physique des Particules (IN2P3), Villeurbanne, France
- ⁹⁹Departamento de Física Teórica C-15 and CIAFF, Universidad Autónoma de Madrid, Madrid, Spain
- ¹⁰⁰Institut für Physik, Universität Mainz, Mainz, Germany
- ¹⁰¹School of Physics and Astronomy, University of Manchester, Manchester, United Kingdom
- ¹⁰²CPPM, Aix-Marseille Université, CNRS/IN2P3, Marseille, France
- ¹⁰³Department of Physics, University of Massachusetts, Amherst, Massachusetts, USA
- ¹⁰⁴Department of Physics, McGill University, Montreal QC, Canada
- ¹⁰⁵School of Physics, University of Melbourne, Victoria, Australia
- ¹⁰⁶Department of Physics, University of Michigan, Ann Arbor, Michigan, USA
- ¹⁰⁷Department of Physics and Astronomy, Michigan State University, East Lansing, Michigan, USA
- ¹⁰⁸B.I. Stepanov Institute of Physics, National Academy of Sciences of Belarus, Minsk, Belarus
- ¹⁰⁹Research Institute for Nuclear Problems of Byelorussian State University, Minsk, Belarus
- ¹¹⁰Group of Particle Physics, University of Montreal, Montreal QC, Canada
- ¹¹¹P.N. Lebedev Physical Institute of the Russian Academy of Sciences, Moscow, Russia
- ¹¹²National Research Nuclear University MEPhI, Moscow, Russia
- ¹¹³D.V. Skobeltsyn Institute of Nuclear Physics, M.V. Lomonosov Moscow State University, Moscow, Russia
- ¹¹⁴Fakultät für Physik, Ludwig-Maximilians-Universität München, München, Germany
- ¹¹⁵Max-Planck-Institut für Physik (Werner-Heisenberg-Institut), München, Germany
- ¹¹⁶Nagasaki Institute of Applied Science, Nagasaki, Japan
- ¹¹⁷Graduate School of Science and Kobayashi-Maskawa Institute, Nagoya University, Nagoya, Japan
- ¹¹⁸Department of Physics and Astronomy, University of New Mexico, Albuquerque, New Mexico, USA
- ¹¹⁹Institute for Mathematics, Astrophysics and Particle Physics, Radboud University Nijmegen/Nikhef, Nijmegen, Netherlands
- ¹²⁰Nikhef National Institute for Subatomic Physics and University of Amsterdam, Amsterdam, Netherlands
- ¹²¹Department of Physics, Northern Illinois University, DeKalb, Illinois, USA
- ^{122a}Budker Institute of Nuclear Physics and NSU, SB RAS, Novosibirsk, Russia
- ^{122b}Novosibirsk State University Novosibirsk, Russia
- ¹²³Institute for High Energy Physics of the National Research Centre Kurchatov Institute, Protvino, Russia
- ¹²⁴Institute for Theoretical and Experimental Physics named by A.I. Alikhanov of National Research Centre "Kurchatov Institute", Moscow, Russia
- ¹²⁵Department of Physics, New York University, New York, New York, USA
- ¹²⁶Ochanomizu University, Otsuka, Bunkyo-ku, Tokyo, Japan
- ¹²⁷Ohio State University, Columbus, Ohio, USA
- ¹²⁸Homer L. Dodge Department of Physics and Astronomy, University of Oklahoma, Norman, Oklahoma, USA
- ¹²⁹Department of Physics, Oklahoma State University, Stillwater, Oklahoma, USA
- ¹³⁰Palacký University, RCPTM, Joint Laboratory of Optics, Olomouc, Czech Republic
- ¹³¹Institute for Fundamental Science, University of Oregon, Eugene, Oregon, USA
- ¹³²Graduate School of Science, Osaka University, Osaka, Japan
- ¹³³Department of Physics, University of Oslo, Oslo, Norway

- ¹³⁴*Department of Physics, Oxford University, Oxford, United Kingdom*
- ¹³⁵*LPNHE, Sorbonne Université, Université de Paris, CNRS/IN2P3, Paris, France*
- ¹³⁶*Department of Physics, University of Pennsylvania, Philadelphia, Pennsylvania, USA*
- ¹³⁷*Konstantinov Nuclear Physics Institute of National Research Centre “Kurchatov Institute”, PNPI, St. Petersburg, Russia*
- ¹³⁸*Department of Physics and Astronomy, University of Pittsburgh, Pittsburgh, Pennsylvania, USA*
- ^{139a}*Laboratório de Instrumentação e Física Experimental de Partículas—LIP, Lisboa, Portugal*
- ^{139b}*Departamento de Física, Faculdade de Ciências, Universidade de Lisboa, Lisboa, Portugal*
- ^{139c}*Departamento de Física, Universidade de Coimbra, Coimbra, Portugal*
- ^{139d}*Centro de Física Nuclear da Universidade de Lisboa, Lisboa, Portugal*
- ^{139e}*Departamento de Física, Universidade do Minho, Braga, Portugal*
- ^{139f}*Departamento de Física Teórica y del Cosmos, Universidad de Granada, Granada (Spain), Spain*
- ^{139g}*Dep Física and CEFITEC of Faculdade de Ciências e Tecnologia, Universidade Nova de Lisboa, Caparica, Portugal*
- ^{139h}*Instituto Superior Técnico, Universidade de Lisboa, Lisboa, Portugal*
- ¹⁴⁰*Institute of Physics of the Czech Academy of Sciences, Prague, Czech Republic*
- ¹⁴¹*Czech Technical University in Prague, Prague, Czech Republic*
- ¹⁴²*Charles University, Faculty of Mathematics and Physics, Prague, Czech Republic*
- ¹⁴³*Particle Physics Department, Rutherford Appleton Laboratory, Didcot, United Kingdom*
- ¹⁴⁴*IRFU, CEA, Université Paris-Saclay, Gif-sur-Yvette, France*
- ¹⁴⁵*Santa Cruz Institute for Particle Physics, University of California Santa Cruz, Santa Cruz, California, USA*
- ^{146a}*Departamento de Física, Pontificia Universidad Católica de Chile, Santiago, Chile*
- ^{146b}*Universidad Andres Bello, Department of Physics, Santiago, Chile*
- ^{146c}*Instituto de Alta Investigación, Universidad de Tarapacá, Chile*
- ^{146d}*Departamento de Física, Universidad Técnica Federico Santa María, Valparaíso, Chile*
- ¹⁴⁷*Department of Physics, University of Washington, Seattle, Washington, USA*
- ¹⁴⁸*Department of Physics and Astronomy, University of Sheffield, Sheffield, United Kingdom*
- ¹⁴⁹*Department of Physics, Shinshu University, Nagano, Japan*
- ¹⁵⁰*Department Physik, Universität Siegen, Siegen, Germany*
- ¹⁵¹*Department of Physics, Simon Fraser University, Burnaby BC, Canada*
- ¹⁵²*SLAC National Accelerator Laboratory, Stanford, California, USA*
- ¹⁵³*Physics Department, Royal Institute of Technology, Stockholm, Sweden*
- ¹⁵⁴*Departments of Physics and Astronomy, Stony Brook University, Stony Brook, New York, USA*
- ¹⁵⁵*Department of Physics and Astronomy, University of Sussex, Brighton, United Kingdom*
- ¹⁵⁶*School of Physics, University of Sydney, Sydney, Australia*
- ¹⁵⁷*Institute of Physics, Academia Sinica, Taipei, Taiwan*
- ^{158a}*E. Andronikashvili Institute of Physics, Iv. Javakhishvili Tbilisi State University, Tbilisi, Georgia*
- ^{158b}*High Energy Physics Institute, Tbilisi State University, Tbilisi, Georgia*
- ¹⁵⁹*Department of Physics, Technion, Israel Institute of Technology, Haifa, Israel*
- ¹⁶⁰*Raymond and Beverly Sackler School of Physics and Astronomy, Tel Aviv University, Tel Aviv, Israel*
- ¹⁶¹*Department of Physics, Aristotle University of Thessaloniki, Thessaloniki, Greece*
- ¹⁶²*International Center for Elementary Particle Physics and Department of Physics, University of Tokyo, Tokyo, Japan*
- ¹⁶³*Graduate School of Science and Technology, Tokyo Metropolitan University, Tokyo, Japan*
- ¹⁶⁴*Department of Physics, Tokyo Institute of Technology, Tokyo, Japan*
- ¹⁶⁵*Tomsk State University, Tomsk, Russia*
- ¹⁶⁶*Department of Physics, University of Toronto, Toronto ON, Canada*
- ^{167a}*TRIUMF, Vancouver BC, Canada*
- ^{167b}*Department of Physics and Astronomy, York University, Toronto ON, Canada*
- ¹⁶⁸*Division of Physics and Tomonaga Center for the History of the Universe, Faculty of Pure and Applied Sciences, University of Tsukuba, Tsukuba, Japan*
- ¹⁶⁹*Department of Physics and Astronomy, Tufts University, Medford, Massachusetts, USA*
- ¹⁷⁰*Department of Physics and Astronomy, University of California Irvine, Irvine, California, USA*
- ¹⁷¹*Department of Physics and Astronomy, University of Uppsala, Uppsala, Sweden*
- ¹⁷²*Department of Physics, University of Illinois, Urbana, Illinois, USA*
- ¹⁷³*Instituto de Física Corpuscular (IFIC), Centro Mixto Universidad de Valencia—CSIC, Valencia, Spain*
- ¹⁷⁴*Department of Physics, University of British Columbia, Vancouver BC, Canada*
- ¹⁷⁵*Department of Physics and Astronomy, University of Victoria, Victoria BC, Canada*
- ¹⁷⁶*Fakultät für Physik und Astronomie, Julius-Maximilians-Universität Würzburg, Würzburg, Germany*

¹⁷⁷*Department of Physics, University of Warwick, Coventry, United Kingdom*¹⁷⁸*Waseda University, Tokyo, Japan*¹⁷⁹*Department of Particle Physics and Astrophysics, Weizmann Institute of Science, Rehovot, Israel*¹⁸⁰*Department of Physics, University of Wisconsin, Madison, Wisconsin, USA*¹⁸¹*Fakultät für Mathematik und Naturwissenschaften, Fachgruppe Physik,
Bergische Universität Wuppertal, Wuppertal, Germany*¹⁸²*Department of Physics, Yale University, New Haven, Connecticut, USA*^aDeceased.^bAlso at Department of Physics, King's College London, London, United Kingdom.^cAlso at Instituto de Fisica Teorica, IFT-UAM/CSIC, Madrid, Spain.^dAlso at TRIUMF, Vancouver BC, Canada.^eAlso at Department of Physics and Astronomy, University of Louisville, Louisville, Kentucky, USA.^fAlso at Physics Department, An-Najah National University, Nablus, Palestine.^gAlso at Department of Physics, University of Fribourg, Fribourg, Switzerland.^hAlso at Departament de Fisica de la Universitat Autònoma de Barcelona, Barcelona, Spain.ⁱAlso at Moscow Institute of Physics and Technology State University, Dolgoprudny, Russia.^jAlso at Department of Physics, Ben Gurion University of the Negev, Beer Sheva, Israel.^kAlso at Università di Napoli Parthenope, Napoli, Italy.^lAlso at Institute of Particle Physics (IPP), Canada.^mAlso at Dipartimento di Matematica, Informatica e Fisica, Università di Udine, Udine, Italy.ⁿAlso at Department of Physics, St. Petersburg State Polytechnical University, St. Petersburg, Russia.^oAlso at Borough of Manhattan Community College, City University of New York, New York, New York, USA.^pAlso at Department of Physics, California State University, Fresno, USA.^qAlso at Department of Financial and Management Engineering, University of the Aegean, Chios, Greece.^rAlso at Centro Studi e Ricerche Enrico Fermi, Italy.^sAlso at Department of Physics, California State University, East Bay, USA.^tAlso at Institutio Catalana de Recerca i Estudis Avancats, ICREA, Barcelona, Spain.^uAlso at IJCLab, Université Paris-Saclay, CNRS/IN2P3, 91405, Orsay, France.^vAlso at Graduate School of Science, Osaka University, Osaka, Japan.^wAlso at Physikalisches Institut, Albert-Ludwigs-Universität Freiburg, Freiburg, Germany.^xAlso at University of Chinese Academy of Sciences (UCAS), Beijing, China.^yAlso at Institute of Physics, Azerbaijan Academy of Sciences, Baku, Azerbaijan.^zAlso at Institute for Mathematics, Astrophysics and Particle Physics, Radboud University Nijmegen/Nikhef, Nijmegen, Netherlands.^{aa}Also at CERN, Geneva, Switzerland.^{bb}Also at Joint Institute for Nuclear Research, Dubna, Russia.^{cc}Also at Hellenic Open University, Patras, Greece.^{dd}Also at The City College of New York, New York, New York, USA.^{ee}Also at Department of Physics, California State University, Sacramento, USA.^{ff}Also at Département de Physique Nucléaire et Corpusculaire, Université de Genève, Genève, Switzerland.^{gg}Also at Louisiana Tech University, Ruston, Louisiana, USA.^{hh}Also at Institute for Nuclear Research and Nuclear Energy (INRNE) of the Bulgarian Academy of Sciences, Sofia, Bulgaria.ⁱⁱAlso at Faculty of Physics, M.V. Lomonosov Moscow State University, Moscow, Russia.^{jj}Also at Institut für Experimentalphysik, Universität Hamburg, Hamburg, Germany.^{kk}Also at CPPM, Aix-Marseille Université, CNRS/IN2P3, Marseille, France.^{ll}Also at National Research Nuclear University MEPhI, Moscow, Russia.^{mmm}Also at Institute for Particle and Nuclear Physics, Wigner Research Centre for Physics, Budapest, Hungary.ⁿⁿAlso at Giresun University, Faculty of Engineering, Giresun, Turkey.^{oo}Also at Department of Physics and Astronomy, Michigan State University, East Lansing, Michigan, USA.